



THE HONG KONG  
POLYTECHNIC UNIVERSITY

香港理工大學

Pao Yue-kong Library

包玉剛圖書館

---

## Copyright Undertaking

This thesis is protected by copyright, with all rights reserved.

**By reading and using the thesis, the reader understands and agrees to the following terms:**

1. The reader will abide by the rules and legal ordinances governing copyright regarding the use of the thesis.
2. The reader will use the thesis for the purpose of research or private study only and not for distribution or further reproduction or any other purpose.
3. The reader agrees to indemnify and hold the University harmless from and against any loss, damage, cost, liability or expenses arising from copyright infringement or unauthorized usage.

### IMPORTANT

If you have reasons to believe that any materials in this thesis are deemed not suitable to be distributed in this form, or a copyright owner having difficulty with the material being included in our database, please contact [lbsys@polyu.edu.hk](mailto:lbsys@polyu.edu.hk) providing details. The Library will look into your claim and consider taking remedial action upon receipt of the written requests.

**THREE-DIMENSIONAL ASSESSMENTS OF  
ADOLESCENT IDIOPATHIC SCOLIOSIS USING  
THREE-DIMENSIONAL ULTRASOUND**

**WANG QIAN**

**PhD**

**The Hong Kong Polytechnic University**

**This programme is jointly offered by The Hong Kong Polytechnic  
University and Sichuan University**

**2018**

**The Hong Kong Polytechnic University**  
**Department of Biomedical Engineering**  
**Sichuan University**  
**Department of Rehabilitation Medicine**

**Three-dimensional Assessments of Adolescent Idiopathic  
Scoliosis Using Three-dimensional Ultrasound**

**WANG Qian**

A thesis submitted in partial fulfilment of the requirements for the  
degree of Doctor of Philosophy

September 2017

## **CERTIFICATE OF ORIGINALITY**

I hereby declare that this thesis is my own work and that, to the best of my knowledge and belief, it reproduces no material previously published or written, nor material that has been accepted for the award of any other degree or diploma, except where due acknowledgement has been made in the text.

\_\_\_\_\_ (Signed)

WANG Qian (Name of student)

## **ABSTRACT OF THESIS**

Adolescent idiopathic scoliosis (AIS) is a three-dimensional spinal deformity characterized by lateral curvature and vertebral rotation of spine. It occurs in approximately 3% of adolescents with unknown reasons. Nowadays, the radiographic assessment of scoliotic spine continues to be the most widely used method in a scoliosis clinic. In routine clinical practice, radiographic assessments are performed throughout the course of treatment of the patients with AIS. However, the frequency of radiation exposure in monitoring scoliosis concerns many adolescents and their parents in light of evidence that cumulative radiation exposure could increase cancer risk. In addition, radiographic assessment of scoliotic spine is limited in the coronal and sagittal planes, which represent a simplification of the true 3-dimensional (3-D) spinal deformity involved in scoliosis. Thus, attempts to reduce or eliminate radiation exposure in adolescents and visualization of 3-D characteristics of scoliotic spine have led researchers to develop new imaging technologies, such as stereo-radiography (EOS), ultrasound imaging, and magnetic resonance imaging (MRI).

Currently, ultrasound has gained considerable attention in the assessment of scoliosis. Ultrasound imaging is a non-radiation and cost-effective method, which is accessible in the majority of medical institutes. The posterior structure of vertebrae could be displayed by ultrasound imaging in the transverse plane. The development of the 3-D ultrasound system can enable the 3-D reconstruction of vertebral images and facilitate the measurement of scoliotic spine in various anatomical planes that could not be accomplished previously. A series of the related research have been conducted in Canada, Hong Kong, Japan, Australia, Netherlands and other places. Spinous processes, laminae and transverse processes can be

visualized and used as landmarks to measure the lateral curvature and vertebral rotation in the coronal and transverse planes of the ultrasound images.

The center of laminae (COL) method has been proposed to measure the spinal curvature and vertebral rotation in the coronal and transverse planes of the 3-D ultrasound images. The reliability and validity of this proposed method have been demonstrated. However, the evidence is limited to the experiment phantom studies. Thus, the objective of this study was to explore the possibility of using the proposed 3-D ultrasound methods to assess the coronal curvature, vertebral rotation, kyphotic and lordotic angles in the subjects with AIS under the clinical setting, and to evaluate its reliability and validity with the concurrent MRI methods.

Due to the gravitational effect, spinal orientation between standing and supine positions may change their corresponding lateral curvatures and vertebral rotations. Thus, the second purpose of this study was to investigate the gravitational effect on the coronal curvature and vertebral rotation between standing and supine postures using 3-D radiation-free ultrasound assessments in the patients with AIS.

Sixteen female AIS subjects were recruited from the Prince of Wales Hospital, Hong Kong. The ultrasound examinations were performed using a 3-D ultrasound unit with a SonixGPS system. A purpose-design couch with central slot was used for supine ultrasound scanning. Ultrasound scanning was performed continuously along the coronal plane from C7 to S1, with the subjects in the standing and supine positions, respectively. Two observers performed the ultrasound scanning and 3 times of angle measurements for each parameter after 3-D image reconstructions. In the coronal plane, the spinal curvatures were measured using the center of laminae (COL) method. In the transverse plane, the apical vertebral rotations were

also assessed with the center of laminae (COL) method. In the sagittal plane, the kyphosis and lordosis angles were estimated by the spinous process angle (SPA) method.

To compare with the ultrasound measurements, magnetic resonance imaging (MRI) examination was conducted within the same morning. A 3.0T MR scanner (Achieva, Philips Medical Systems, Netherlands) and a spine array coil were used. The spinal curvature was measured with the Cobb method in the coronal plane. The apical vertebral rotation was calculated using the Aaro-Dahlborn method in the transverse plane. The kyphotic and lordotic angles were assessed by the Cobb method in the sagittal plane.

The raters 1 and 2 had 5- year and 2-year experience of using ultrasound to measure the scoliotic spine respectively. Prior to the study, each rater was required to practice ultrasound scanning at the supine position and measurements for more than 10 subjects. During this study, the 3-D ultrasound and MRI images were randomly assigned without specific order for measurements. The two raters were blinded to the subjects' clinical information and they performed the 3-D ultrasound and MRI measurements independently in 3 trials each with one week interval.

The intra-class correlation coefficient (ICC, [2, k]) with 95% confidence intervals (CI) was used to evaluate the intra- and inter-observer reliabilities of the 3-D ultrasound and MRI assessments. In addition, the mean absolute deviation (MAD), standard deviation (SD) and standard error of measurement (SEM) were used to assess the intra- and inter-observer measurement variability of these two methods. In order to determine the validity of 3-D ultrasound assessments, the comparison of means, the Bland-Altman method and the Pearson

correlation analysis were applied between the 3-D ultrasound and MRI measurements in the patients with AIS.

The results suggested that the 3-D ultrasound presented high intra- and inter-rater reliability when measuring the coronal curvature (COL method), the apical vertebral rotation (COL method), the kyphosis and lordosis (SPA method) in the patients with AIS. In addition, the validity of 3-D ultrasound measurements has been verified, including the spinal curvature angle in the coronal plane (COL method); the vertebral rotation in the transverses plane (COL method); the kyphotic other than lordotic angles in the sagittal plane (SPA method). Besides, the difference between the supine and standing positions was  $1.9^{\circ}\sim 11.7^{\circ}$  and  $0.0^{\circ}\sim 5.9^{\circ}$  for the coronal curvature and the vertebral rotation respectively. Multi-linear regression revealed that the possible relevant factors were the coronal curvature, the vertebral rotation and the variation in the selected upper-end vertebra to these changes. Furthermore, a high correlation between the supine and standing postures was demonstrated.

The radiation-free 3-D ultrasound presented to be a reliable & valid method for measuring the spinal curvature in the coronal plane and the vertebral rotation in the transverse plane in the patients with AIS under the clinical setting. The reliable assessments of kyphotic and lordotic angles in the sagittal plane have been obtained using the 3-D ultrasound method (SPA), however, its validity has yet been proved in this study. The possibility of using 3-D ultrasound to measure the lateral curvature and the vertebral rotation of AIS at the supine and standing positions were verified, the difference and correlation between these two positions have been demonstrated. Further studies on the 3-D changes of AIS using the radiation-free ultrasound are deserved in order to optimize the 3-D ultrasound scanning and measuring procedures, and to further validate the 3-D ultrasound measurements in a larger clinical trial.



With these efforts, 3-D ultrasound will become a potential option used as an alternative to radiography for screening and routine assessment of scoliosis.

## **PUBLICATIONS ARISING FROM THE THESIS**

### ***Peer-reviewed journal papers (published or accepted)***

WANG Q, LI M, LOU H. M. E, WONG M. S.

Reliability and Validity Study of Clinical Ultrasound Imaging on Lateral Curvature of Adolescent Idiopathic Scoliosis. PLoS One, 2015,10(8): e0135264.

WANG Q, LI M, LOU H. M. E, CHU C.W.W, LAM TP, CHENG C.Y.J, WONG M. S.

Validity Study of Vertebral Rotation Measurement Using Three-dimensional Ultrasound in Adolescent Idiopathic Scoliosis. Ultrasound Med Biol, 2016, 42(7):1473-1481.

WANG Q, LEI ZJ, MA ZH, WONG M. S.

Application of Medical Imaging Technologies in Adolescent Idiopathic Scoliosis. Chin J Rehabil Theory Pract. 2017, 23(11): 1304-1307.

WANG Q, LI M, LOU H. M. E, WONG M. S, HE CQ.

Three-dimensional Ultrasound Assessment of Apical Vertebral Rotation in Patients with Adolescent Idiopathic Scoliosis: Reliability and Validity Analysis. J Sichuan Univ (Med Sci Edi), 2018, 49(3):36-44.

WANG Q, LI M, LOU H. M. E, WONG M. S, HE CQ.

Three-dimensional Ultrasound Imaging of Coronal Curvature and Vertebral Rotation Changes between Supine versus Standing Postures in Patients with Adolescent Idiopathic Scoliosis. J Sichuan Univ (Med Sci Edi), 2018.

***Peer-reviewed journal papers (submitted)***

WANG Q, LOU H. M. E, ZHANG M, LEUNG AKL, WONG M. S.

Ultrasound Application in the Assessment of Patients with Adolescent Idiopathic Scoliosis. Submitted to Spine Journal. April, 2017.

WANG Q, LI M, LOU H. M. E, CHU C.W.W, LAM TP, CHENG C.Y.J, WONG M. S.

Reliability of Three-dimensional Ultrasound on Vertebral Rotation Assessment of Adolescent Idiopathic Scoliosis. Submitted to PLOS One Journal. March, 2017.

***Peer-reviewed conference papers***

WANG Q, LI M, LOU H. M. E, CHU C.W.W, LAM TP, CHENG C.Y.J, WONG M. S. 3-D

Ultrasound Assessment of Coronal Curvature Change from Standing to Supine in Patients with Adolescent Idiopathic Scoliosis. In: Proceedings of Hong Prosthetic and Orthotic Scientific Meeting 2015, Hong Kong, 17th October 2015.

WANG Q, LI M, LOU H. M. E, CHU C.W.W, LAM TP, CHENG C.Y.J, WONG M. S.

Validation of 3-D Clinical Ultrasound Assessments to Scoliosis. In: Proceedings of International Society of Prosthetic and Orthotic World Congress 2015 in France, Lyon, 22th-25th June 2015.

WANG Q, LI M, LOU H. M. E, CHU C.W.W, LAM TP, CHENG C.Y.J, WONG M. S. 3-D

Clinical Ultrasound Assessments to Scoliosis in Supine and Standing Positions: A Pilot Study. In: Proceedings of Asian Prosthetic and Orthotic Scientific Meeting 2014 in conjunction with The Second Meeting of the International Society for Restorative Neurology in Taipei, Taiwan, 28th-30th November 2014.

WANG Q, LI M, LOU H. M. E, CHU C.W.W, LAM TP, CHENG C.Y.J, WONG M. S.

Intra-and Inter-observer Reliability Study of 3-D Clinical Ultrasound Measurements to Scoliosis: A Pilot Study. In: Proceedings of Hong Kong Prosthetic and Orthotic Scientific Meeting 2014, Hong Kong, 20th September 2014.

## **ACKNOWLEDGEMENTS**

I would like to express my heartest thanks to my chief supervisor, Dr. M.S. WONG for their patience, guidance and support during my PhD research work and to prepare this thesis. I will be forever grateful for what he has taught and suggested which will be the precious wealth of my life.

I also want to take this opportunity to thank my co-supervisor, Prof. Chengqi HE for his helpful suggestions and support.

I would especially thank Prof. Edmond H. M. Lou for his technical support and insightful advice and thank my partner, Meng LI, for her kind help and suggestion during the research experiment of PhD study.

I am grateful to Prof. Jack C.Y. Cheng, Prof. T. P. Lam and Prof. Winnie C.W. Chu for supporting patient's recruitment in the Prince Welsh hospital, Chinese University of Hong Kong.

Thanks to Babak Hassan Beygi, Hazel Chen He, Yummy Y.M. Lin, Hui Dong Wu and Cheng Fei Gao for their help and accompany during my PhD study.

To all the subjects who were involved in this project, I would like to thank for their participation to my study.

Thanks to the Research Grants Council of Hong Kong Special Administrative Region, PRC

(Project No. PolyU 5634/13M) for offering General Research Fund to support work described in this thesis.

I would also like to thank the Hong Kong Jockey Club for providing the Scholarship to support the PhD study in Hong Kong.

Last but not least, I would like to thank my parents and wife for their love, understanding and support during the course of the pursuit of PhD degree.

## TABLE OF CONTENTS

CERTIFICATE OF ORIGINALITY .....	I
ABSTRACT OF THESIS .....	II
PUBLICATIONS ARISING FROM THE THESIS.....	VII
ACKNOWLEDGEMENTS .....	X
TABLE OF CONTENTS.....	XII
LIST OF FIGURES .....	XVII
LIST OF TABLES .....	XX
LIST OF ABBREVIATIONS .....	XXIII
CHAPTER 1 INTRODUCTION .....	25
1.1 Background .....	25
1.2 Objectives.....	26
CHAPTER 2 LITERATURE REVIEW .....	28
2.1 Spine and Vertebra.....	28
2.2 Scoliosis .....	30
2.3 Adolescent idiopathic scoliosis .....	31
2.3.1 Prevalence of AIS .....	31
2.3.2 Symptoms and Progression of AIS.....	31
2.3.3 Screening of AIS .....	32
2.3.4 Assessment of AIS.....	33
2.3.5 Treatment of AIS .....	35
2.4 Imaging Assessment Methods of AIS .....	36
2.4.1 Spinal Radiography .....	37
2.4.2 Stereoradiography.....	57
2.4.3 Computed tomography .....	58

2.4.4 Magnetic resonance imaging .....	61
2.4.5 Surface topography .....	64
2.5 Ultrasound Assessments of AIS .....	68
2.5.1 Muscle Thickness and Dimension Measurements.....	69
2.5.2 Skeletal Maturity Determination .....	73
2.5.3 Bone Quality Assessment.....	75
2.5.4 Development and validation of 3-D ultrasound systems.....	75
2.5.5 Coronal Curvature Measurements .....	78
2.5.6 Vertebral Rotation Measurements .....	83
2.5.7 Other Application of Ultrasound Assessments.....	85
2.6 Summary of Literature Review .....	87
<b>CHAPTER 3 Reliability Study of 3-D Ultrasound Assessments in Patients with Adolescent Idiopathic Scoliosis.....</b>	<b>89</b>
3.1 Introduction .....	89
3.2 Materials and Methods .....	92
3.2.1 Reliability Study of 3-D Ultrasound Assessments in AIS.....	92
3.2.2 Subjects.....	92
3.2.3 3-D Ultrasound System .....	93
3.2.4 Observers .....	94
3.2.5 3-D Ultrasound Scan in the Supine Position .....	94
3.2.6 3-D Ultrasound Images Reconstruction and Landmarks Identification .....	97
3.2.7 3-D Ultrasound Assessments of Spinal Curvature in the Coronal Plane .....	99
3.2.8 3-D Ultrasound Assessments of Vertebral Rotation in the Transverse Plane .	101
3.2.9 3-D Ultrasound Assessments of Kyphotic and Lordotic Angles in the Sagittal Plane .....	101



3.2.10 Statistical Analysis .....	102
3.3 Results .....	103
3.3.1 Anthropometric Information of the Recruited Subjects .....	103
3.3.2 Reliability of 3-D Ultrasound Assessment of Coronal Curvature in AIS .....	104
3.3.3 Reliability of 3-D Ultrasound Assessment of Vertebral Rotation in AIS .....	106
3.3.4 Reliability of Kyphotic/Lordotic Angles Measurements using 3-D Ultrasound in AIS.....	108
3.4 Discussions.....	111
3.5 Conclusions .....	114
CHAPTER 4 Validity Study of 3-D Ultrasound Assessments in Patients with Adolescent Idiopathic Scoliosis.....	115
4.1 Introduction .....	115
4.2 Materials and Methods .....	116
4.2.1 Validity Study of 3-D Ultrasound Assessments in AIS .....	116
4.2.2 Subjects.....	116
4.2.3 Observers .....	117
4.2.4 3-D Ultrasound Scan and Assessments .....	117
4.2.5 MRI Scan and Measurements .....	118
4.2.6 Statistical Analysis .....	122
4.3 Results .....	123
4.3.1 Anthropometric Information of the Recruited Subjects .....	123
4.3.2 Validity of 3-D Ultrasound Assessment of Coronal Curvature in AIS .....	123
4.3.3 Validity of 3-D Ultrasound Assessments of Vertebral Rotation in AIS.....	130
4.3.4 Validity of 3-D Ultrasound Assessment of Kyphotic/Lordotic Angles in AIS .....	140

4.4 Discussions.....	146
4.4.1 Validity Study of 3-D Ultrasound Assessment of Coronal Curvature in AIS.	146
4.4.2 Validity Study of 3-D Ultrasound Assessment of Vertebral Rotation in AIS.	148
4.4.3 Validity Study of 3-D Ultrasound Assessment of Kyphotic/Lordotic Angles in AIS.....	150
4.5 Conclusion.....	153
CHAPTER 5 Supine versus Standing Change of Coronal Curvature and Vertebral Rotation of 3-D Ultrasound Measurements in Adolescent Idiopathic Scoliosis .....	155
5.1 Introduction .....	155
5.2 Materials and Methods .....	157
5.2.1 Subjects.....	157
5.2.2 3-D Ultrasound System .....	157
5.2.3 Observers .....	157
5.2.4 3-D Ultrasound Scan in the Supine / Standing Positions .....	157
5.2.5 3-D Ultrasound Assessments of Patients with AIS .....	159
5.2.6 Statistical Analysis .....	159
5.3 Results .....	160
5.3.1 Comparison of 3-D Ultrasound Measurements in Supine versus Standing Positions.....	160
5.3.2 Relevant Factors to 3-D Ultrasound Measurement Difference in Supine versus Standing Positions .....	164
5.3.3 Correlation of 3-D Ultrasound Measures between Supine and Standing Positions.....	166
5.4 Discussions.....	168
5.5 Conclusions .....	171

CHAPTER 6 Conclusions and Recommendations .....	173
6.1 Conclusions .....	173
6.2 Recommendations .....	174
APPENDICES .....	175
APPENDIX A -- CONSENT TO PARTICIPATE IN RESEARCH .....	175
APPENDIX B -- CONSENT TO PARTICIPATE IN RESEARCH .....	176
APPENDIX C -- INFORMATION SHEET .....	177
APPENDIX D -- INFORMATION SHEET (CHINESE VERSION) .....	178
APPENDIX E -- PROJECT PROTOCOL .....	179
REFERENCES .....	181

## LIST OF FIGURES

<b>Figure 2. 1 The anatomical planes of human body .....</b>	<b>28</b>
<b>Figure 2. 2 The coronal and sagittal views of a normal spine.....</b>	<b>29</b>
<b>Figure 2. 3 The superior and lateral views of the thoracic vertebra.....</b>	<b>30</b>
<b>Figure 2. 4 The use of Scoliometer. ....</b>	<b>33</b>
<b>Figure 2. 5 The analysis of the frontal radiograph.. ....</b>	<b>38</b>
<b>Figure 2. 6 Measurements of curve magnitude in the frontal radiograph. ....</b>	<b>40</b>
<b>Figure 2. 7 Methods of vertebral rotation measurements in radiograph. ....</b>	<b>49</b>
<b>Figure 2. 8 Ultrasound measurements of muscle thickness .....</b>	<b>72</b>
<b>Figure 2. 9 Ultrasound determination of skeletal maturity .....</b>	<b>74</b>
<b>Figure 2. 10 The 3-D ultrasound systems.....</b>	<b>77</b>
<b>Figure 2. 11 Ultrasound images of vertebral landmarks.....</b>	<b>79</b>
<b>Figure 2. 12 Ultrasound measurements of coronal curvature. ....</b>	<b>82</b>
<b>Figure 2. 13 Ultrasound measurements of vertebral rotation .....</b>	<b>85</b>
<b>Figure 3. 1 3-D Clinical Ultrasound System .....</b>	<b>94</b>
<b>Figure 3. 2 3-D Ultrasound Experiment Setting and a Purpose-design Coach with a Rectangular Slot.....</b>	<b>95</b>
<b>Figure 3. 3 3-D ultrasound scan in the supine position. ....</b>	<b>96</b>
<b>Figure 3. 4 Self-developed medical image analysis software (MIAS) for 3-D reconstruction of ultrasound images and measurements for scoliotic spine.....</b>	<b>98</b>
<b>Figure 3. 5 The reconstructed 3-D ultrasound images of a scoliotic spine in the 3 orthogonal planes.....</b>	<b>98</b>
<b>Figure 3. 6 Coronal curvature measurement .....</b>	<b>100</b>
<b>Figure 3. 7 Apical vertebral rotation (AVR) measurements.....</b>	<b>101</b>

<b>Figure 3. 8 Kyphotic and lordotic angles measurements. ....</b>	<b>102</b>
<b>Figure 4. 1 Magnetic resonance imaging (MRI) systems for scoliosis assessments .....</b>	<b>118</b>
<b>Figure 4. 2 Coronal curvature measurement .....</b>	<b>120</b>
<b>Figure 4. 3 Apical vertebral rotation (AVR) measurements.....</b>	<b>121</b>
<b>Figure 4. 4 Kyphotic and lordotic angles measurements. ....</b>	<b>122</b>
<b>Figure 4. 5 Comparison of 3-D ultrasound versus MRI measurements for AIS patients with .....</b>	<b>124</b>
<b>Figure 4. 6 Bland–Altman plot assessing the agreement of coronal curvature measurements using 3-D ultrasound and MRI methods in the sample categories .....</b>	<b>127</b>
<b>Figure 4. 7 Correlation of coronal curvature measurements using 3-D ultrasound and MRI methods in the sample categories .....</b>	<b>129</b>
<b>Figure 4. 8 Comparison of measurements of apical vertebral rotation using 3-D ultrasound versus MRI methods in the sample categories.....</b>	<b>132</b>
<b>Figure 4. 9 Bland–Altman plot assessing the agreement of apical vertebral rotation measurements using 3-D ultrasound versus MRI methods in the sample categories ...</b>	<b>134</b>
<b>Figure 4. 10 Bland–Altman plot assessing the agreement of apical vertebral rotation measurements using 3-D ultrasound versus MRI methods in the sample categories ...</b>	<b>136</b>
<b>Figure 4. 11 Bland–Altman plot assessing the agreement of apical vertebral rotation measurements using 3-D ultrasound versus MRI methods in the sample categories. ...</b>	<b>137</b>
<b>Figure 4. 12 Correlation of apical vertebral rotation measurements using 3-D ultrasound versus MRI methods in the sample categories.....</b>	<b>138</b>
<b>Figure 4. 13 Correlation of apical vertebral rotation measurements using 3-D ultrasound versus MRI methods in the sample categories.....</b>	<b>139</b>

<b>Figure 4. 14 Correlation of apical vertebral rotation measurements using 3-D ultrasound versus MRI methods in the sample categories.....</b>	<b>139</b>
<b>Figure 4. 15 Bland–Altman plot assessing the agreement of kyphotic angle measurements using 3-D ultrasound versus MRI methods in the sample categories. ..</b>	<b>142</b>
<b>Figure 4. 16 Bland–Altman plot assessing the agreement of lordotic angle measurements using 3-D ultrasound versus MRI methods in the sample categories .....</b>	<b>143</b>
<b>Figure 4. 17 Correlation of kyphotic angle measurements using 3-D ultrasound versus MRI methods in the sample categories .....</b>	<b>145</b>
<b>Figure 4. 18 Correlation of lordotic angle measurements using 3-D ultrasound versus MRI methods in the sample categories. ....</b>	<b>146</b>
<b>Figure 5. 1 3-D Ultrasound Scanning in the Supine (a) and Standing (b) Positions.....</b>	<b>158</b>
<b>Figure 5. 2 Comparison of coronal curvature measurements using 3-D ultrasound between supine versus standing positions in patients with AIS.....</b>	<b>161</b>
<b>Figure 5. 3 Comparison of vertebral rotation measurements using 3-D ultrasound between supine and standing positions in patients with AIS. ....</b>	<b>163</b>
<b>Figure 5. 4 Correlation of coronal curvature measurements using 3-D ultrasound between supine and standing positions in patients with AIS. ....</b>	<b>167</b>
<b>Figure 5. 5 Correlation of vertebral rotation measurements using 3-D ultrasound between supine and standing positions in patients with AIS. ....</b>	<b>168</b>

## LIST OF TABLES

<b>Table 2. 1 Results of reliability of manual Cobb angle measurements in radiograph ....</b>	<b>41</b>
<b>Table 2. 2 Results of variability of manual Cobb angle measurements in radiograph ..</b>	<b>42</b>
<b>Table 2. 3 Results of reliability of digital Cobb angle measurements in radiograph .....</b>	<b>46</b>
<b>Table 2. 4 Results of variability of digital Cobb angle measurements in radiograph .....</b>	<b>47</b>
<b>Table 2. 5 Results of reliability of vertebral rotation measurements in radiograph .....</b>	<b>51</b>
<b>Table 2. 6 Results of variability of vertebral rotation measurements in radiograph .....</b>	<b>52</b>
<b>Table 2. 7 Ultrasound measurements of muscle thickness and dimension.....</b>	<b>70</b>
<b>Table 2. 8 Ultrasound measurements of spinal curvature in the coronal plane .....</b>	<b>80</b>
<b>Table 2. 9 Ultrasound measurements of vertebral rotation in the transverse plane .....</b>	<b>84</b>
<b>Table 3. 1 Anthropometric data of the recruited subjects .....</b>	<b>104</b>
<b>Table 3. 2 Intra – and inter- rater reliability of coronal curvature assessments using 3-D ultrasound.....</b>	<b>105</b>
<b>Table 3. 3 Intra – and inter-rater variability of coronal curvature assessments using</b>	<b>106</b>
<b>Table 3. 4 Intra – and inter-rater reliability of apical vertebral rotation assessments using 3-D ultrasound.....</b>	<b>107</b>
<b>Table 3. 5 Intra -rater variability of apical vertebral rotation assessments using 3-D ultrasound compared with MRI.....</b>	<b>108</b>
<b>Table 3. 6 Intra- and inter-rater reliability of kyphotic angle assessments using.....</b>	<b>109</b>
<b>Table 3. 7 Intra- and inter-rater reliability of lordotic angle assessments using .....</b>	<b>110</b>
<b>Table 3. 8 Intra- and inter-rater variability of kyphotic angle assessments using 3-D ultrasound.....</b>	<b>110</b>
<b>Table 3. 9 Intra- and inter-rater variability of lordotic angle assessments using.....</b>	<b>111</b>

<b>Table 4. 1 Comparison of means of coronal curvature assessments between 3-D ultrasound and MRI methods.....</b>	<b>125</b>
<b>Table 4. 2 Agreement of coronal curvature assessments between 3-D ultrasound and MRI methods.....</b>	<b>128</b>
<b>Table 4. 3 Pearson correlation analyses of coronal curvature assessments between 3-D ultrasound and MRI methods.....</b>	<b>130</b>
<b>Table 4. 4 Comparison of means of apical vertebral rotation assessments between 3-D ultrasound and MRI methods.....</b>	<b>133</b>
<b>Table 4. 5 Evaluation of agreement of apical vertebral rotation assessments between 3-D ultrasound and MRI methods.....</b>	<b>135</b>
<b>Table 4. 6 Pearson correlation analysis of apical vertebral rotation assessments between 3-D ultrasound and MRI methods.....</b>	<b>140</b>
<b>Table 4. 7 Comparison of means of kyphotic angle assessments between 3-D ultrasound and MRI methods .....</b>	<b>141</b>
<b>Table 4. 8 Comparison of means of lordotic angle assessments between 3-D ultrasound and MRI methods .....</b>	<b>141</b>
<b>Table 4. 9 Agreement of kyphotic angle assessments between 3-D ultrasound and MRI method.....</b>	<b>143</b>
<b>Table 4. 10 Agreement of lordotic angle assessments between 3-D ultrasound and MRI methods.....</b>	<b>144</b>
<b>Table 4. 11 Pearson correlation analysis of kyphotic angle assessments between 3-D ultrasound and MRI methods.....</b>	<b>145</b>
<b>Table 4. 12 Pearson correlation analysis of lordotic angle assessments between 3-D ultrasound and MRI methods.....</b>	<b>146</b>



<b>Table 5. 1 Average difference of coronal curvature angle between supine versus standing positions using 3-D ultrasound measurements in AIS .....</b>	<b>161</b>
<b>Table 5. 2 Average difference of coronal curvature angle between supine versus standing positions using 3-D ultrasound measurements in AIS .....</b>	<b>163</b>
<b>Table 5. 3 Multiple linear regression of coronal curvature difference in supine versus standing positions.....</b>	<b>165</b>
<b>Table 5. 4 Multiple linear regression of vertebral rotation difference in supine versus standing positions.....</b>	<b>166</b>
<b>Table 5. 5 Pearson correlation coefficient (r) between supine and standing positions.</b>	<b>167</b>

## LIST OF ABBREVIATIONS

<u>Abbreviations</u>	<u>Full Spelling</u>
3-D US	Three-dimension Ultrasound
AIS	Adolescent Idiopathic Scoliosis
ASISs	Anterior Superior Iliac Spines
AVR	Apical Vertebral Rotation
CI	Confidence Intervals
COL	Center of Laminae
CT	Computed Tomography
CVSL	Central Vertical Sacral Line
DAPI	Axial plane index
ICC	Intra-class Correlation Coefficient
LEV	Lower-end Vertebra
MAD	Mean Absolute Deviation
MRI	Magnetic Resonance Imaging
n	Number of Subjects
p	Probability
PI	Pelvic Incidence
POTSI	Posterior Trunk Symmetry Index
r	Pearson's Correlation Coefficients
SD	Standard Deviation
SEM	Standard Error of Measurement
SPA	Spinous Process Angle

SRS	Scoliosis Research Society
TRA	Transverse Process Angle
UEV	Upper-end Vertebra

# CHAPTER 1 INTRODUCTION

## 1.1 Background

Adolescent idiopathic scoliosis (AIS) is a three-dimensional spinal deformity characterized by lateral curvature in the coronal and sagittal planes and vertebral rotation in the transverse plane. It occurs in approximately 3% of adolescents with unknown reasons [1, 2]. Nowadays, the radiographic assessment of scoliotic spine continues to be the most widely used method in a scoliosis clinic. In the standing posterior-anterior radiographs, the spinal curvature can be assessed with the Cobb method, which was adopted by the Scoliosis Research Society (SRS) as the standard reference method to diagnose and monitor AIS [3].

In the routine clinical practice, radiographic assessments are performed throughout the course of treatment of the patients with AIS. However, the frequency of radiation exposure in monitoring scoliosis concerns many adolescents and their parents in light of evidence that the cumulative radiation exposure could increase cancer risk [4, 5]. The Society on Scoliosis Orthopaedic and Rehabilitation Treatment (SOSORT) 2012 consensus statements advocated the effective strategies for reducing the number of radiographs in each of the pediatric and adolescent sub-populations who are subjective to scoliosis [6]. In addition, radiographic assessment of scoliotic spine is limited in the coronal and sagittal planes, whereas the vertebral rotation in the transverse plane cannot be displayed in the radiographic images of scoliosis. The assessments provided by radiograph only represent a simplification of the true 3-dimensional (3-D) spinal deformity involved in scoliosis [3]. Thus, attempts to reduce radiation exposure in adolescents and visualization of 3-D characteristics of scoliotic spine have led researchers to develop new imaging technologies, such as stereo-radiography (EOS), 3-D ultrasound imaging, and magnetic resonance imaging (MRI).

Among various imaging technologies, ultrasound imaging has some superior characteristics such as radiation-free, cost effective and easy to operate. The development of the 3-D ultrasound system can enable the 3-D reconstruction of vertebral images and facilitate the measurement of scoliotic spine in various anatomical planes that could not be accomplished previously [7-16]. A series of the related research have been conducted in Canada, Hong Kong, Japan, Australia, Netherlands and other places. The landmarks such as spinous processes, transverse processes and laminae have been identified in the 3-D ultrasound images [9, 11, 17, 18]. It is the key point how to use these structural landmarks of vertebrae to assess the 3-D characteristics of scoliosis. Currently, the center of laminae (COL) method has been proposed to assess the spinal curvature in the coronal plane of scoliotic spine [19-21]. However, the evidence is limited to the phantom studies [17]. Moreover, studies using ultrasound to evaluate scoliosis on the other anatomical planes, as well as in the different scanning positions are limited. Therefore, this study aims to study the feasibility, reliability and validity of the 3-D ultrasound assessments for the patients with AIS under the clinical setting.

## **1.2 Objectives**

The objectives of the current study are:

- To explore the possibility of using 3-D ultrasound to scan and measure AIS under the clinical setting.
- To assess the reliability and validity of the 3-D ultrasound assessment of spinal curvature in the coronal plane for the patients with AIS.
- To evaluate the reliability and validity of the 3-D ultrasound assessment of vertebral rotation in the transverse plane for the patients with AIS.

- To verify the reliability and validity of the 3-D ultrasound assessments of kyphotic and lordotic angles in the sagittal plane for the patients with AIS.
- To investigate the gravitational effect on the changes of coronal curvature and vertebral rotation between the standing and supine postures using the 3-D ultrasound assessments in the patients with AIS.

## CHAPTER 2 LITERATURE REVIEW

### 2.1 Spine and Vertebra

The terminologies of anatomical planes with regard to the spine and vertebra in this thesis are described in the following. The coronal plane, also known as the frontal plane, is a vertical plane dividing the body into anterior and posterior parts. The sagittal plane, also known as the lateral plane, is a vertical plane that divides the body into right and left parts [22]. The transverse plane, also known as the axial plane, lies horizontally and divides the body into superior and inferior parts (Figure 2.1).

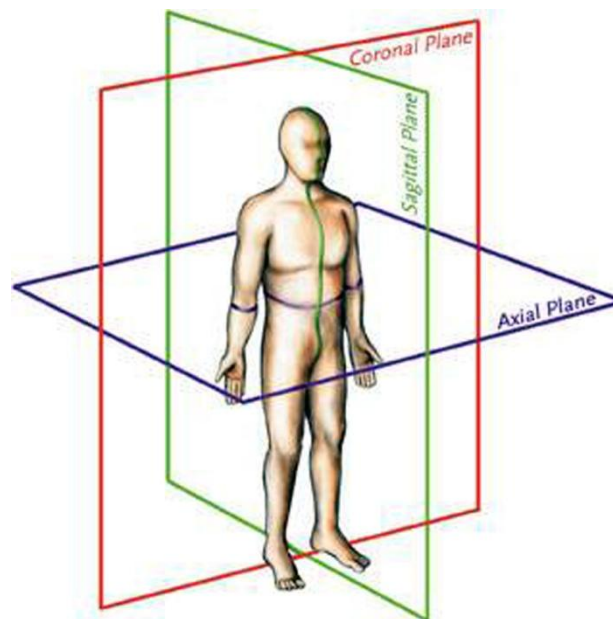


**Figure 2. 1 The anatomical planes of human body**

The spine is known as the vertebral column, which is the mainstay of the body located centrally and extended from the base of the skull to the pelvis. It serves to protect the spinal cord, support the human in the upright posture and allow the movement and lococation. The

spine is composed of 7 cervical vertebrae (C1-C7), 12 thoracic vertebrae (T1-T12), 5 lumbar vertebrae (L1-L5), 5 fused vertebrae in the sacrum (S1-S5) and the coccyx from the top to the bottom. The vertebrae with different shape and size are bounded together by the ligaments and separated by the intervertebral discs between their bodies. Four natural curvatures are formed in the sagittal plane of a normal spine, while there is no curvature or minor lateral curvature in the coronal plane [23]. Figure 2.2 shows the coronal and sagittal views of a normal spine, respectively.



**Figure 2. 2 The coronal and sagittal views of a normal spine.**



Although the vertebrae of spine have regional differences, they possess a common pattern, which typically consists of a rounded vertebral body anteriorly and a vertebral arch posteriorly. The vertebral arch is composed of a pair of pedicles forming the sides of the arch and a pair of laminae connecting at the end of the arch posteriorly. In addition, the vertebral arch gives rise to 7 processes, including 1 spinous process, 2 transverse processes, 2 inferior articular processes and 2 superior articular processes [23]. Figure 2.3 displays the superior and lateral views of the thoracic vertebra, respectively.

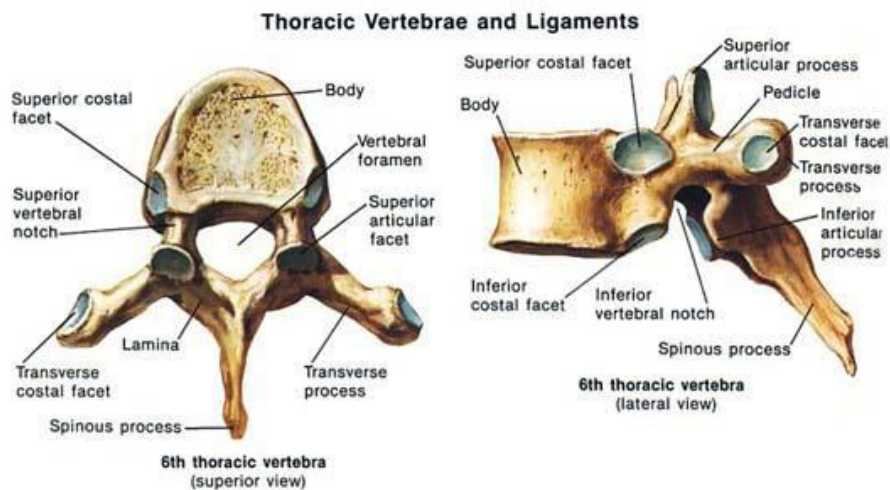


**Figure 2. 3 The superior and lateral views of the thoracic vertebra.**

## 2.2 Scoliosis

Scoliosis is a general term, introduced by Hippocrates, which can be defined as three-dimensional torsional deformity of the spine and trunk. It caused a lateral curvature in the coronal plane, an axial rotation in the transverse plane, and a disturbance of the kyphotic and lordotic angles in the sagittal plane, mostly reducing them in direction of a flat back [1, 2, 24]. According to etiology, scoliosis is typically classified to congenital scoliosis, neuromuscular scoliosis and idiopathic scoliosis [25, 26]. Approximately 80% of all scoliosis cases are

idiopathic scoliosis, by definition, which is of unknown origin and is probably due to several causes. Idiopathic scoliosis is further classified as infantile (in children from birth up to 3 years of age), juvenile (in children 3 to 10 years of age), adolescent (in children 10 to 18 years of age), or adult (older than 18 years of age) [1, 25].

## **2.3 Adolescent idiopathic scoliosis**

### **2.3.1 Prevalence of AIS**

Adolescent idiopathic scoliosis (AIS) is the most common type of idiopathic scoliosis, which occurs in the general population in a wide range from 0.93 to 12% reported in the literature. A meta-analysis showed that the prevalence of scoliosis was 1.02% among the primary and middle school students in Mainland China [27]. In addition, a large population-based cohort study revealed the prevalence of curves of  $>20^\circ$  was 1.8% among a total of 306,144 students in Hong Kong [28]. The female to male ratio ranges from 1.5:1 to 3:1 and rises substantially with the age or lateral curvature increased. When the Cobb angle is within 10 to  $20^\circ$ , the ratio of the affected girls to boys is similar (1.3:1), increasing to 5.4:1 for Cobb angles between 20 and  $30^\circ$ , and 7:1 for angle values above  $30^\circ$ [24].

### **2.3.2 Symptoms and Progression of AIS**

If the scoliosis angle at completion of growth exceeds a “critical threshold” (most authors assume it to be between  $30^\circ$  and  $50^\circ$ ), there is a higher risk of health problems in adult life, such as decreased quality of life, cosmetic deformity and visible disability, pain and progressive functional limitations. Severe AIS cases (Cobb angle larger than  $50^\circ$ ) often lead to the cardiac dysfunction and pulmonary constraints. In the growing child with AIS, the major concern is the cosmetic disfigurement of shoulder or waist and rib hump, which are likely to result in the psychological disturbances of adolescents [1, 29, 30].

The likelihood of progression of AIS is dependent on the maturity (chronological age, menarchal status or skeletal age), the curve magnitude and the position of the curve apex [2, 31, 32]. The more skeletally and sexually immature the patient is, the greater the probability of curve progression. There is a much lower potential for progression of AIS after the spinal growth is complete. Likewise, the larger the curve magnitude is at presentation, the higher the likelihood of progression. Many studies agree that the curves with a thoracic apex often have the probability ranging from 58% to 100% of curve progression [2]. In addition, natural history studies have shown that the scoliosis deformity that is less than 30° at the end of growth rarely worsens throughout the adulthood, whereas the scoliosis of greater than 50° predictably worsens at a rate of 0.8 to 1.0° per year [33]. Therefore, the patient with scoliosis of more than 30° will be at risk for progression if the skeleton is immature.

### **2.3.3 Screening of AIS**

Scoliosis screening program is used to identify the suspected cases of AIS who will be referred for diagnostic evaluation or conservative brace treatment. The purpose of school scoliosis screening is to achieve the early detection of AIS and consequently reduce the risk of requiring invasive spinal fusion surgery and its high costs [34, 35]. A two-step procedure is recommended for the school-based scoliosis screening. Adam's forward-bending test (FBT) is the first step, in which the patient bends forward to 90° in an upright position and the examiner identifies the rotation of trunk (rib hump) from the behind and side of the patient's back [36]. Then in the second step, the Scoliometer is used to quantify the degree of trunk rotation based on the Adam's test. The Scoliometer is placed at the apex of the curvature, perpendicular to the long axis of the body, with the patient in a forward bending position (Figure 2.4) [36]. The referral for diagnostic evaluation of X-ray is recommended when the

degree is between 7° and 9° on the Scoliometer [35, 37].

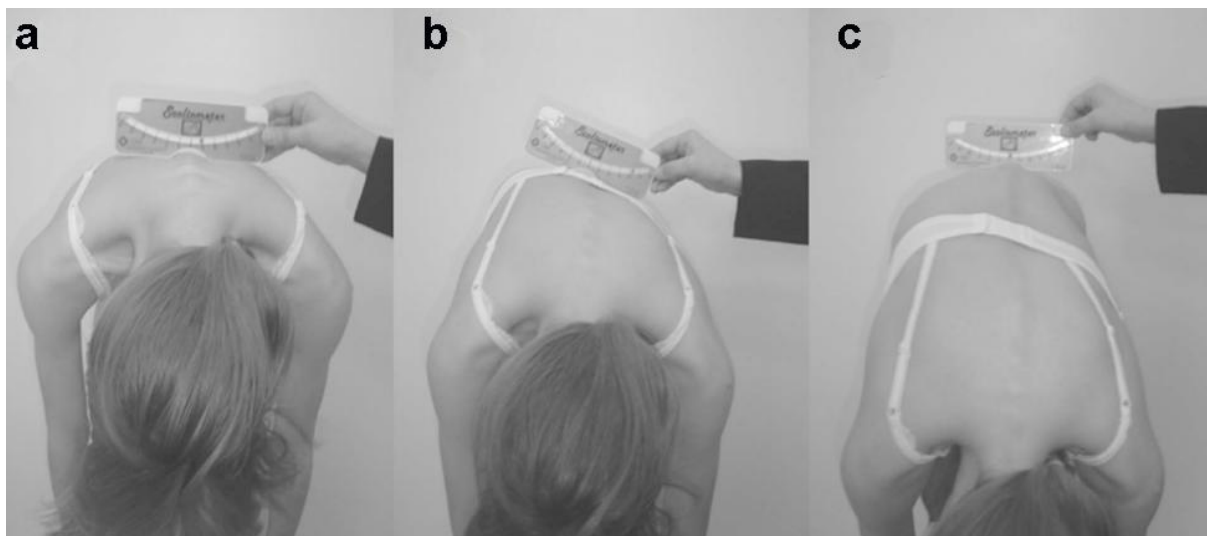


**Figure 2. 4 The use of Scoliometer:** to quantify the degree of trunk rotation, with the patient in a forward bending position (Kotwicki 2008).

The mandate for school-based screening program of AIS as a routine health service is highly controversial around the world. Due to the uncertainty of screening effects, national institutions and professional organizations in the different countries currently hold the opposite view with respect to the need for school-based screening program [34, 38-40]. Indeed, the clinical effectiveness of scoliosis screening program has been demonstrated in the early detection of AIS with a low referral rate for radiography [36, 41-45]. Furthermore, a large population-based cohort study with a 10-year follow-up supported the sustained effectiveness of scoliosis screening program of the patients with AIS [28].

#### **2.3.4 Assessment of AIS**

The diagnosis of AIS is by exclusion, and it is mandatory at the first evaluation to collect family and personal clinical history and perform a full medical and neurological exam. The

examiner needs to rule out the other causes of scoliosis, such as vertebral malformation, connective-tissue disorders (e.g., Marfan's syndrome), neurofibromatosis or other neuromuscular conditions [1-3].

The main assessment test in the clinical examination of patients with AIS is the Adam's forward bending test described as above. The test's positive predictive value varies since it is proportional to the degree of vertebral rotation and depends on the operator's experience. As a consequence of the Adam's test, the Scoliometer measures the rib hump as the angle of trunk inclination [3, 46, 47].

A major concern for AIS patients is the aesthetics problem. In this respect, the Trunk Aesthetic Clinical Evaluation (TRACE) scale has been recently proposed and validated: it's a 12 point scale based on a visual assessment of shoulders, scapulae, waist and hemithorax asymmetries [48]. Also the validated scales like the Walter-Reed and the Trunk Appearance Perception Scale (TAPS) have been proposed as the self-evaluation of asymmetric trunk of the patients with AIS [49].

Quality of life (QoL) and disability are other main aspects to be considered in the treatment of AIS patients [50]. A series of instruments (questionnaires) have been proposed to assess the QoL, such as the scoliosis specific questionnaires (SRS-22) [51-53], the Brace Questionnaire (BrQ) [54] and the Bad Sobernheim Stress Questionnaire (BSSQ) [55, 56].

Radiographic examination of scoliotic spine continues to be the main reference standard in a scoliosis clinic. On the basis of medical history and physical examination, the diagnosis of AIS is made by measuring the lateral curvature in the coronal plane of radiographic image

and is confirmed as the lateral curvature with a Cobb angle more than  $10^\circ$  while the patient is in a standing position [1]. Radiographic assessment of the vertebral rotation using Perdriolle's torsionmeter has been shown to be reproducible [57]. Based on the same principle, the application of Raimondi's tables or ruler makes the assessment easier and slightly more reproducible [57]. Furthermore, the Risser sign is assessed as an important parameter indicating the patient's growth or skeletal status [3].

### **2.3.5 Treatment of AIS**

The primary goal of treatment of AIS is to reduce the progression of curves, thereby to decrease the risk of secondary impairment, to relieve the back pain, to improve the functional mobility and the cosmetic deformities. Nowadays, the intervention modalities, such as the physical therapy, the orthotic intervention and the surgery have been advocated around the world [1, 2, 24, 30]. Physical therapy can be applied to prevent the aggravation of the deformity in the mild scoliosis (i.e., curves less than  $25^\circ$ ) and to enhance the effect of a brace and counteract its side-effects in the moderate scoliosis (i.e., curves between  $25^\circ$  and  $45^\circ$ ) [24, 58-60]. These aims are met, theoretically, by the individualized sports activities, the protocol of which should be designed on the basis of the patient's needs, the curve pattern, and the intervention phase. Based on the SOSORT 2012 Consensus Statement, it is recommended that the Physiotherapeutic Specific Exercise (PSE) increase the the coordination, the spinal proprioception, and the posture control of the patients with AIS. The appropriate exercise program will be regarded as the important step to prevent/limit the progression of AIS [24].

In addition, the orthotic intervention is preferred for the patient with a curve magnitude of  $25^\circ\sim 45^\circ$ , with the aim of arresting the curve progression below the level requiring the orthopaedic surgery [24, 61, 62]. Different orthotic designs have been proposed through the

modifications of the typical rigid thoracolumbosacral orthoses (TLSO), the basic principle of which is to restore the normal contour and alignment of the spine by means of the external forces [63]. The effectiveness of orthotic treatment in reducing the rate of surgical procedures required in AIS patients has recently been demonstrated in a multicenter randomized controlled trial [64].

Besides, the orthopaedic surgery is indicated when the scoliotic curve progresses greater than 45° in the patients with an immature skeleton [1, 2, 30]. The main purpose of surgical treatment is to achieve a maximum 3-D correction of spinal deformity and to restore the trunk asymmetry and balance, while minimizing the morbidity and pain [1, 2, 65]. Posterior or anterior instrumentations have been both applied in the surgery of scoliosis [66-68]. The use of the segmental pedicle screws in the thoracic spine allows even better three-column mechanical fixation, saving of fusion levels and reduction of risk of mid- to long-term complications as compared with the standard hook-wire constructs [69-71].

## **2.4 Imaging Assessment Methods of AIS**

The assessment of AIS requires a comprehensive imaging technique to fully reveal the 3-D spinal deformity. Medical imaging techniques play an important role in the diagnosis and assessment of the patients with AIS [3]. This section presents a literature review of the medical imaging techniques for AIS, including spinal radiography, stereoradiography (EOS), computed tomography (CT), magnetic resonance imaging (MRI) and surface topography. The assessment methods of these imaging techniques will be shown, followed by a discussion with regard to its reliability and validity.

### **2.4.1 Spinal Radiography**

Spinal radiography serves as the basic imaging assessment method to determine the curve type and severity of the patients with AIS [72, 73]. Frontal and lateral radiographs are commonly taken in the standing position. For the frontal plane radiograph, the postero-anterior projection is recommended due to the less ionizing radiation produced to the breasts and thyroid tissue as compared with the antero-posterior one. For the lateral plane radiograph, the upper limbs have to be taken away or the fists put on the clavicles, which allow adequate radiographic visualization of the lateral thoracic spine. Lateral images are indicative of the patients with low back pain or lumbar scoliosis, in order to identify if the spondylolisthesis occurs as a cause of the scoliosis [1]. In addition, digital radiography can provide a good image resolution, whereas the exposition seems to be reduced. A long cassette (90 cm) makes it possible to visualize the cervical, thoracic and lumbar spine as well as the pelvic [73].

#### **2.4.1.1 The assessments in the frontal radiograph**

The analysis of the frontal (coronal) radiograph often starts with drawing a central vertical sacral line (CVSL), passing through the center of the sacrum (Figure 2.5). The spinal curvature of scoliosis is harmonious and usually cross this line. In the frontal radiographic images, the accurate identification of the apical, upper- & lower-end vertebrae is essential for the assessment of scoliotic spine. The apical vertebra is the most distant from the CVSL, most rotated and deformed, but not titled. The upper- & lower-end vertebrae are located closely to the CVSL, most titled but least deformed and rotated [3] (Figure 2.5).



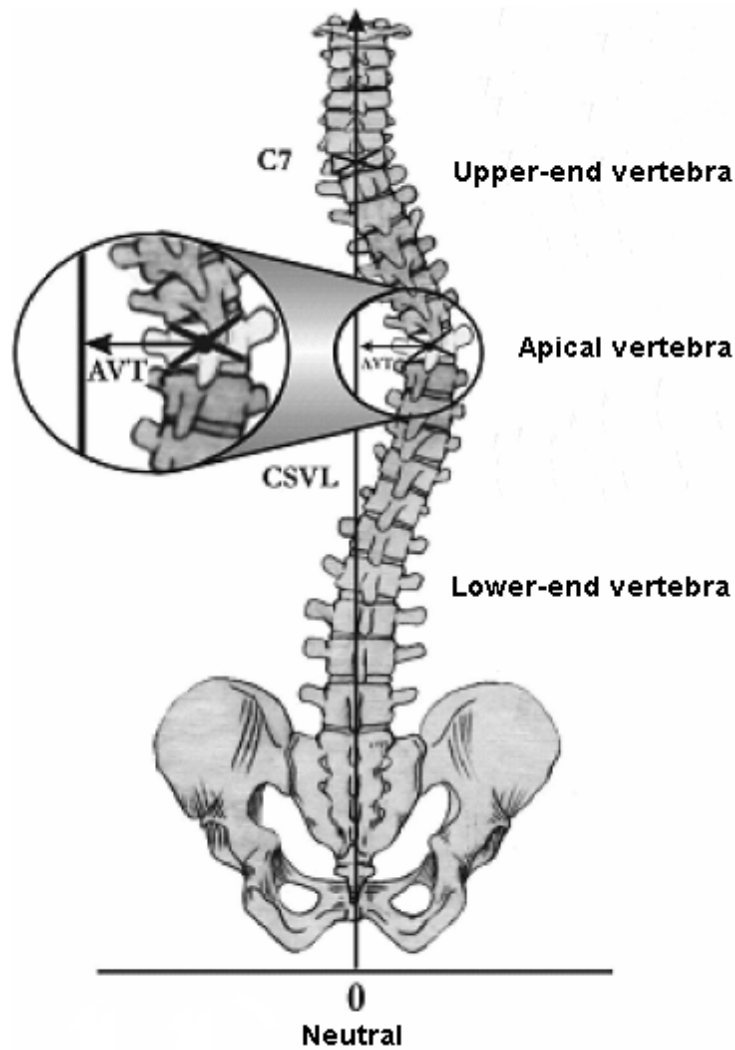


**Figure 2. 5 The analysis of the frontal radiograph.** Central vertical sacral line (CVSL), Upper-end vertebra, Lower-end vertebra and Apical vertebra (Kuklo et al. 2005).

### Curve magnitude

The curve magnitude is assessed by measuring the angle of scoliotic spine in the frontal (coronal) radiograph. Quantitative measurement of the curve magnitude is valuable for diagnose and monitor of the progression of scoliosis, as well as decision making of the treatment modalities for AIS [74]. The earliest method proposed to assess the curve magnitude is the Ferguson method, in which the angle is defined between the two straight

lines that connect the centers of the end vertebrae with the center of the apical vertebra (Figure 2.6 a). Similarly, the Cobb method was proposed, and the Cobb angle was measured as the angle between the lines parallel to the superior and inferior endplates of the upper-end and lower-end vertebrae of the curve (Figure 2.6 b). Due to the simple and reproducible measurement of the curve magnitude, the Cobb method was applied extensively in the clinical practice of AIS, even for the cases with severe spinal curvatures. In 1966, the Scoliosis Research Society (SRS) adopted the Cobb method as the standard reference for the quantification of the curve magnitude [74]. The diagnosis of scoliosis is defined on the basis of Cobb angle of 10 degrees or greater. There is a consensus that the difference of more than 5 degrees between the two radiographic measurements of Cobb angle was regarded as the clinical significance to detect the curve progression of scoliosis [1, 2]. The Cobb method, though simply in technique operation, is actually limited to reflect the extent of the tilt between the upper and lower end-vertebrae, neglecting the information of curve length or lateral translation of the apex [3]. In attempt to reflect the true curve magnitude of scoliosis as far as possible, many different methods were proposed by Diab et al., Chen et al. and Greenspan et al. [74] (Figure 2.6 c-e) .

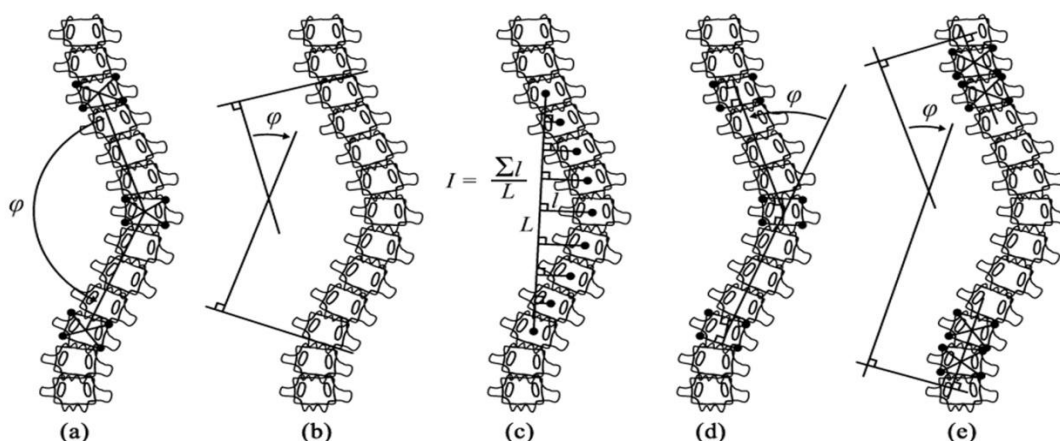


**Figure 2. 6 Measurements of curve magnitude in the frontal radiograph.** (a) Ferguson method (b) Cobb method (c) Greenspan index (d) Diab et al. method (e) Centroid method (Vrtovec T, 2009)

### **Cobb method: Reliability and Variability**

Since the Cobb method has been accepted as the standard reference, a number of studies have been conducted to investigate its reliability and variability, including the manual or digital methods when measuring the spinal curvature of the patients with AIS. Table 2.1 and 2.2 summarize the literatures regarding to the assessment of reliability and variability of the manual Cobb angle measurements in the radiographic images from the year of 2000 to 2017. The manual Cobb angle measurements presented good to excellent intra- and inter-rater reliability with the intra-class correlation coefficients (ICCs)>0.78 in the previous literatures (Table 2.1). In the case of the surgical patients with AIS, it is found that the preoperative Cobb angle measurement could be more reliable than the postoperative measurements, as evidenced by Kuklo's study. The analysis of variability was calculated as the mean absolute difference (MAD), standard deviation (SD) and standard error of measurement (SEM), above of which are commonly used in the related literatures. The results showed that the intra-rater MAD of the Cobb angle measurement ranged from 2.22° to 3.04° and the inter-rater MAD

varied from 3.35° to 3.85°. The reported intra-rater SD was from 2.23° to 4.12°, and the inter-rater SD was from 2.24° to 4.62° (Table 2.2).

**Table 2. 1 Results of reliability of manual Cobb angle measurements in radiograph**

Study	X-ray (Range)	Raters			Pre-defined	Intra-rater (ICC)	Inter-rater (ICC)
		No.	experience	trials			
Dang et al. 2005[75]	10 PA 20-45°	2	varying	5 x	-	>0.8	>0.8
Kuklo et al. 2005[76]	30 PA	3	senior	2 x	Yes	0.96	0.96
De Carvalho et al. 2007[77]	40 PA 20-45°	8	varying	2 x	-	0.97	0.939
Gstoettner et al. 2007[78]	48 PA 20-130°	6	senior	3 x	Yes	0.97	0.97
Gupta et al. 2007[79]	48 PA 10-40°	7	varying	-	Yes	0.78-0.98	0.991
Allen et al. 2008[80]	22 PA 20°-50°	3	varying	-	-	0.95	0.94
Mok et al. 2008[81]	20 PA 32-80°	4	senior	-	Yes	0.96	0.93
Tanure et al. 2010[82]	49 PA 12-80°	3	varying	3 x	-	0.96	0.95

Data are taken from the Result section of the articles

PA: posterior-anterior radiograph

ICC: intra-class correlation coefficient

CR: coefficient of reliability

**Table 2. 2 Results of variability of manual Cobb angle measurements in radiograph**

Study	X-ray (Range)	Raters			Pre- defined	Intra-rater	Inter-rater
		No.	experience	trials			
Facanha-Filho et al. 2001[83]	55 AP	7	varying	3 x	Yes	MAD:2.8° 95% CI: ±3°	MAD:3.35° 95% CI: ±7.86°
Kuklo et al. 2005[84]	60 PA	2	-	2 x	-	MAD: 2.87° 95%CI: 2.35° -3.38°	
De Carvalho et al. 2007[77]	40 PA 20-45°	8	varying	2 x	-	MAD: 2.22°~2.63° SD: 2.23°~2.24°	MAD: 3.43°~3.59° SD: 2.24°~3.42°
Allen et al. 2008[80]	22 PA 20-50°	3	varying	-	-	SEM: 2.185°	SEM: 3.17°
Mok et al. 2008[81]	20 PA 32-80°	4	senior	-	Yes	SD: 4.12°	SD: 4.62°
Tanure et al. 2010[82]	49 PA 12-80°	3	varying	3 x	-	MAD: 3.04° SD: 2.43°	MAD: 3.85° SD: 3.45°

Data presented are taken from the Result section of the articles.

AP: anterior-posterior radiograph; PA: posterior-anterior radiograph

MAD: mean absolute difference

SD: standard deviation

95% CI: 95% confidential limit

SEM: standard error of measurement

The factors which may influence the variability of the Cobb angle measurements have been reported to be depended mainly on the raters' experience, measurement error, range of curve

magnitude and image quality. Additionally, the pre-defined apical vertebra and end-vertebrae would be expected to reduce the variability when measuring the Cobb angle in radiographs. Nevertheless, the reported results didn't demonstrate that the pre-defined apical and upper & lower end-vertebrae could reduce the raters' error and the variability when measuring the Cobb angle. In addition, the intra- and inter-rater variability of the measurement of Cobb angle was found not to be associated with the raters' experience. It is opposite to the results obtained from the Facanha-Filho's study, in which the raters' experience was regarded as the key factor to minimize the measurement error.

The sources of errors of the manual measurements of Cobb angle have been summarized, including the selection of end-vertebral, drawing of variable best-fit lines to the vertebral endplates, bias of the different raters, inaccurate protractors, image acquisition techniques, patient positioning, and acquisition time. It has been shown that the variation of the manual Cobb angle measurements was roughly 9 degrees between the supine *versus* the standing postures of the patients with AIS; mean difference of 2.4 degrees between the antero-posterior and the posteroanterior radiographs; average increase of 5.2 degrees from morning to afternoon acquisition.

Compared with the manual Cobb angle measurement, the digital or computer-assisted methods are less sensitive to the raters' skill levels or experiences. As the digital radiographic images become available in the clinical setting, clinicians are required to perform the Cobb angle measurements by means of the computerized tools and related software. Table 2.3 and 2.4 summarize the reliability and variability of the digital or computer-assisted measurements of the Cobb angle during the past ten years. The results showed that the intra-rater reliability determined by the ICC value was within 0.76 to 0.985 and the inter-rater reliability from 0.70

to 0.988 (Table 2.3). As shown in Table 2.4, the intra-rater mean absolute difference (MAD) of the computer-assisted Cobb angle measurements ranged from 1.2° to 3.4° and the inter-rater MAD from 1.22° to 3.71°; the intra-rater standard deviation (SD) varied from 1.2° to 6.45° and the inter-rater SD from 1.8° to 4.9°; the intra-rater standard error of measurement (SEM) from 0.739° to 3.18° and inter-rater SEM from 1.22° to 3.71°. Taking into account the different regions of spine, the intra- and inter-rater reliability of Cobb angle measurement using the computerized tools were better in the main thoracic and thoracolumbar/lumbar curves than those in the proximal thoracic curve; the average intra- and inter-rater SD were lower in the proximal thoracic curve than those in the main thoracic and thoracolumbar/lumbar curves.

The comparison of the Cobb angle measurements using the manual and computer-assisted methods has been studied during the past ten years. It has been shown that the reliability was similar between these two measurement methods of the Cobb angle. Although the digital radiographic images did not improve the measurement accuracy, the computer-aided techniques have more advantages when measuring the Cobb angle of scoliotic spine in the clinical practice, such as the fast and efficient storage of images, the improved quality of radiographic images, the easy access to the comparison and follow-up, as well as the automated interpretation of data. Chockalingam et al. [85] developed a computer-aided method of the Cobb angle measurement, in which the vertebral edges were required to be assigned manually and the curvature angle would be calculated automatically by the relevant programs. The accuracy of Chockalingam's method depended on how well the edges of the vertebrae were identified. Allen et al. also proposed a computer-assisted program based on active shape models. During the Cobb angle measurement, this program was able to recognize the specific contour of the vertebrae in the radiographic images on the basis of the

inputted information of characteristics of vertebra in a series of sample images. However, this measurement was not accurate for the curve magnitude more than 40°. To minimize human involvement, a computer-aided system based on the Fuzzy Hough Transform was developed by Zhang et al.[86] to automatically detect the directions of the end-vertebrae from which the Cobb angle was then calculated. In this automatic system, the end-vertebrae could be selected by the method through the fixed regions of interest (ROI), in which ROI flexibly fit to the boundary of the vertebra better. The intra- and inter-rater measurement errors were reported to be less than 2° for ROI-mediated Cobb angle measurement.



**Table 2. 3 Results of reliability of digital Cobb angle measurements in radiograph**

Study	X-ray (Range)	Raters			Pre- defined	Intra-rater (ICC)	Inter-rater (ICC)
		No.	experience	trials			
Chockalingam et al. 2002[85]	9 PA	10	varying	3 x	-	0.985	0.988
Kuklo et al. 2005[87]	60 PA	3	-	2 x	Yes	0.887 (post-operation)	0.85 (post-operation)
Gstoettner et al. 2007[78]	48 PA 20-130°	6	senior	3 x	Yes	0.96	0.93
Srinivasalu et al. 2008[88]	318 AP	3	varying	-	Yes	0.969	0.986
Allen et al. 2008[80]	22 PA 20-50°	3	varying	-	-	0.935 (Active shape model)	0.91 (Active shape model)
Mok et al. 2008[81]	20 PA 32-80°	4	senior	-	Yes	0.87	0.96
Mehta et al. 2009[89]	318 AP	3	varying	2 x	Yes	0.978	0.986
Zhang et al. 2010[86]	70 PA <90°	3	varying	2 x	Yes	0.962 0.994 (fuzzy hough transform)	0.929 0.985 (fuzzy hough transform)
Tanure et al. 2010[82]	49 PA 12-80°	3	varying	3 x	-	0.97	0.96
Aubin et al. 2011[90]	32 PA 9-88°	3	varying	2 x	-	0.76 (Proximal thoracic) 0.95 (Main thoracic) 0.92(Thoracolumbar/lumbar)	0.7 (Proximal thoracic) 0.94 (Main thoracic) 0.93(Thoracolumbar/lumbar)
Chan et al. 2014[91]	60 PA 10-44°	3	varying	2 x	-	0.98	0.94

Data taken from the Result section of the articles

AP: anterior-posterior radiograph; PA: posterior-anterior radiograph

ICC: intra-class correlation coefficient.

**Table 2. 4 Results of variability of digital Cobb angle measurements in radiograph**

Study	X-ray (Range)	Raters			Pre- defined	Intra-rater	Inter-rater
		No.	experience	trials			
Chockalingam et al. 2002[85]	9 PA	10	varying	3 x	-	SEM: 0.739°	SEM: 1.22°
Kuklo et al. 2005[87]	60 PA	2	senior	2 x	-	MAD: 2.80° 95%CI: 2.43° -3.16°	
Stokes and Aronsson 2006[92]	27 PA 45-105°	5	varying	3 x	-	SD: 2.0° (Main thoracic) SD: 2.0° (Thoracolumbar/lumbar)	SD: 2.5° (Main thoracic) SD: 2.6° (Thoracolumbar/lumbar)
Allen et al. 2008[80]	22 PA 20-50°	3	varying	-	-	SEM: 3.18° SEM: 2.005° (Active shape model)	SEM: 3.71° SEM: 2.37° (Active shape model)
Mok et al. 2008[81]	20 PA 32-80°	4	senior	-	Yes	SD: 6.45°	SD: 3.82°
Zhang et al. 2010[86]	70 PA <90°	3	varying	2 x	Yes	MAD: 3.4° MAD: 1.4° SD: 1.2° (fuzzy hough transform)	MAD: 5.1° MAD: 2.2° SD: 1.8° (fuzzy hough transform)
Tanure et al. 2010[82]	49 PA 12-80°	3	varying	3 x	-	MAD: 2.79° SD: 2.23°	MAD: 3.61 SD: 3.18°
Aubin et al. 2011[90]	32 PA 9-88°	3	varying	2 x	-	SD:2.1° (Proximal thoracic) SD:3.5°(Main thoracic) SD:4.2°(Thoracolumbar/lumbar)	SD: 2.8°(Proximal thoracic) SD:4.9° (Main thoracic) SD:4.4°(Thoracolumbar/lumbar)
Chan et al. 2014[91]	60 PA 10-44°	3	varying	2 x	-	MAD: 1.2° SD: 1.3° SEM: 1.26°	MAD: 2.2° SD: 1.9° SEM: 2.06°

Data is taken from the Result section of the articles.

PA: posterior-anterior radiograph

MAD: mean absolute difference

SD: standard deviation

95% CI: 95% confidential limit

SEM: standard error of measurement

### **Vertebral Rotation**

The vertebral rotation is an important parameter of the deformity in AIS, which can be used to assess the severity of scoliotic spine, to monitor the risk of curve progression, and to evaluate the outcome of treatments [57]. It is also associated with the lateral curvature and the ribcage asymmetry, leading to reduced respiratory capacity and cosmetically disfiguring rib hump of the patients with scoliosis [93, 94]. Thus, the accurate and reliable measurement of the vertebral rotation is of key significance in the prognosis and intervention of scoliotic curves.

Several methods have been proposed to assess the vertebral rotation using radiographic images, based on the position of the projected spinous process (Cobb method) or pedicles shadows (Nash and Moe, Perdriolle, Drerup, Stokes method) in relation to the vertebral body [57, 95]. However, the measurements taken from radiographic images only represent a projected rotation, which is not directly measured in the transverse plane. The Figure 2.7 summarized the radiographic methods of measurement of the vertebral rotation. The first documented method has been proposed by the Cobb, in which the five grades of vertebral rotation can be determined by dividing the vertebral body into six segments and then identifying which segment is located by the spinous process. However, the Cobb method is only able to provide an approximation but not a quantification of the angle of vertebral rotation. In addition, the Nash-Moe method has been modified on the basis of the Cobb method. This method describes the percentage of the displacement of the convex pedicle with respect to the vertebral body width. However, the shape and symmetry of the vertebral body are neglected in this method, leading to the variability of the measurement results. To overcome this issue, Stokes et al. has proposed that the vertebral rotation could be assessed by the position of the pedicles relative to the vertebral body center, in combination with the

parameters of the vertebral shape, i.e., the actual distance between the pedicles and the vertebral body center. Furthermore, the specific torsionmeter has been developed by Perdriolle and Vidal to measure the vertebral rotation angle directly from the center of the inner pedicle. The edges of the torsionmeter are aligned with the inner points on the vertebral margin; the degree of the rotation angle is then read from a vertical line drawn through the convex pedicle. The torsionmeter is marked with a scale of  $5^\circ$  increments, which is also the minimum variation when measuring the vertebral rotation in the patients with AIS. Despite this disadvantage, the Perdriolle method has been reported to be a precise and simple method, making it applicable in the clinical setting.

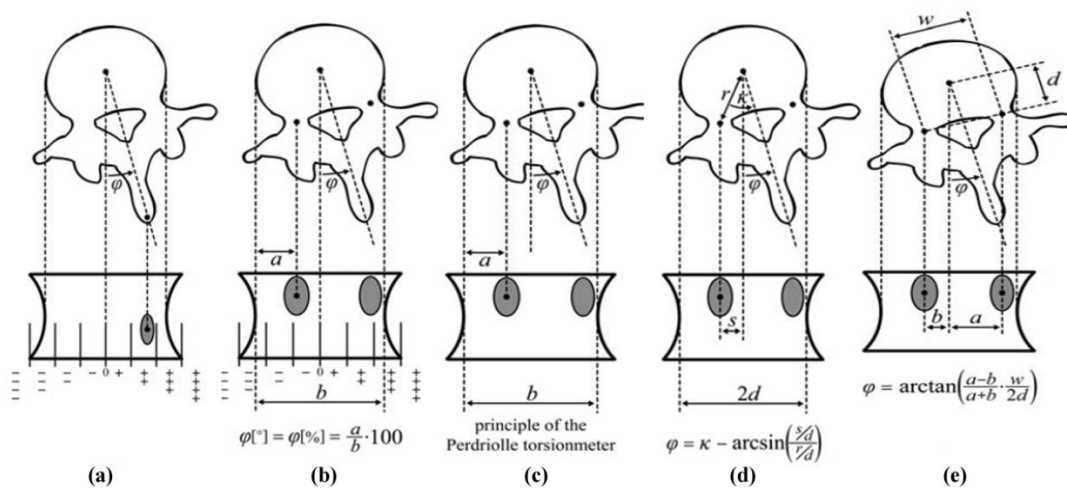


**Figure 2. 7 Methods of vertebral rotation measurements in radiograph.** (a) Cobb method. (b) Nash-Moe method. (c) Perdriolle method. (d) Drerup method. (e) Stokes method. (Vrtovec T, 2009)

Tables 2.5 and 2.6 summarized the results of reliability and variability of the radiographic measurements of the vertebral rotation from the literature during the past ten years. The intra- and inter-rater reliabilities (ICC values) were reported to be within 0.53 and 0.84 for the

Nash-Moe method when measuring the vertebral rotation between the pre- and post-operation of the scoliosis patients. As shown in Table 2.5, the Drerup method presented the intra-rater reliability of ICC value 0.743 for the manual measurement, compared to the 0.821 for the computer-assisted measurement through the fuzzy hough transform model. This computer-assisted program improved the intra- and inter-rater reliability of the Drerup method when assessing the vertebral rotation in the patients with AIS. The same research team found that the fuzzy hough transform model could also increase the intra- and inter-rater reliability of the measurements of the vertebral rotation using the Stokes method.

As shown in Table 2.6, the mean absolute difference (MAD) of the Nash-Moe method was  $0.23^\circ$  and  $0.43^\circ$  for the manual and digital measurement procedures, respectively. The results indicated that the digital radiographic measure of vertebral rotation demonstrated to be less variable than the manual measures using the Nash-Moe method. It has been suggested that the variability of measurement could be reduced by means of the computer-assisted program, i.e., the fuzzy hough transform model, when measuring the vertebral rotation through the Drerup method or the Stokes method. Based on the fuzzy hough transform program, the measurement error varied from  $1.7^\circ$  to  $4.1^\circ$  for the Drerup method, and  $1.5^\circ$  to  $3.1^\circ$  for the Stokes method.

**Table 2. 5 Results of reliability of vertebral rotation measurements in radiograph**

Study	X-ray (Range)	Raters			Pre- defined	Procedure	Intra-rater (ICC)	Inter-rater (ICC)
		No	experience	trials				
Kuklo et al. 2005[76]	30 PA	3	senior	2 x	Yes	Manual (Nash-Moe method)	0.84(pre-operation)	0.59(pre-operation)
							0.63(post-operation)	0.53(post-operation)
Kuklo et al. 2005[84]	60 PA	3	varying	2 x	Yes	Digital (Nash-Moe method)	0.81(pre-operation)	0.59(pre-operation)
							0.63(post-operation)	0.53(post-operation)
Zhang et al. 2010[86]	70 PA <90°	3	varying	2 x	Yes	Digital (Drerup method)	0.743	0.692
							0.821 (fuzzy hough transform)	0.809 (fuzzy hough transform)
						Digital (Stokes method)	0.803	0.756
							0.857 (fuzzy hough transform)	0.826 (fuzzy hough transform)
Abul- Kasim et al. 2010[96]	25 Lateral 32.7-83°	1	senior	2 x	Yes	Digital (Perdriolle method)	0.76	
Chan et al. 2014[91]	60 PA 10-44°	3	varying	2 x	-	Digital (Stokes method)	0.95	0.87

Data is taken from the Result section of the articles

PA: posterior-anterior radiograph

ICC: intra-class correlation coefficient.

**Table 2. 6 Results of variability of vertebral rotation measurements in radiograph**

Study	X-ray	Raters			Pre-defined	Procedure	Intra-rater	Inter-rater
		No.	experience	trials				
Kuklo et al. 2006[87]	60 PA	2	varying	2 x	-	Manual (Nash-Moe method)	MAD: 0.23° 95% CI:0.14° -0.31°	
						Digital (Nash-Moe method)	MAD: 0.43° 95% CI:0.33° -0.52°	
Zhang et al. 2010[86]	70 PA <90°	3	varying	2 x	Yes		MAD: 3.0°	MAD: 4.1°
						Digital (Drerup method)	MAD: 1.7° SD: 1.6° (fuzzy hough transform)	MAD: 2.7° SD: 2.6° (fuzzy hough transform)
							MAD: 2.5°	MAD: 3.1°
						Digital (Stokes method)	MAD: 1.5° SD: 1.1° (fuzzy hough transform)	MAD: 2.3° SD: 1.9° (fuzzy hough transform)
Abul-Kasim et al. 2010[96]	25 Lateral 32.7-83°	1	senior	2 x	Yes	Digital (Perdriolle method)	MAD: 1°	
Chan et al. 2014[91]	60 PA 10-44°	3	varying	2 x	-	Digital (Stokes method)	MAD: 1.9° SD: 2.1° SEM:1.97°	MAD: 3.2° SD: 3.1° SEM: 3.01°

Data is taken from the Result section of the articles

PA: posterior-anterior radiograph

MAD: mean absolute difference

SD: standard deviation

95% CI: 95% confidential limit

SEM: standard error of measurement

### *Curve flexibility*

Curve flexibility is a valuable indicative parameter used to provide the information of the structural changes of the major and compensatory curves. The measurement of curve flexibility is crucial in the estimation of the orthotic and surgical treatment outcomes, the determination of the level to be instrumented, and the amount of the correction to be achieved. Optimal positions used in the assessment of curve flexibility have been investigated to improve the accuracy of predication. Various positions have been devised to evaluate the pre-orthotic and pre-operative curve flexibility, including the standing or supine side-bending [97, 98], push-prone, traction (with or without general anesthesia) [99-102], and fulcrum-bending radiographs (FBR) [103, 104].

Currently, supine side-bending radiographs are the most commonly used methods to determine the curve flexibility because of its ease of use and role in curve classification. However, with the advance of segmental spinal instrumentation techniques, especially like the utilization of pedicle screw, supine side-bending flexibility radiographs gradually lost the ability to predict the correction accurately [103, 104]. Additionally, lack of standardization in the operation procedure is another limitation of the supine side-bending radiographic assessment of the curve flexibility.

Push-prone radiographic imaging, originally described by Kleinman et al., can reveal the changes of the structural and compensatory curves on the same radiograph, but fall short of predicting the comparative correction in the recent studies. Besides, radiographic imaging through the traction under general anesthesia (UGA) is a relatively new technique firstly reported by Davis et al. [99]. It has been reported that the radiographs obtained using the



traction with UGA were better at predicting the maximum curve flexibility; especially in the cases with the Cobb angle  $> 65^\circ$  and the rigid curves [99-102].

Fulcrum-bending radiographs (FBR), developed by Cheung and Luk, have been demonstrated to reflect the flexibility of thoracic curves more accurately, and the proposed fulcrum-bending correction index (FBCI) was better at predicating the correction rate [105, 106]. An innovative FBR technique was introduced by Li et al., who applied the maximal weight to the curve apex in order to attain the maximum heights lifted. The results showed that the flexibility assessed by this modified FBRs approximated the postoperative correction more closely from posterior pedicle screw instrumentation than that from the traditional FBR or supine side-bending radiographs [103]. Therefore, the modified FBR with combining the traction and translation forces will be more applicable in the era of modern segmental spinal instrumentation [104].

#### **2.4.1.2 The Assessments in the Lateral Radiograph**

The analysis of the lateral radiograph refers to the measurement of cervical lordosis, thoracic kyphosis and lumbar lordosis, as well as pelvic incidence. However, the measurement taken in the lateral (sagittal) radiograph is more difficult than that in the frontal one, because the scoliotic deviation is superposed on the normal lateral (sagittal) curvatures [3, 107]. The assessment of sagittal profile is also of great value in providing reference for bracing and surgical intervention [1]. The thoracic kyphosis and lumbar lordosis are measured with the angles using the Cobb method, in which the vertebral endplate lines are used to construct the angles in the sagittal radiographs. However, the kyphotic and lordotic angles estimated by the Cobb method predominantly reflect the angle of the upper- and lower-end vertebral inclination, but not the corresponding angle of the regional curvature [108]. In order to

explore the local disturbances of thoracic kyphosis, the segmental sagittal analysis are undertaken by the Cobb method. The segmental curvature could be measured by the angle between the lines of the upper- and lower-end vertebrae in the corresponding regions in the sagittal plane [109, 110]. Besides, the pelvic incidence can be assessed in the lateral radiograph as proposed by Duval-Beaupere. The angle of the pelvic incidence is estimated between the line perpendicular to the upper plate of the first sacral vertebra, and the line connecting the center points of the first sacral vertebra and the bi-coxo-femoral axis [111-113].

#### **2.4.1.3 Estimation of Skeletal Maturity**

The determination of skeletal maturity is crucial in the management of patients with AIS. Based on the extent of the skeletal maturity, the decision whether to use the excise, orthotic treatment or surgical intervention could be made to control the curve progression [1, 2]. One of the most frequently used methods to determine the skeletal maturity is described as the Risser sign. Six stages of the skeletal development could be assessed from zero to five, denoting the extent of ossification of the apophysis from the antero-lateral to the postero-medial aspect of the iliac crest [114]. The absence of ossification of the iliac crest is defined as the Risser Grade 0. Ossification within the first quarter of the iliac crest (0–25%) is defined as the Risser Grade I. Ossification extending the second quarter of the iliac crest (25–50%) is recorded as the Risser Grade II. The Risser Grade III represents that the ossification progresses into the third quarter (50–75%) while the Grade IV is defined as the ossification into the fourth quarter of the iliac crest (>75%). Complete fusion of the apophysis to the ilium is rated as the Risser Grade V [115].

#### **2.4.1.4 Other Application of Radiographic Assessments**

Currently, various innovative applications of the radiographic measurements have been investigated to improve the management of the patients with AIS. To reduce the measurement error from the different observers (raters), the axis-line-distance technique (ALDT) has been proposed [116]. It has been reported that ALDT method may be applicable for the therapeutic evaluation of scoliosis during treatment and at follow-up visits due to no significant differences between the observers when measuring the change of the spinal curvature angles [117]. For the postoperative measurement of the apical vertebral rotation, a novel method based on the inter-rod distance in the lateral and posteroanterior radiographic images has been developed and validated by a high correlation with the computed tomography [118]. For the outcome measures of treatment in the early onset scoliosis, the measurement of the pelvic inlet width (PIW) in the radiographic images is useful for predicting the individual, age-independent thoracic dimensions, which are related to cardiopulmonary dysfunction [119]. To estimate the segmental movement, Noh et al. developed a novel computational method to calculate the linear displacement of pedicles from the target segment precisely [120].

The hazardous effect of radiography is associated with the frequent and prolonged exposure to radiation, which has been of primary concern for scoliotic patients often undergoing the critical growth and the developmental stages [6]. Consequently, there has been growing emphasis on developing new technologies that do not involve patients' exposure to the ionizing radiation. Despite this disadvantage of radiography, the measurements taken from the radiographic methods remain the standard reference, to which the current developing techniques will compare for validating their validity.

## **2.4.2 Stereoradiography**

### **2.4.2.1 Biplanar X-ray Imaging System**

The attempts to reduce the radiation exposure of the conventional radiography and reconstruct the accurate 3-D image of spine have led researchers to develop new technologies in the assessment of scoliosis, such as the relatively low-dose stereoradiography (EOS). EOS is a biplanar X-ray imaging system, in which the slot scan technology is applied to take the posteroanterior and lateral radiographic images simultaneously, allowing the reconstruction of a three-dimensional model of spine [121] and rib cage [122]. The upright weight bearing position is required in the EOS images acquisition, with the benefit of allowing the spinal visualization in a manner consistent with the conventional X-ray methods when assessing the scoliotic spine [123]. In addition, the EOS involves only a fraction of the radiation exposure of the conventional radiography. The dosage for the whole spine could be reduced to between 1/6 and 1/9 of the standard doses [6], while delivering the images of the full length of body, especially for a lateral image of the pelvic girdle, which can enhance our knowledge of the pelvic-spinal balance [124, 125]. Taken together, the weight-bearing upright position, the minimal radiation exposure, and the full imaging acquisition of spine and pelvis raised the potential use of the EOS for the 3-D assessments of the patients with AIS.

### **2.4.2.2 Reliability and Variability of EOS Measurements**

The intra- and inter-rater reliability of the 3-D measurements of AIS obtained by the EOS imaging have been demonstrated to be good for the cases with mild [121], moderate [126] and severe [123] scoliotic curves. The mean absolute difference of the 3-D EOS measurements varied between 4° and 6° for the spine curves, between 1° and 4° for the pelvic parameters, and between 2° and 4° for the vertebral rotation [121, 127]. Due to the severity of the curve, the precision of the corresponding parameters measured would be slightly

increased by no more than 1°. In addition, Somoskeoy et al., found that the intra- and inter-rater reliability would be higher for the EOS 3-D imaging than the 2-D radiography in the assessments of scoliotic curvature in the coronal and sagittal planes [128]. Furthermore, it has been also indicated that the 3-D postoperative reconstruction of the scoliotic spine could be as reproducible as the 3-D preoperative ones using the EOS imaging. The reproducibility was not affected by the type of implant used for the surgical correction. Moreover, the reconstructed accuracy of the EOS imaging has also been demonstrated in the shape, position, and orientation of each vertebra and the entire spine [123]. Overall, these results of studies provide the evidence pertaining to the EOS imaging technology that may aid in the clinical diagnosis and assessments for the patients with AIS.

#### **2.4.2.3 Other Application of EOS Assessments**

Recently, the 3-D reconstruction of the spine and rib cage by the EOS imaging has been validated in the healthy volunteers, the patients with early onset scoliosis undergoing the growing rod procedures [129], and the patients with AIS treated by the bracing [126] or the surgery [130]. In addition, EOS imaging could be used to predict the restrictive respiratory impairment by the spinal penetration index (SPI) and to determine the progression risk of mild scoliosis based on the parameters in the transverse plane of spine [125]. At the same time, a series of innovative programs have been developed to promote the efficient and effective utilization of the EOS imaging, such as the deformable articulated model [131] and the introduced vertebra vectors [130, 132].

### **2.4.3 Computed tomography**

#### **2.4.3.1 Measurement of Vertebral Rotation and Distortion**

Computed tomography (CT) enables the direct visualization of the transverse plane of vertebrae, which can facilitate to assess the vertebral rotation and distortion [133]. The methods used to measure the vertebral rotation through the CT scans include Aaro-Dahlborn, Ho, Krismer and Gocen, Haughton, Adam-Askin, Kouwenhoven, and Vrtovec. Among these methods, the Aaro-Dahlborn and Ho methods are widely applied in the scoliosis clinic [134, 135]. The computerized program was developed by the Forsberg et al's research team to achieve the fully automatic measurement of vertebral rotation using the Aaro-Dahlborn method in the transverse plane of CT images [136]. Based on the measurement of vertebral rotation, the vertebral distortion could be measured by comparing the rotation degrees between the anterior and posterior components of the scoliotic curves [137].

Besides, the spinal curvature could be also measured in the coronal plane of the reformatted CT images. The Cobb angles measured in the reformatted coronal CT images have been verified with the measurements in the frontal radiographs. Therefore, the CT imaging could allow the assessments of scoliotic deformity in the both coronal and transverse planes with the same dataset, avoiding the changes of the spinal geometry between the standing and supine positions [138].

#### **2.4.3.2 Assessment of Pedicle Morphology**

Measurement of vertebral rotation in the CT images has been demonstrated to be feasible in the prone position, which is identical to that the surgeons usually are faced with on the operating table [96]. In addition, CT images can provide the information of the pedicle morphology, which is considered as another important factor involved in the surgical correction of scoliotic spine. Gstoettner and colleagues reported that the measurement of pedicle dimensions is time-consuming but reliable using the 3-D CT imaging, especially for

the special cases with the anatomic vertebral structure unclear in the radiographic images [139]. Furthermore, Kuraishi et al. explored the possibility of using the CT-based navigation system to calculate the pedicle diameter, which is narrower on the concave side of the scoliotic spine than on the convex side. The application of the CT-based navigation system would provide the guidance for the surgeon when inserting the pedicle screw on the concave side of the patients with the AIS [140].

#### **2.4.3.3 Evaluation of Pulmonary Capacity**

Reduced pulmonary capacity is a complex issue to be treated in the scoliosis patients with the severe curves. It has been shown that the CT-based volumetric reconstruction technique could reconstruct the pulmonary system of the patients with AIS and evaluate the change of the lung volume on the concave and convex sides of the scoliotic spine [141, 142]. The CT-based volumetric reconstruction technique revealed that the severity of curve magnitude and apical vertebral rotation could restrict the lung volume on the concave side considerably than that on the convex side, and there would be an inverse correlation between the kyphotic angle and the convex to concave lung volume ratio [142]. The similar results were reported by Adam and colleague, who investigated the correlation of the rotation of the thoracic curves with the lung volume in the patients with AIS using the advanced CT-based volumetric reconstruction technique [141].

#### **2.4.3.4 Other Application of CT Assessments**

The development of CT imaging allowed for the 3-D evaluation of volumetric bone mineral density and bone micro-architecture of the scoliosis patients, as discussed in the high-resolution peripheral quantitative computed tomography [143] and the micro-computed tomography [144]. Besides, in order to overcome the drawback of CT imaging with high

radiation does, the innovative CT imaging system with low radiation does is under the research for the evaluation of the patients with AIS [145].

#### **2.4.4 Magnetic resonance imaging**

##### **2.4.4.1 Three Dimensional Assessments of Vertebrae**

Magnetic resonance imaging (MRI) could provide the high-quality 3-D images of the vertebrae with non-ionizing radiation. In the coronal plane of MRI images, the spinal curvature angle is measured using the Cobb method. Even though the MRI tends to underestimate the Cobb angle by 10° on average, there is a strong positive correlation between the MRI and radiograph on the lateral curvature measurements [146]. In the sagittal plane, MRI could assess the kyphotic and lordotic angles using the Cobb method, the results of which are superior to the radiographic assessments for the upper thoracic region [147]. In the transverse plane, it is easy for MRI to measure the vertebral rotation through the methods which are similar to the CT measurements.

However, the main issue of MRI assessments is the scanning position. During the MRI scanning, the patients with AIS are often required to lie in the MRI scanning table, which is different from the position used in the radiography. The horizontal position would eliminate the effect of the gravity force and the postural reflexes on the scoliotic spine, leading to the corresponding change of the 3-D measurements of MRI. Hence, the axially loaded MRI has been proposed by means of a compression device to overcome the difference resulted from the horizontal position and simulate the imaging of spine in the standing position [148]. Several studies reported that the Cobb angles measured by the supine MRI with the axial loading were highly correlated with the measurements by the standing radiograph [149]. Little et al. revealed that the difference existed mainly in the curve magnitude rather than in



the vertebral rotation or the intra-vertebral rotation between the unloaded and loaded MRI measurements [149]. Recently, Diefenbach and colleague explored the application of the upright MRI in the assessments of the patients with scoliosis. Compared with the standing radiographic measurements, the upright MRI could produce the similar measurements of the lateral curvature in the coronal and sagittal planes [150]. However, the measurement of axial vertebral rotation of the upright MRI is still not well understood.

#### **2.4.4.2 Detection of Abnormality of the Neural Axis**

The MRI imaging could also play an important role in detecting the abnormality of the neural axis, thus being clinically applicable for the preoperative assessment. The Chiari malformation, the syringomyelia, the tethered spinal cord and diastematomyelia will be suspected if the patients with idiopathic scoliosis are found to have some indications, such as onset before 10 years of age, abnormal neurological examination, unusual curve pattern, and severe pain [151].

#### **2.4.4.3 Other Application of MRI Assessments**

The various applications of MRI assessments have been proposed to improve the knowledge and management of scoliosis, including the measurements of pedicle diameter [152-155], pulmonary function [156-158], vertebral disc characteristics [159-161] and rotation of spinal cord [162].

The measurement of pedicle morphology could assist the surgeon to select the appropriate screw sizes [153, 156]. In contrast with other methods, MRI seems to be superior in that it could ensure the acquisition of the transverse images which are parallel to the superior endplate of each vertebra [156]. The pedicle morphology in the scoliotic spines differs from

those in the normal spines. The study of Rajwani et al. didn't indicate whether the pedicle would grow longer on the convexity or the concavity [154]. In addition, Parent et al. and Catan et al. both suggested that the pedicle width was significantly diminished on the concave side of the scoliotic curves [153, 155]. Similar results have been reported that the pedicle width measured by MRI images were significantly thinner on the concave side than on the convex side in patients with AIS [152].

With the advent of ultrafast dynamic breath-hold MRI and multi-planar reformat technique, the lung volume, chest wall, and diaphragmatic motions between the inspiration and expiration phases could be measured with a high reliability in the subjects with or without AIS [157]. The ultrafast dynamic breath-hold MRI revealed that the impaired pulmonary function might be attributed to the limited chest wall motion in the patients with AIS [156]. Chu and colleague have demonstrated the effective role of the posterior spinal fusion on the lateral chest wall and diaphragmatic motions by means of the ultrafast dynamic breath-hold MRI in the patients with severe scoliosis, even though there was not significantly change in the lung volumes after surgery [158].

The characteristics of the vertebral disc of the scoliotic spine could be reflected by the MRI imaging. Birchall et al. demonstrated that the mechanical torsion between the vertebral bodies and discs contributed to average 45% of the overall deformity in the transverse plane of the MRI images [163]. In addition, the 3-D geometrical properties of intervertebral discs could be revealed by the MRI imaging, such as the location of disc centers, the nucleus pulpous as well as the ratio between the nucleus pulpous volume and the disc volume. The results of MRI observations suggested that there was no significant relative volume variation in the whole spine except at the apex of the scoliotic curvature [159]. Furthermore, MRI imaging

was used to investigate the relationship of vertebral disc characteristics with pain of the patients with AIS. The results showed that the discogenic pain would commonly happen at the apex of curvature or at the proximal lumbar levels in the adult scoliosis [160]. Gervais et al. introduced a novel MRI method which could discriminate between the scoliosis and spondylolisthesis by detecting the change of distribution of the MRI signal intensity in the special indices [161].

## **2.4.5 Surface topography**

### **2.4.5.1 Various Surface Topography Systems**

Different surface topography systems have been developed in the assessments and follow-up examinations of the patients with scoliosis as well as other spinal deformities. The core technologies involved in the different systems including moiré technology and raster stereography. Moiré technology was one of the earliest forms of surface topography. The contour of the back surface could be analyzed in light of the distortion that occurs when a grid is projected onto the patient's trunk [164]. Similar to the Moiré technology, the Raster stereography could project a series of narrow black and white stripes of light rather than a grid onto the patient's trunk; and its distortion is also used to assess the curvature angle of the patients with scoliosis [165]. Currently, the commonly used surface topography systems which adopt the raster technology in the scoliosis clinic include ISIS (version 1 and 2) [166], Quantec [167, 168], Frometric [169, 170], and InSpeck [171, 172].

The commercialized systems differ in the techniques of image acquisition, the degree of resolution, the scanning time, the degree of automation and the parameters proposed by the software. For example, the novel techniques such as the optical motion capture and the automation processing algorithm have been applied to the surface topography systems to

improve the imaging quality and measurement accuracy. Dynamic surface topography is established on the basis of the optical motion capture technique which can observe the dynamic changes of positions of the anatomical reference landmarks on the back surface. This technique allows for establishing the correlations between the breathing, postures, dynamic capability and the changes of the surface topography of the back [173]. Additionally, an automation 3-D surface topography system has been developed with the processing algorithm, which can automatically identify the anatomical landmarks of the human back [174]. Furthermore, Komeili et al. has proposed a 3-D marker-free analysis technique, which can be used to assess the torso asymmetry in the patients with scoliosis by means of the visually intuitive asymmetry map. Based on the distinct patterns of asymmetry, the patients with scoliosis would be classified into three groups and six subgroups. This technique promoted the utilization of the surface topography system with the marker-free placement, which has not been accomplished in the assessments of the patients with AIS [175].

#### **2.4.5.2 Three Dimensional Assessments of Back Surface**

Surface topography is a non-invasive method that uses a non-contact optical system to capture and assess the 3-D geometry changes of the torso. Compared with the radiography, surface topography has radiation-free imaging and concentrates on the external assessments of the spinal deformity [165], closely associated with the cosmetic problems of the patients with AIS [176]. Usually, the posterior aspect of the trunk is scanned by the surface topography in the upright position. At the same time, the “folding” or “clavicle” postures could be applied so as to highlight the thoracic gibbositities or humps [177, 178]. Besides, the lateral bending test could also be used to assess the flexibility of the trunk asymmetry of the patients with AIS [179]. However, the forward bending posture is not feasible due to the

misinterpretation of the spinal deformity and the increase of axial surface rotation about  $3.2^\circ$  on average compared with standing posture [180].

#### **2.4.5.3 Parameters of Surface Topography Systems**

A variety of parameters have been proposed by the different surface topography systems. The measurements of these parameters are based on the distances and angles between the landmarks identified on the torso, or on the geometric properties of the 2-D cross sections through the torso [167, 181]. Among them, the most common parameters used in the scoliosis clinics and researches include: the POTSI index, the Hump Sum and the DAPI index. In order to quantify the degree of left–right asymmetry in the coronal plane, posterior trunk symmetry index (POTSI) was proposed by Suzuki et al. [182]. It is a sum of six indices, calculated by looking at the relative positions of C7, shoulders, axillas and waists. The intra- and inter-raters measurement error of POTSI was 5.5 and 6.4, respectively; the value of POTSI below 27.5 was reported to be within the normal limits [182, 183]. To date, POTSI could be applied to evaluate the correction outcomes of the spinal deformity through the surgical intervention [184]. In the transverse plane, the deformity in the axial plane index (DAPI) has been developed to assess the left-right asymmetry at the level of the most protruding points of scapulae and at the deepest lumbar lordosis [185]; the value of DAPI inferior to 3.9% was reported as the normal limits. Additionally, a combined diagnostic criterion has been proposed accordingly: cases with the normal DAPI and POTSI could be regarded as the non-pathologic scoliosis ( $DAPI \leq 3.9\%$  and  $POTSI \leq 27.5\%$ ), but cases with the high DAPI or POTSI were considered as the pathologic [185]. Similarly, the Hump Sum has been developed to quantify the rotational prominence in the transverse plane. The Hump Sum is a sum of the three hump indices, corresponding to the three levels of the spine: the proximal thoracic, the main thoracic and the thoracolumbar or lumbar. Currently, the

assessment of the surface deformity has been limited to the sagittal plane and needs the further research.

#### **2.4.5.4 Reliability and Variability of Surface Topography Measurement**

Irrespective the type of the systems and parameters, the detailed configuration of the back surface is reproduced, with the precision sufficient for the clinical assessments of scoliotic spine. Several different systems have been demonstrated to be highly reliable to assess the external asymmetry of the patients with AIS and to be correlated well with the radiographic measurements [186, 187]. It has been shown that the InSpeck system could provide the accurate and reliable assessments for the scoliosis patients with different types of spinal curvatures [177]. Berryman and his colleague demonstrated the reliability of the measurements produced by the ISIS system in the lateral asymmetry, rib hump height and thoracic kyphosis, with the mean difference between pairs of measurements of 1mm, -0.08 mm and  $-0.02^{\circ} \pm 7.4^{\circ}$  respectively [188-190]. In addition, the Quantec system was found to have a standard deviation (SD) value of  $3.8^{\circ}$  when assessing the thoracic kyphosis in the sagittal plane prior to the surgery [191]. Similarly, the measurements of the major curve presented an average SD value of  $3.2^{\circ}$  in the Formetric system [169].

Additionally, raster-stereography could also reflect the curve progression of scoliosis, which is similar to the radiograph during a mean follow-up period of 8 years [192]. However, the measurement provided by the raster-stereography would be limited to the patients with extreme obesity or very muscularity [190]. Knott et al. found that the higher the patients' BMI, the more variability the measurements of scoliotic spine by the surface topography; however, even at the highest BMIs, the variability of surface topography measurements was only  $4.6^{\circ}$  [193]. By contrast, Mohokum et al.'s study did not support the findings that BMI

could affect the reliability of surface topography measurements [194]. To conclude, the reliabilities of the above four surface topography systems have been demonstrated in the measurements of the spinal curvature in the coronal plane. Further research will be needed to validate the use of surface topography in the other anatomical planes.

## **2.5 Ultrasound Assessments of AIS**

An accurate 3-D assessment of the patients with AIS is crucial to facilitate the diagnosis of scoliotic deformation and optimize the treatment strategies. The use of ultrasound has a growing popularity in the orthopedic practice for a variety of reasons, including decreased equipment costs, no radiation exposure and higher resolution images [195, 196]. In order to reduce the radiation exposure from repeated radiographic examinations, the application of ultrasound has become a potential option in the assessment of patients with AIS. A series of the related research have been conducted in Canada [17, 18, 21, 197], Hong Kong [198-201], Japan [202], America [203], Australia [204], Netherlands [14, 16] and other places. It has been shown that ultrasound can be used to assess the spinal curvature, vertebral rotation, muscle thickness, skeletal maturity and bone mineral status in the patients with AIS. Furthermore, the advent of 3-D reconstruction technique promoted the development of 3-D ultrasound system and facilitated the application of 3-D ultrasound in the assessments of scoliotic spine.

Therefore, this part of literature review was to critically summarize the existing studies regarding the use of ultrasound in the scoliosis assessment practices, and estimate its future potential. In addition, the potential roles of 3-D ultrasound in the assistance of brace treatment and surgical intervention for the patients with AIS would also be discussed.

### **2.5.1 Muscle Thickness and Dimension Measurements**

The abnormality of muscles is often found between the concave and convex sides in the patients with AIS. It has been suggested that the muscle abnormality may be one of the important factors which involved in the etiology and development of AIS. Compared with other imaging technologies, ultrasound is superior to reflect the real-time change of muscle in scoliosis patients. The online literature search identified 5 research articles [205-209] and 1 conference abstract [210]. Table 2.7 summarized the main characteristics of these studies.



**Table 2. 7 Ultrasound measurements of muscle thickness and dimension**

Studies	Ultrasound system	Subjects	Assessors	Muscles measured	Parameters	Reliability
1993 Kennelly[205]	①Ultrasound B-scanner ②5 MHz linear transducer	20 AIS subjects (13°~53°) prone position	1 assessors	Lumbar multifidus at L4 level	Muscle dimension (cross-sectional area)	-
2013 Pawel[206]	①Ultrasound B-scanner ②7.5 MHz linear transducer	71 AIS subjects supine position	-	External oblique, internal oblique, and transversus abdominalis muscles	Muscle thickness	-
2013 Richte[210]	①Ultrasound machine ②linear transducer	9 AIS subjects (39.4±9.1°); prone position	1 assessors	Erector spinae at L3,apical vertebral, end-vertebrae level	Muscle thickness	intra-rater: 0.75-0.99 ICC (2,1)
2014 Yang[207]	①Ultrasound SonoAce X4 ②5-9 MHz linear transducer	15 AIS subjects (15.4±4.8°); supine position	2 assessors with experience	External oblique, internal oblique, and transversus abdominalis muscles	Muscle thickness	intra-rater:>0.8 ICC (3,1) inter-rater:>0.8 ICC (2,1)
2015 Pawel[206]	①Ultrasound B-scanner ②7.5 MHz linear transducer	42 AIS subjects supine/standing position	-	External oblique, internal oblique, and transversus abdominalis muscles	Muscle thickness	-
2015 Zapata[209]	① Ultrasound machine ②1-4 MHz curve transducer	10 AIS subjects (15°~24°); prone/standing position	2 assessors with varying experience	①Deep thoracic paraspinals muscles (thoracic multifidus, semispinalis, and rotator muscles) at T8 level; ②Lumbar multifidus at L1/L4 level	Muscle thickness	intra-rater: 0.83-0.99 ICC (3,3) inter-rater:0.93-0.99 ICC (2,3)

The emphasis of these studies were placed on the muscle asymmetry of paraspinal muscles (erector spinae [210] and multifidus [205, 209]) and lateral abdominal muscles (external oblique, internal oblique, and transverses abdominals) [206-208] between the concave-convex sides in the patients with AIS. The main parameters detected by ultrasound imaging included the muscle thickness and muscle dimension (cross-sectional area). Specifically, the muscle thickness was determined as the length from the most posterior portion of the zygapophyseal joints to the inner edge of the fascia for the lumbar multifidus/thoracic paraspinal muscles [209] (Fig. 2.8a), whereas the vertical distance between the musculofascial layers for the lateral abdominal muscles [207] (Fig. 2.8b). Additionally, the measurement of muscle dimension (cross-sectional area) was directly made by an electronic calipers tracing around the muscle border [205, 209]. Moreover, the reliability of the ultrasound measurements has been established for quantifying the muscle asymmetry of the lumbar multifidus [209], erector spinae [210] and lateral abdominal muscles [207].

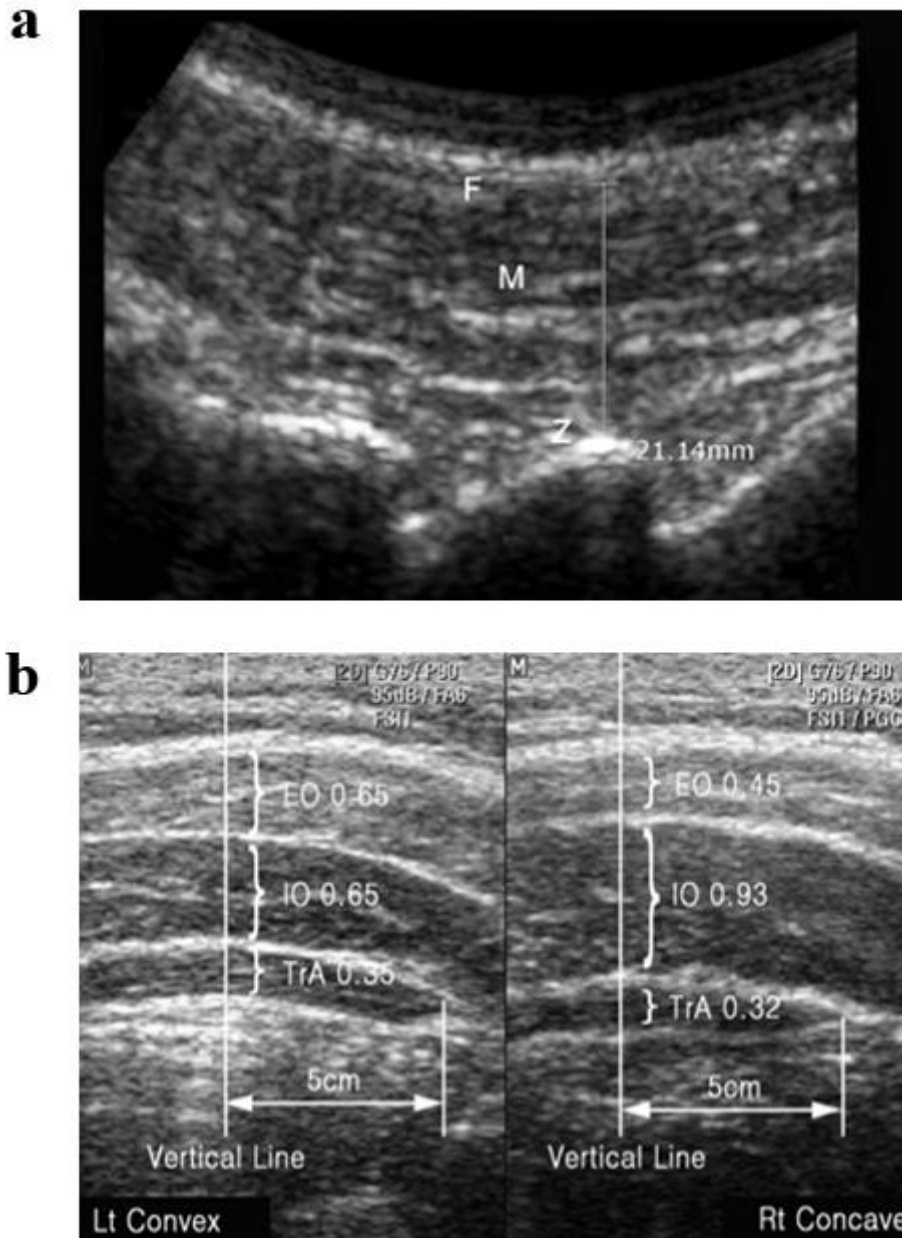


**Figure 2. 8 Ultrasound measurements of muscle thickness:** (a) Multifidus muscle thickness of L4 measured by ultrasound; (b) Abdominal muscles thickness of bilateral external oblique (EO), internal oblique (IO), and transverse abdominal (TrA) muscles in patients with AIS. F = fascia; M = muscle tissue; Z = zygapophyseal joint (Yang et al. 2014 and Zapata et al. 2015).

Knowledge of paraspinal and abdominal muscle asymmetries may improve the understanding of the pathogenesis in AIS. The real-time ultrasound measurements of the dynamic change of muscle thickness and dimension will help to monitor and guide the conservative treatments in the patients with AIS. Thus, further studies are deserved to investigate the correlation of the efficacy of rehabilitative exercise with the dynamic change of muscle asymmetry detected by the ultrasound imaging.

### **2.5.2 Skeletal Maturity Determination**

The determination of skeletal maturity is essential in the management of patients with AIS, especially when deciding whether conservative or surgical treatment is indicated. Risser Grades is the most commonly used method to determine the skeletal maturity from the radiograph of iliac apophysis. The grades of the Risser sign (0–V) were defined by the extent of ossification of the apophysis of iliac crest (Fig. 2.9a). In order to reduce the radiation exposure of repeated X-ray examination, the ultrasound has been proposed as an alternative method to X-ray in the Risser Grades determination. Electronic literature search identified 4 studies, which investigated how to use ultrasound to determine the skeletal maturity [204, 211-213].

It has been demonstrated that Risser Grades was also applied in the ultrasound assessment of the skeletal maturity [204, 212, 213]. According to the Risser Grades, ultrasound scanning was performed from the antero-lateral to the postero-medial aspect of the iliac crest. In the ultrasound images, the iliac wing is shown as the notched image, and the hypertensive region over the iliac wing shows the apophysis (Fig. 2.9b,c). The reliability and validity of the ultrasound method of Risser Grades have been demonstrated in comparison with the radiographic method [211, 212]. In addition, Hrovje et al. proposed to subdivide Risser Grade

IV into Grade IVa and IVb in the ultrasound images, according to the amount of cartilage left unossified between iliac apophysis and iliac wing, in order to determine exactly when to discontinue brace treatment of scoliosis [213]. On the basis of the existing studies, further research is required to validate the proposed Risser Grades determined by ultrasound in a larger sample size, and explore its clinical application of scoliosis treatments.

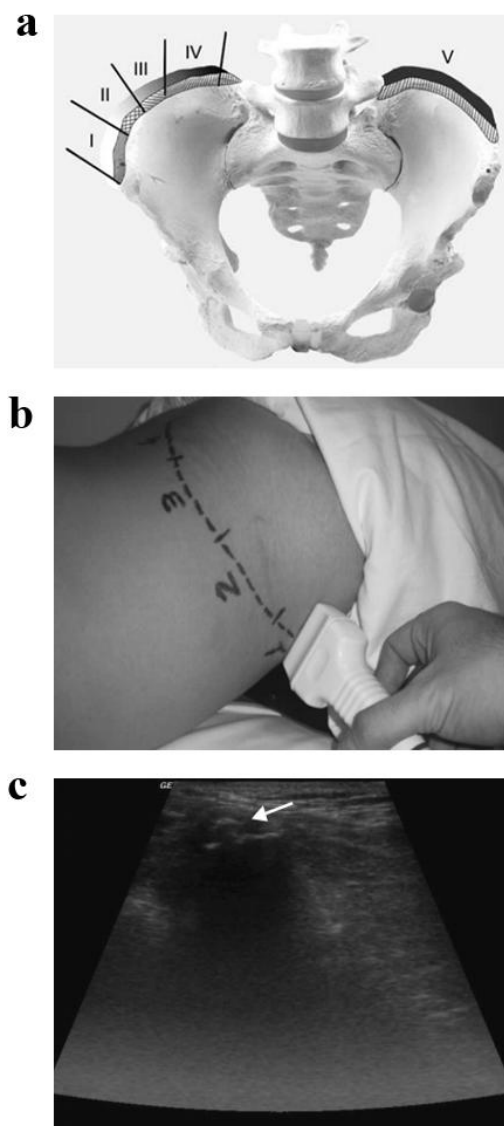


**Figure 2. 9 Ultrasound determination of skeletal maturity:** (a) Risser grades (0–V); (b) Ultrasound scanning from the antero-lateral to the postero-medial aspect of the iliac crest wing of the subject with Risser grade II; (c) The ultrasound image of the iliac wing is the

notched image, and the hypertensive region over the iliac wing shows the apophysis (arrow) (Torlak et al. 2012).

### **2.5.3 Bone Quality Assessment**

Decline of bone quality is associated with the development of scoliotic spine. To assess the extent of bone quality, the use of quantitative ultrasound (QUS) has been studied in patients with AIS [214]. From the electronic literature search, 6 studies have been identified, including 3 research articles [215-217] and 2 conference abstracts [218, 219].

Three parameters were proposed to evaluate the bone quality using QUS: the ultrasound velocity or speed of sound (SOS), broadband ultrasound attenuation (BUA) and stiffness index (SI). The QUS was undertaken along the longitudinal axis of the radial bones or over the non-dominant calcaneus [201, 215, 217]. Lam et al. reported that calcaneus BUA and SI were found to be lower in AIS as compared with controls [215]; SI was an independent prognostic factor when estimating the risk of curve progression [201]. Chen et al. found that radial SOS measured by QUS was significantly reduced in AIS patients. In addition, they suggested that the bone quality may be correlated with the maturation status rather than the curve type and severity in patients with AIS [217-219]. Further studies are deserved to make use of QUS to clarify the role of bone quality in the etiopathogenesis of AIS, and to assist the conservative treatment planning in clinical setting.

### **2.5.4 Development and validation of 3-D ultrasound systems**

In order to reflect the 3-D spinal deformation of scoliosis, the 3-D ultrasound system has been developed, which is composed of B-mode ultrasound scanner, tracking system and specific computer programs [12, 14, 21, 199]. The tracking system can record the 3-D orientation of

the ultrasound transducer when ultrasound scanning is performed. Based on the 3-D orientation data recorded, the 3-D information of the posterior section of vertebrae could be determined and calibrated for further image processing and analysis. Then the 3-D reconstruction of spine could be done by means of specific computer programs. Recently, the optical and electromagnetic tracking systems have been developed and used in the 3-D imaging of scoliotic spine.

A series of research have been conducted to develop and validate the 3-D ultrasound system in the assessment of scoliotic spine. From electronic literature search, 15 studies have been identified [7-14, 16-18, 220-222], of which 8 studies were from conference papers [7, 8, 11-13, 15, 16, 18]. Purnama et al. introduced a framework for human spine imaging using a freehand 3-D ultrasound system with an optical tracking system [14, 16]. Optical trackers need to use wireless markers, which are not affected by metallic or electronic objects in the environment [221] (Fig. 2.10a). However, the varying position of the attached markers relative to the vertebral landmarks will affect the extracted 3-D data of scoliotic spine. The validation of 3-D ultrasound system with optical trackers has been proved. The errors of the axial rotation and vertebral tilt measurements using the centers of mass were in the range of  $0.4 \sim 3.3^\circ$  and  $0.1 \sim 2.9^\circ$ , respectively [16].

In the electromagnetic tracking system, an electromagnetic spatial sensing device and a spatial sensor mounted onto the ultrasound probe were used to collect the spatial information [9, 12] (Fig. 2.10b). Cheung et al. have developed a 3-D ultrasound system which projects the virtual 3-D model of spine phantom into three orthogonal planes and Cobb angle could be measured in the coronal plane [10, 12]. Meanwhile, a novel surface rendering technique has been successfully applied in the 3-D ultrasound system by Lou and his colleague [9, 17, 18,

222]. The accuracy of reconstructed 3-D image of spine was validated by the small dimension measurement error and a difference of 2~5° in Cobb angle [9, 12] and 0.8~3.6° in vertebral rotation assessments [9].

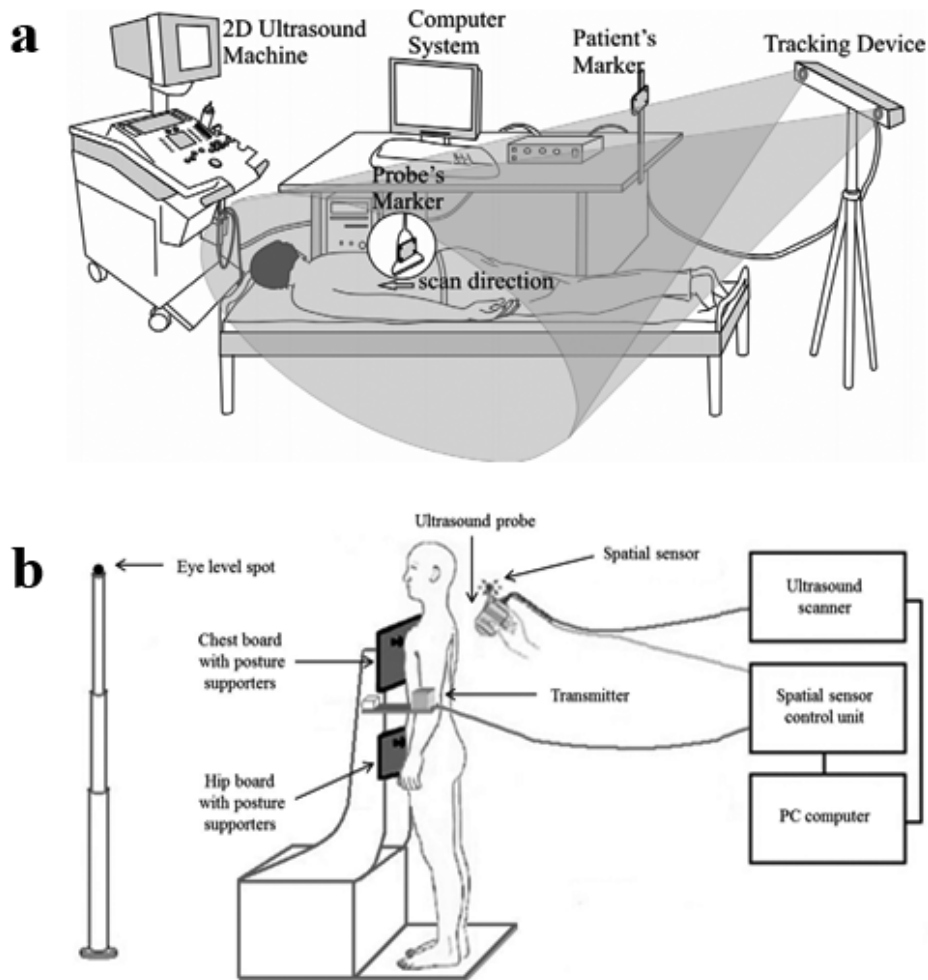


**Figure 2. 10 The 3-D ultrasound systems:** (a) with optical tracking markers; (b) with electromagnetic spatial device and sensor (Cheung et al. 2015 and Purnama et al. 2010).

The recent studies have shown that it was feasible to use 3-D ultrasound system to reconstruct the 3-D surface of the posterior section of vertebrae [9, 17, 18], spine phantom [12] and scoliotic spine from AIS patients [10, 17]. However, some limitations still exist in 3-D ultrasound system due to the inherent characteristics of ultrasound. Firstly, it is difficult for



ultrasound to image the vertebral body due to the acquisition configuration and the lack of ultrasound energy penetrating through bone. Secondly, the increase of the axial vertebral rotation has a tendency to make some of the areas behind the spinal process have no ultrasound signal. The reason is the side of the spinous process facing toward the transducer blocks the emitted ultrasound signals. Thirdly, the developed 3-D ultrasound reconstruction technique still needs an operator to manually or semi-automatically identify the contours of the vertebrae surface on each B-mode image and to perform digitization. Therefore, future studies are deserved to improve the technology of 3-D ultrasound imaging process to create better 3-D ultrasound images, to accomplish the automatic extraction and measurement. In addition, more patients' data are required to further validate the measurement accuracy of 3-D ultrasound system in the clinical setting.

### **2.5.5 Coronal Curvature Measurements**

Accurate measurement of the coronal curvature is essential in the scoliosis clinical practice. The Cobb angle measured from the standing postero-anterior (PA) radiograph is the standard method to measure the coronal curvature. Compared with radiographic imaging, ultrasound appears to be unable to image the whole scoliotic spine in the coronal plane. Soft tissue-bone interface is a strong reflector for ultrasound signals, making ultrasound imaging for the posterior structure of vertebrae possible. It has been shown that the landmarks located in the posterior structure of vertebra could be observed in the ultrasound images, including the landmarks such as spinous process, laminae, transverse process and superior articular processes (Fig. 2.11) [17, 18]. The development of 3-D imaging reconstruction technique makes it possible to reconstruct 3-D ultrasound images by means of the posterior landmarks identified. This is the basis of using ultrasound to reflect and measure the coronal curvature of scoliotic spine.

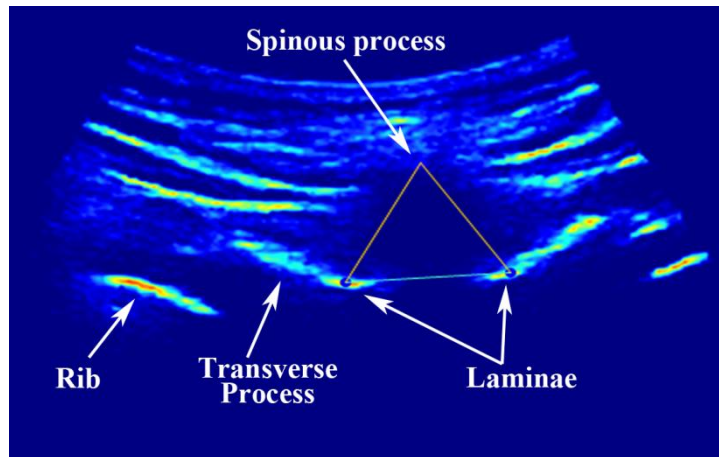


**Figure 2. 11 Ultrasound images of vertebral landmarks:** Spinous process, Laminae, and Transverse process (arrow) (Chen et al. 2013).

Table 2.8 summarizes the studies of ultrasound measurements of coronal curvature. The studies evaluating the reliability and/or validity of using ultrasound to measure the coronal curvature were identified. Of these, 3 studies were from the conference abstracts [12, 198, 223], 1 study was the purely technique paper [203], and 4 studies investigated the application of ultrasound measurements [10, 21, 199, 224]. Various approaches to the measurement of coronal curvature were proposed in terms of the different landmarks identified, including the Ferguson method [197], spinous process angle (SPA) method [198, 199], center of laminae (COL) method [21, 223], transverse process angle (TxA) method [224] and the “Cobb” method [10, 12].

**Table 2. 8 Ultrasound measurements of spinal curvature in the coronal plane**

Studies	Ultrasound system	Subjects	Assessors	Measurement method	Landmarks	Measurement Procedure	Reliability
1986 Letts[197]	①Ultrasonic digitizer; ②Microphone sensors; ③Specially designed software.	30 AIS subjects (15°~73°); standing position	-	Ferguson	spinous process	-	intra-rater:0.997 (spearman coefficient)
2012 Li [199]	①Esaoe MPX ultrasound unit; ②7.5MHz linear transducer; ③Tom Tec 3-D tracking system; ④SPA calculator software.	12 AIS subjects (20°~40°); standing position	1 assessor	SPA	spinous process	blind; 3 xmeasurements	intra-rater: >0.9 ICC (3,3)
2013 Chen[21]	①Olympus TomoScan Phased Array ultrasound; ②5MHz linear transducer; ③TomoView™ software.	cadaver spinal column phantom	3 assessors with varying experience	COL	laminae	2 xmeasurements with 1 week interval	intra- rater:0.976 (ICC) inter-rater:0.877 (ICC)
2013 Chen[21]	①Olympus TomoScan Phased Array ultrasound; ②5MHz linear transducer; ③TomoView™ software.	5 AIS subjects (14°~34°); standing position	1 assessor	COL	laminae	2 xmeasurements	-
2013 Cheung[12]	① Hitachi ultrasound scanner; ②5-10MHz linear transducer; ③Electromagnetic spatial sensing device.	cadaver spinal column phantom	-	“Cobb” (TP-TP/TP-SAP)	transverse process/ superior articular process	2 xmeasurements	intra- rater:0.99 inter-rater:0.89 (ICC)
2014 Ungi[224]	①Sonix Tablet with GPS; ②5MHz linear transducer; ③3-D Slicer application software.	cadaver spinal column phantom	3 assessors	TxA	transverse process	-	-
2015 Cheung[10]	①Hitachi ultrasound scanner; ②6-14MHz linear transducer; ③Electromagnetic spatial sensing device.	28 subjects (1.9°~29.9°); standing position	2 assessors	“Cobb” (TP-TP/TP-SAP)	transverse process/ superior articular process	2 xmeasurements	intra- rater:0.57 for TP-TP inter- rater:0.75 for TP-TP intra- rater:0.93 for TP-SAP inter- rater:0.89 for TP-SAP (ICC)

Data is taken from the Result section of the articles

ICC: intra-class correlation coefficient; SPA: spinous process angle; COL: center of laminae;

TxA: transverse process angle; TP: transverse process; SAP: superior articular processes.

The first attempt to use ultrasound to measure the coronal curvature was done by Letts et al., who applied ultrasonic digitization to record the spatial position of spinous process along the scoliotic curve and calculated the curve magnitude through specific computerized procedure [197]. The modified Ferguson method was applied, in which the coronal curvature was measured by the angle between the two lines that connect the spinous process of the end vertebrae with that of the apical vertebra. The other studies were reported in the recent 5 years, when the 3-D reconstruction technique had been successfully developed and applied in ultrasound imaging. Wong and his colleagues proposed to assess the scoliotic curvature using the spinous process angle (SPA) method, and demonstrated its high correlation with Cobb angle [198, 199]. SPA is described as the accumulating angle formed by every two lines joining three neighboring spinous processes of a scoliotic spine (Fig. 2.12a). In addition, Ungi et al. tried to choose the transverse processes as the landmarks to measure the coronal curvature using the transverse process angle (TxA) method [224] (Fig. 2.12b). However, this method was verified only in an adult and a pediatric scoliotic model. At the same time, the center of laminae (COL) method was proposed by Lou's research group [17, 18, 21]. The spinal curvature was calculated by the angle between the two lines that connected the centers of laminae at the upper-end and lower-end vertebrae (Fig. 2.12c). The reliability and validity of the COL method have been demonstrated in both the cadaver spinal column of scoliotic model [17, 18] and the patients with AIS<sup>[21]</sup>. Similarly, Cheung et al. presented the Cobb method using the transverse process and/or superior articular processes (TP-TP/TP-SAP) at the level of end-vertebrae to assess the spinal curvature (Fig. 2.12d) in phantom studies [12] and clinical trials [10], respectively.

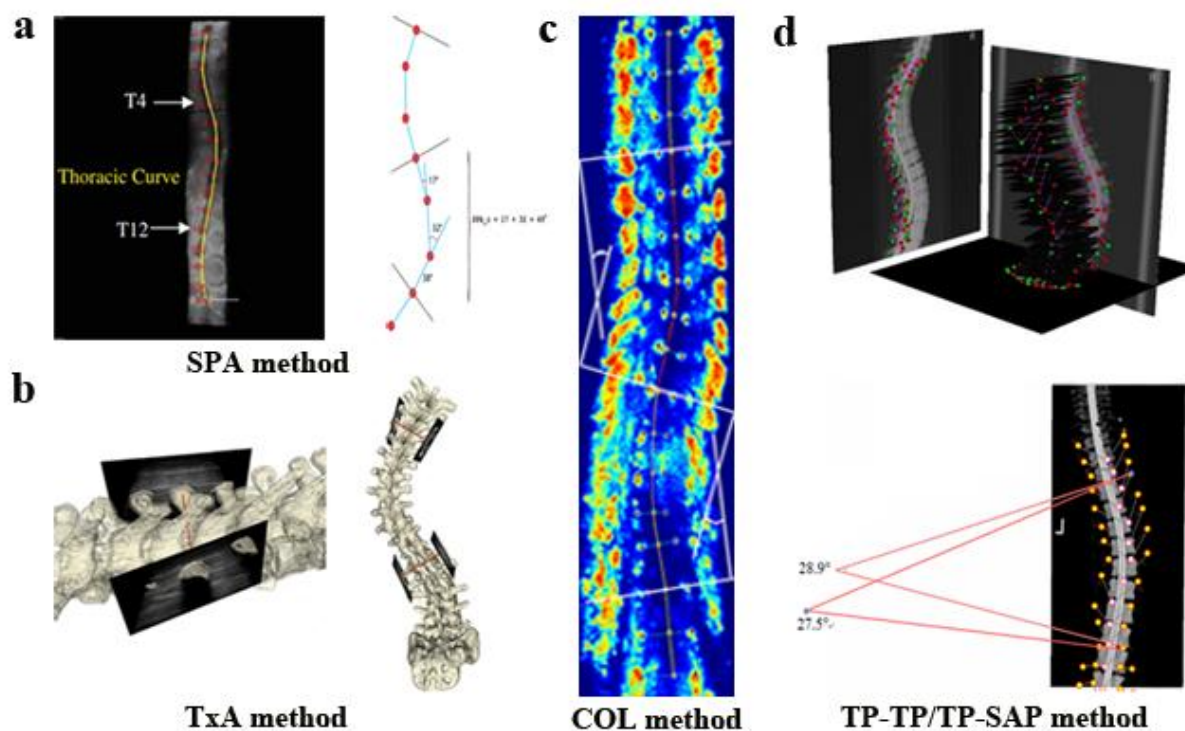


**Figure 2. 12** Ultrasound measurements of coronal curvature using (a) Spinous process angle (SPA) method; (b) Transverse process angle (TxA) method; (c) Center of laminae (COL) method; and (d) “Cobb” method using the transverse process and/or superior articular proces (Li et al. 2012; Ungi et al. 2014; Chen et al. 2013 and Cheung et al. 2013).

Several issues of the methodological quality in these studies should be noticed: (1) The evidence was limited in the validation of ultrasound measurements of coronal curvature in the clinical setting due to the small sample size. In addition, only 4 studies provided description or source of the assessors [10, 12, 199, 224], which made it difficult to understand the assessor's qualifications, skills, and length of training for future clinical comparisons. (2) Among the reviewed studies, the most widely used statistical method for the calculation of reliability was the ICC, which is a recommended option for continuous scales [225]. However, only 1 study provided no information of the ICC type [199]. The Spearson coefficient was used as a

measure of reliability in one study which is likely to provide overly optimistic estimates of reliability. (3) Five studies did not describe blinding of the assessors either to the subjects' clinical information or to the other assessors' measurement results. This would cause the bias of measurement procedure.

In summary, the feasibility of using ultrasound to measure the coronal curvature has been demonstrated. Further research is required to validate the proposed ultrasound measurements in a larger sample size, and to further standardize the measurement procedure.

### **2.5.6 Vertebral Rotation Measurements**

The posterior structure of vertebrae could be displayed by ultrasound imaging in the transverse plane. Similar to CT/MRI measurements, ultrasound could also visualize and measure the vertebral rotation in the transverse plane of scoliotic spine. A total of 7 studies [202, 226-231] have been identified, of which 6 studies were the conference abstracts [226-231]. The detailed information of these studies was shown in Table 2.9. Burwell et al. reported their results in 4 conference papers [226-229], which were related to ultrasound assessments of vertebral rotation and rib rotation. However, the authors did not provide any information about how to use ultrasound to measure the rotation and how reliable the measurements were.

**Table 2. 9 Ultrasound measurements of vertebral rotation in the transverse plane**

Studies	Ultrasound system	Subjects	Assessors	Measurement method	Landmarks	Measurement Procedure	Reliability
1989 Suzuki[202]	①Shimazu SDL-300 ultrasound machine; ②5.0MHz linear transducer.	42 scoliosis subjects; prone position	-	direct measurement	laminae	-	-
2015 Chen[230]	①Olympus TomoScan Phased Array ultrasound; ②5MHz linear transducer; ③TomoView™ software.	cadaveric vertebrae	1 assessors with 3 years' experience	L-L	laminae	2xmeasurements with 1 week interval	intra- rater: >0.9 ICC (2,k)
2015 Vo[231]	①Sonix Tablet with GPS; ②4.0MHz convex transducer; ③3-D image processing software	cadaveric vertebrae	3 assessors with six months' experience	L-L/TP-TP	laminae/ transverse process	blind; 3 xmeasurements with 1 week interval	intra- rater: >0.9 inter- rater: >0.9 ICC (2,k)

Data is taken from the Result section of the articles

ICC: intra-class correlation coefficient; COL: center of laminae.

The possibility of using ultrasound to assess vertebral rotation has been firstly studied by Suzuki et al.[202], who combined the ultrasound system with an inclinometer to measure the vertebral rotation from scoliosis patients in a prone posture (Fig. 2.13a). However, this method relied on radiographs to determine the positions of each vertebrae and thus the whole process of measurement was time-consuming. Additionally, the reliability of this method has not been documented. Recently, Lou and his colleagues tried to assess the vertebral rotation by means of 3-D ultrasound technique and specific programs [230, 231]. In the transverse plane of ultrasound images, the rotation of each reconstructed vertebra was automatically determined by the angle between the line going through either the centers of laminae (L-L) or the centers of transverse processes (TP-TP) and a reference horizontal line (Fig. 2.13b). However, the measurement is limited to cadaveric vertebrae. Further studies are deserved to

explore the possibility of using the proposed 3-D ultrasound method to measure the vertebral rotation in subjects with AIS in the clinical setting.

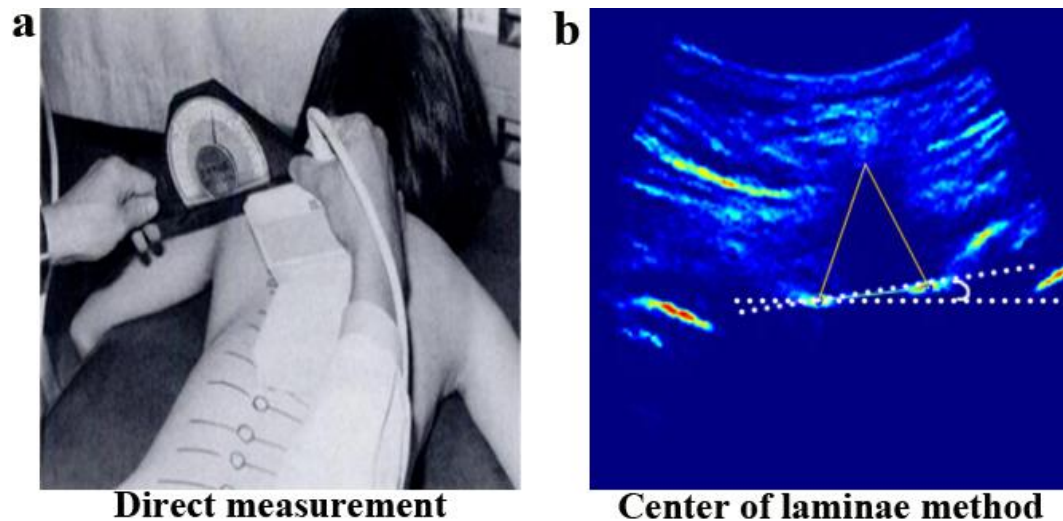


**Figure 2. 13 Ultrasound measurements of vertebral rotation using (a) Combination of ultrasound with an inclinometer; (b) Centers of laminae (L-L) or transverse processes (TP-TP) methods (Suzuki et al. 1989).**

### 2.5.7 Other Application of Ultrasound Assessments

Other than the assessments in the coronal and transverse planes, ultrasound measurement has also been investigated in the sagittal plane. An ultrasound-based motion analysis system has been developed for the purpose of screening for scoliosis, and applied to assess the kyphosis and lordosis of the growing children's spine in the sagittal plane [232, 233]. In addition, several studies have been conducted to explore and test the novel application of ultrasound assessments, including estimation of the curve flexibility [234, 235], 3-D analysis of chest wall motion during breathing [236], and geometrical measurement of the rib hump [237]. However, due to a limited number of participants in these studies, the validation and



reliability of these novel applications of ultrasound assessments should be further investigated.

Due to the non-radiation exposure to patients, ultrasound assessment could be performed repeatedly to provide the dynamic changes of the scoliotic spine during the conservative and surgical treatments [200]. To improve the effectiveness of spinal orthosis, Wong et al. [199] investigated if real-time ultrasound could aid orthotists in determining the optimum magnitude and location of the pressure pad resulting in optimal in-brace correction of the spine. During the fitting procedure of the spinal orthosis, ultrasound scanning was undertaken and spinous process angle (SPA) was measured. The optimal location of pressure pad of spinal orthosis was determined at the spot where the best curvature correction was achieved according to the differences between the pre-brace SPA and the in-brace SPA measurements. As a result, 62% of patients in this study benefitted from the use of ultrasound measurement [199]. Likewise, Lou and his colleagues applied ultrasound-assisted brace casting to obtain the immediate and optimal simulated in-brace correction [238, 239]. In addition, Stokes et al. [240] and Yoon et al. [241] applied ultrasound to assess the rod length in scoliosis patients undergoing surgical treatment with magnetically-controlled growing rod (MCGR). Ultrasound is a viable alternative to radiography and can provide reliable assessment of the MCGR lengthening.

Ultrasound technology could provide a comprehensive imaging assessment of scoliosis from soft tissues to bony structures, but further research is still needed to validate the proposed ultrasound measurements in larger clinical trials.

## **2.6 Summary of Literature Review**

Scoliosis is a complex three-dimensional spinal deformity, characterized by lateral curvature, vertebral rotation, and geometric changes in the trunk and rib cage. Medical imaging evaluation is essential for determination of the severity of scoliotic spine, prediction of the progression and assistance of the decision-making interventions for scoliosis. Traditionally, spinal radiography was the primary means of quantifying the severity of scoliosis patients. However, this method is confined to the assessment of spine in the frontal and lateral planes. The hazardous health implications associated with the frequent and prolonged exposure to radiation have been of primary concern for the scoliotic patients, who are often undergoing the critical growth and developmental stages. Consequently, various imaging modalities which are capable of providing the 3-D assessments of scoliosis and involving no ionizing radiation have been developed and studied.

The purpose of this literature review is to provide better insight into the clinical utilizations and the research progress of radiography, computed tomography, magnetic resonance imaging, surface topography and ultrasonic imaging, along with the critical concerns that should be addressed in the future studies. Classical radiography serves as the most common method to determine the curve type and magnitude. Computer tomography and magnetic resonance imaging enable the direct visualization of the transverse plane of spine. Surface topography, as a non-invasive method, places emphasis on the external assessment of the trunk deformity. Ultrasound has been proposed in the non-invasive 3-D assessments of scoliotic spine. Computed tomography (CT) and magnetic resonance imaging (MRI) are indicated in the patients who are candidates for surgery. At present, stereo-radiography and ultrasound seem to be the most promising techniques, which is able to provide the 3-D assessments of AIS.

Major advances have occurred in the past 5 years in the development and validation of the ultrasound assessments for the patients with AIS. The development of 3-D ultrasound system enabled the 3-D reconstruction of spinal images and assessments of spinal curvature and vertebral rotation in various anatomical planes that could not be accomplished previously. The validity and reliability of 3-D ultrasound measurements have been verified in the vertebral models and the spinal phantom in the experiments, and the patients with AIS in the clinical trials. Continuous studies are deserved to further validate the proposed 3-D ultrasound methods in clinical applications. On the basis of 3-D ultrasound assessments, further optimization of the orthotic treatment and rehabilitation exercise for patients with AIS should be explored in the future studies.

# **CHAPTER 3 Reliability Study of 3-D Ultrasound Assessments in Patients with Adolescent Idiopathic Scoliosis**

## **3.1 Introduction**

Adolescent idiopathic scoliosis (AIS) presents with a lateral and rotational deformity of the spine [1, 2]. The spinal curvature in the coronal plane and vertebral rotation in the transverse plane are both important parameters of the deformity in AIS, which can be used to assess the severity of scoliotic spine, to monitor the risk of curve progression, and to evaluate the treatment outcomes [57]. These two parameters are also associated with the ribcage asymmetry, leading to reduced respiratory capacity and cosmetically disfiguring rib hump [93, 94, 251]. In addition, AIS would often cause a disturbance of spine in the sagittal plane, resulted in the abnormal thoracic kyphosis and lumbar lordosis [24]. This abnormal sagittal profile has been thought to influence the biomechanical stability of spine, which are relevant to the etiology, progression and decision-making intervention of AIS [255- 261]. Therefore, an accurate and reliable assessment of coronal curvature in the coronal plane, vertebral rotation in the transverse plane and kyphotic and lordotic angles in the sagittal plane is of paramount importance for the patients with AIS.

Nowadays, the radiographic assessment of scoliotic spine continues to be the most widely used method in a scoliosis clinic. In routine clinical practice, radiographic assessments are performed throughout the course of treatment of the patients with AIS. However, the frequency of radiation exposure in monitoring scoliosis concerns many adolescents and their parents in light of evidence that cumulative radiation exposure could increase cancer risk [6]. In addition, the radiographic assessment of scoliotic spine is limited in the coronal and

sagittal planes, which represent a simplification of the true 3-dimensional (3-D) spinal deformity involved in scoliosis. Thus, the attempts to reduce or eliminate radiation exposure in adolescents and visualize 3-D characteristics of scoliotic spine have led researchers to develop new imaging technologies, such as stereo-radiography (EOS), ultrasound imaging, and magnetic resonance imaging (MRI).

Among various imaging technologies, ultrasound imaging is a non-radiation and cost-effective method, which is accessible in the majority of medical institutes. The posterior structure of vertebrae could be displayed by ultrasound imaging in the transverse plane [17, 18]. The feasibility of using these landmarks to assess the spinal curvature has been studied. In 1988, the first attempt to use ultrasound to assess the spinal curvature was made by Letts et al., who applied the ultrasonic digitization to identify the spinous process and document the spinal curvature angle using the Ferguson method [197].

The development of 3-D ultrasound systems can enable the 3-D reconstruction of vertebral images and facilitate the measurement of scoliotic spine in various anatomical planes that could not be accomplished previously [7-14, 16-18, 221]. Thus, the use of 3-D ultrasound systems in the scoliosis assessment has gained considerable attention over the past decade. A series of research regarding the 3-D ultrasound assessments have been conducted in Canada, Hong Kong, Japan, Australia, Netherlands and other places. Spinous processes, laminae and transverse processes can be visualized and used as the landmarks to measure the lateral curvature and vertebral rotation in the coronal and transverse planes of the ultrasound images [10, 12, 21, 199, 230, 231].

In the recent years, Wong et al. has shown that the Cobb angle could be estimated through the spinous process angle (SPA) method in the 3-D ultrasound images, by which the optimal location of pressure pad of the spinal orthosis could be determined during the fitting procedure of orthosis [198, 199]. Additionally, Ungi et al. found that the transverse process angle (TRA) obtained from the 3-D ultrasound images could be correlated with the Cobb angle from the radiographic images when measuring the spinal curvature in the coronal plane [224]. In Canada, the center of laminae (COL) method has been proposed by Lou and his colleague using the 3-D ultrasound to measure the coronal curvature of scoliosis in a phantom study. The results indicated that the COL method was applicable for the patients with AIS ranged from  $12^{\circ}$  to  $45^{\circ}$ , with the high intra- and inter-reliability of the 3-D ultrasound measurements. Furthermore, the correlation was found to be high between the COL method in 3-D ultrasound and the Cobb method in radiograph; the measurement difference between these two methods was less than  $5^{\circ}$  [17, 21].

The above studies indicated the importance and future trend of using 3-D ultrasound in the assessment for the patients with AIS. However, most of the relevant results currently available regarding the 3-D ultrasound assessments of spinal curvature and vertebral rotation were derived in the phantom studies, but not in the clinical trials. For this reason, it is warranted to systematically validate the proposed 3-D ultrasound measurements of the patients with AIS in the clinical setting. Thus, the objective of this study was to explore the possibility and reliability of using the proposed 3-D ultrasound method to measure the coronal curvature in the coronal plane, vertebral rotation in the transverse planes, kyphotic and lordotic angles in the sagittal plane for the subjects with AIS under the clinical setting.

## **3.2 Materials and Methods**

### **3.2.1 Reliability Study of 3-D Ultrasound Assessments in AIS**

The feasibility of using 3-D ultrasound to scan and measure the patients with AIS has been investigated under the clinical setting in the present study. This study was conducted according to the Guidelines for Reporting Reliability and Agreement Studies (GRRAS) [225]. To evaluate the reliability of 3-D ultrasound assessments, the 3-D ultrasound images were randomly assigned without specific order for measurements. The two raters were blinded to subjects' clinical information and they measured the spinal curvature in the coronal plane, apical vertebral rotation in the transverse plane, kyphotic and lordotic angles in the sagittal planes independently in 3 trials each with one week interval. The time required was about 3 minutes for 3-D ultrasound measurements.

### **3.2.2 Subjects**

The subject selection criteria were as follows: 1) female adolescents; 2) age: 10-18 years; 3) Cobb angle: 10°-80°; 4) no prior surgical treatment; 5) out-of-brace MRI examination of the whole spine on the same morning.

Human ethical approval was granted from both the Human Subjects Ethics Sub-committee of the Hong Kong Polytechnic University and the Joint Chinese University of Hong Kong-New Territories East Cluster Clinical Research Ethics Committee. All the examination procedures were explained and written informed consents were obtained from the subjects and their parents.

As the subjects are young females (10-16 years), their privacy rights are paramount. A female researcher was involved in the whole data collection procedure and the subjects' parent/guardian could be present during scanning.

### **3.2.3 3-D Ultrasound System**

The 3-D ultrasound scan was performed with a 3-D SonixTABLET ultrasound unit (Analogic, Massachusetts, USA), consisting of a C5-2/60 convex transducer, SonixGPS and a 3D Guidance device (driveBAY, Ascension Ltd., USA) (Fig 3.1a). An electromagnetic tracking sensor is built into the ultrasound transducer. The Ultrasonix program (Version 6.1.0) is bundled with the 3-D ultrasound unit and used to perform the ultrasound data acquisition (Fig 3.1b). During the ultrasound scanning, the parameters of ultrasound scan were set as follows: frequency 2.5 MHz, penetration depth 18cm, gain 10% with linear time gain compensation. To extend the the size of ultrasonic image frames; the UlteriusEx program (Version 3.0) has been developed and installed into the Ultrasonix program. These two programs were working collaboratively to collect the raw data of ultrasound images in the real-time mode (Fig 3.1c).



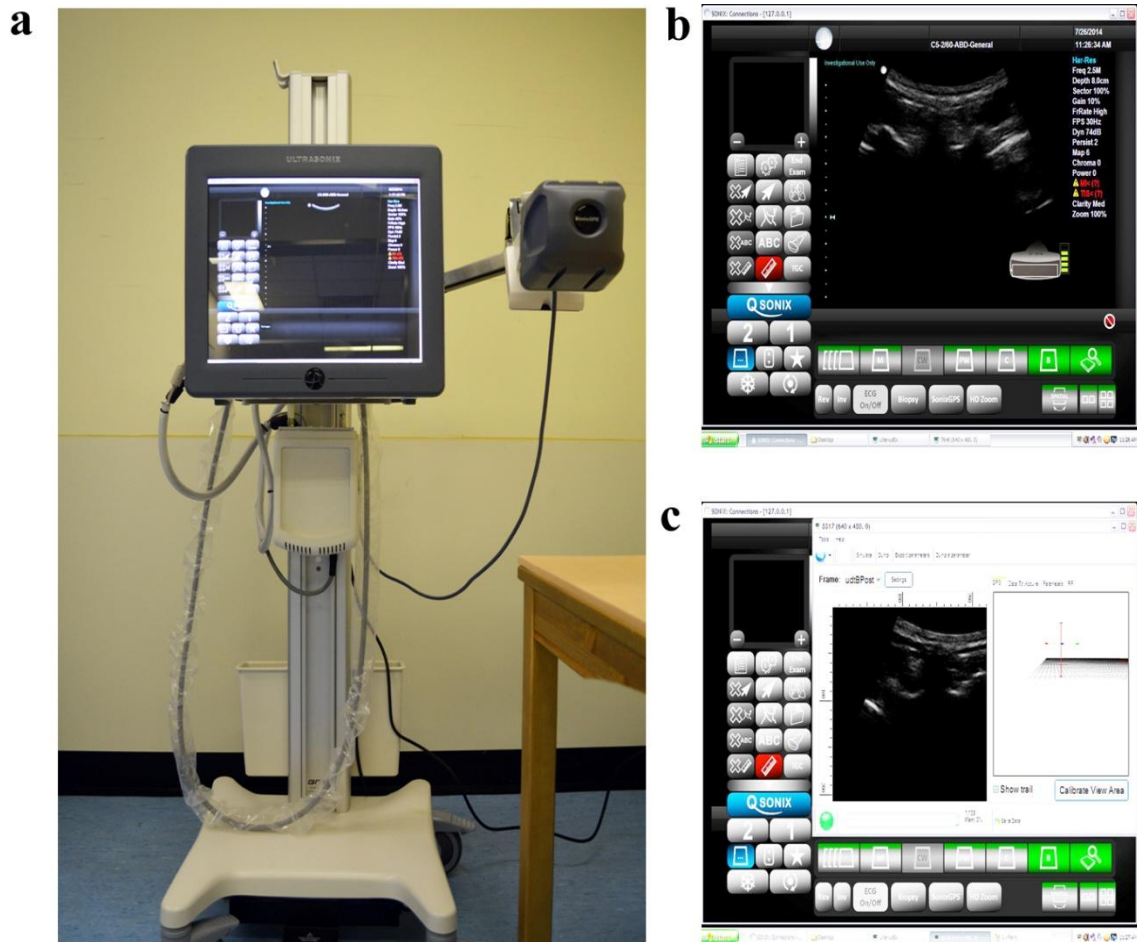


**Figure 3. 1 3-D Clinical Ultrasound System: (a) 3-D Ultrasound Unit with a SonixGPS System; (b) Ultrasonix Program Interface (Version 6.0.7); (c) UlteriusEx Program Interface (Version 2.0)**

### 3.2.4 Observers

Two observers with varying experience of ultrasound measurement participated into this study. Observer 1 was a research fellow with approximately 5 years of experience, while Observer 2 a rehabilitative physician with 2 years of experience. Prior to the study, each observer was trained to practice the 3-D ultrasound scanning in the supine and standing positions, and the 3-D ultrasound measurements for at least 10 volunteers.

### 3.2.5 3-D Ultrasound Scan in the Supine Position

A purpose-design couch with a central rectangular slot (size: 12 cm [width] x 60 cm [length])

was used to facilitate the ultrasound scanning in the supine position (Fig 3.2). The size of the slot could exactly expose the subjects' scoliotic spine when the ultrasound transducer was scanning along the coronal curvature from C7 to S1.

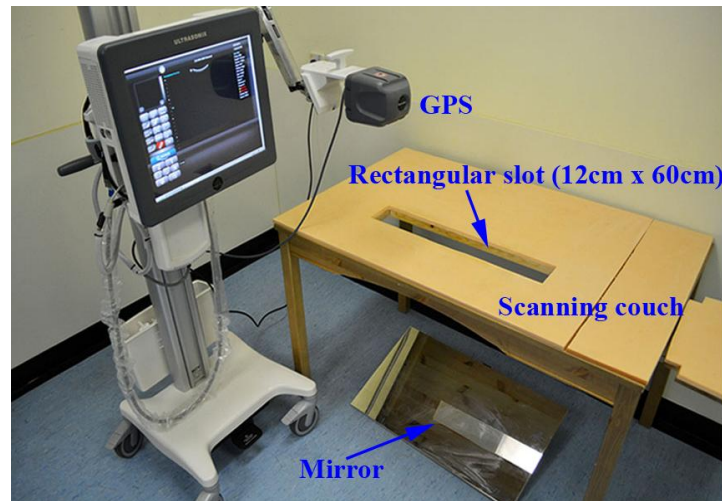


**Figure 3. 2 3-D Ultrasound Experiment Setting and a Purpose-design Couch with a Rectangular Slot**

Each subject wore a gown with the back opened (about 8 cm) to allow the ultrasound scanning. The spinous processes from C7 to S1 were palpated and the general trend of coronal curvature was marked on the subjects' back by a water soluble marker (Fig 3.3a). To ensure a smooth scanning and good coupling between the transducer and skin, sufficient ultrasound gel was applied between the transducer and the subject's back.

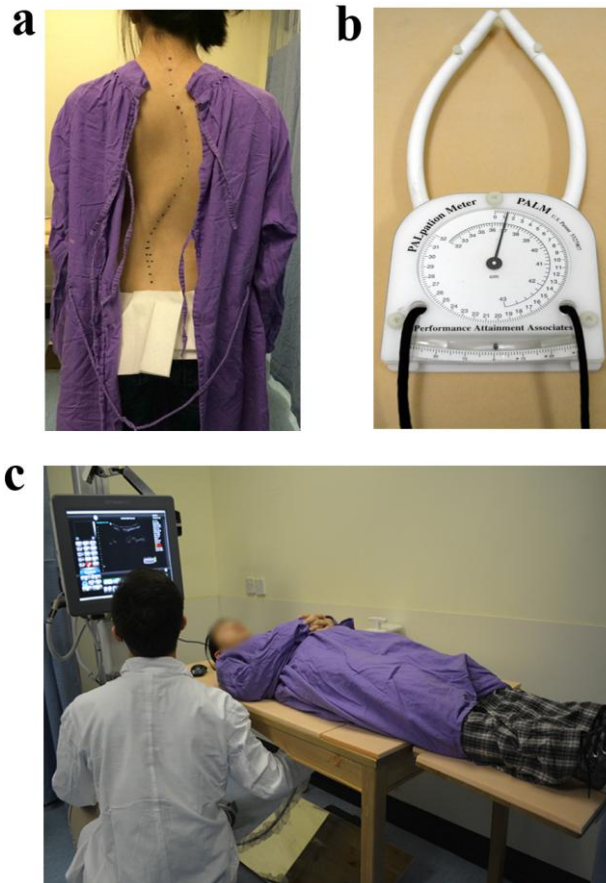


**Figure 3.3 3-D ultrasound scan in the supine position** (a) A subject with AIS; (b) Level meter; (c) Ultrasound scanning was undertaken in the supine position.

Then, the subjects were instructed to lying on the scanning couch in the supine position. Before scanning, a level meter was used to ensure the anterior superior iliac spines (ASISs) of subjects at the horizontal level which was used as a reference for the 3-D ultrasound measurements (Fig 3.3b). In addition, to prevent the shift of the trunk, the position of the subjects' ASISs would also be adjusted to be parallel with the edge of the ultrasound scanning couch.

With the 3-D ultrasound unit activated, the ultrasound probe was moved caudally along the coronal curvature from C7 to S1 inside the slot of the scanning couch (Fig 3.3c). Under the

scanning couch, a mirror was used to reflect the marked trend of the coronal curvature, which assisted to place the probe correctly while moving it along the spine (Fig 3.3c). In addition, it was required that the observer push the ultrasound probe upward to attach on the subjects' back tightly all the time. During the ultrasound scanning, the image of the transverse plane of vertebra was reflected in each of the ultrasonic frames (Fig 3.3c). Three ultrasound scans (with no breaks in between) were acquired for each observer and it took less than a minute for 1 scan. Therefore, each subject underwent 6 scans (2 observers and each with 3 scans).

### 3.2.6 3-D Ultrasound Images Reconstruction and Landmarks Identification

#### 3-D Ultrasound Images Reconstruction

The ultrasound data, which consisted of signal strength and position information, were then exported into the Medical Image Analysis Software (MIAS) (Fig 3.4). This purpose-design software would reconstruct the 3-D ultrasound images of the vertebrae and perform the semi-automatic measurements. The reconstructed 3-D ultrasound images of vertebrae were shown in the 3 orthogonal planes (coronal, sagittal and transverse) (Fig 3.5).

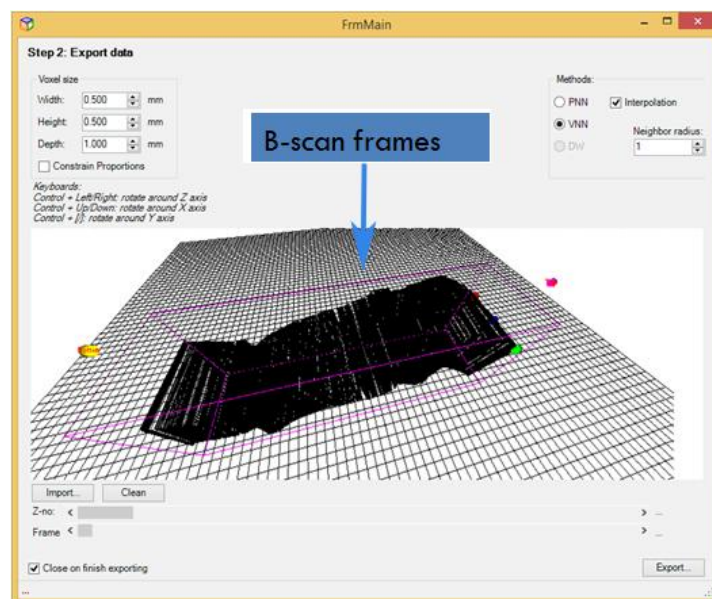


**Figure 3. 4 Self-developed medical image analysis software (MIAS) for 3-D reconstruction of ultrasound images and measurements for scoliotic spine.**

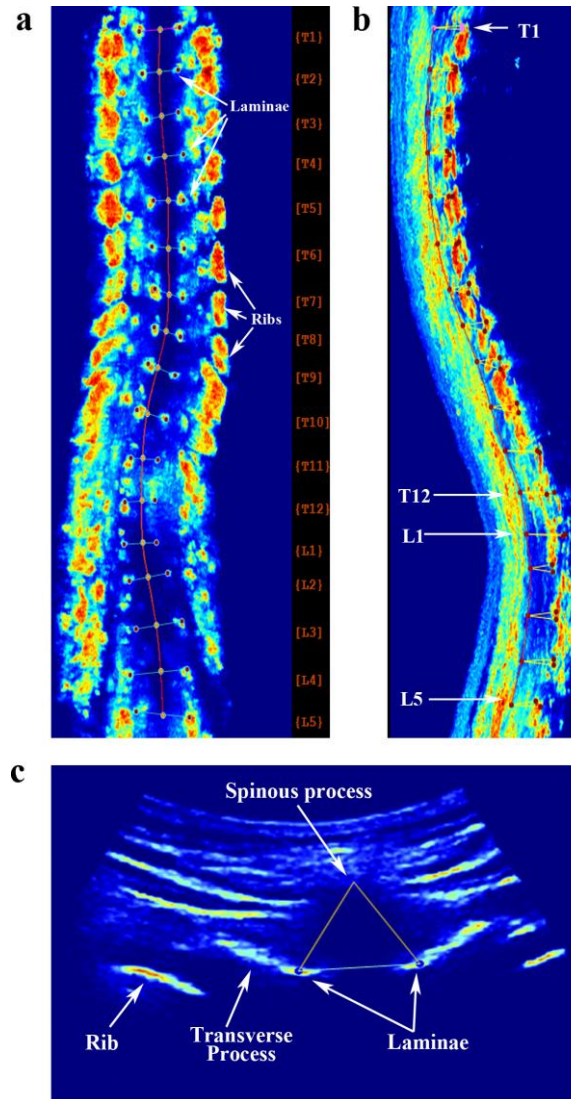


**Figure 3. 5 The reconstructed 3-D ultrasound images of a scoliotic spine in the 3 orthogonal planes: (a) Coronal plane; (b) Sagittal plane; (c) Transverse plane.**

**Identification of Vertebral Landmarks**

In the interface of MIAS, the observer used the mouse to select each vertebral level in the coronal plane of the 3-D ultrasound image, while the corresponding image in the transverse

plane would be also displayed. In the coronal plane of 3-D ultrasound image, the laminae could be easily recognized, while in the transverse plane the landmarks such as the spinous processes, laminae and transverse processes could be clearly identified (Fig 3.5).

Similar to the radiographic method, the vertebral level could be identified in the coronal plane of 3-D ultrasound image. As shown in Fig. 3.5, the ultrasound signals reflected from the ribs are always larger and stronger due to the relative large and flat surface of the ribs (Fig 3.5a). Therefore, the ribs can be easily located pair by pair in the thoracic area, whereas there are no evident signs of rib pairs in the lumbar area. The last pair of ribs was used to identify the T12 vertebra, on the basis of which the other vertebral levels could be determined accordingly.

The apical vertebra and end-vertebrae could be identified in the 3-D ultrasound reconstructed images with reference to the following methods. The apical vertebra was the most distant vertebra from the central vertical sacral line (CVSL) or the apex of a curve in the coronal plane of 3-D ultrasound image; the most rotated and deformed vertebra in the transverse plane of 3-D ultrasound image. The end vertebrae were the most tilted vertebrae situated close to the CVSL in the coronal plane of 3-D ultrasound image; the least rotated and deformed vertebra in the transverse plane of 3-D ultrasound image.

### **3.2.7 3-D Ultrasound Assessments of Spinal Curvature in the Coronal Plane**

#### **Center of Laminae (COL) Method**

The center of laminae (COL) method was used to assess the spinal curvature in the coronal plane of the 3-D ultrasound image. Firstly, the centers of the laminae will be identified manually at each vertebral level. Due to the 3-D characteristics of the ultrasound data, the



adjustment of the center points of the laminae in the coronal view would be reflected in the corresponding transverse and sagittal view. The corresponding transverse plane was shown to assist in the fine-tune of the centers of the selected laminae. Lines were then drawn automatically by the custom-developed software (MIAS) to join the centers of laminae at each level. The most tilted lines above and below each curve along the spinal column could be recognized as the upper-end and lower-end vertebrae. The angle formed between these two lines was defined as the spinal curvature angle (COL angle) in the 3-D ultrasound image that would be compared with the Cobb angle in the MRI image. The COL angle was automatically calculated by the MIAS software (Fig 3.6a). When the spine had more than one curve, the procedure was repeated to measure the additional angle.

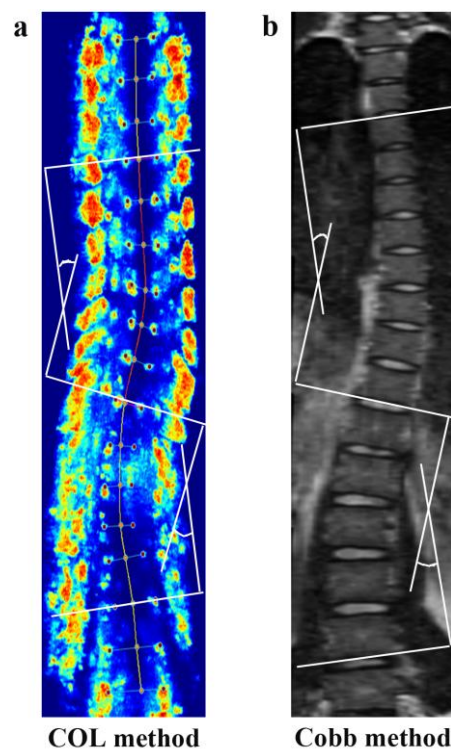


**Figure 3. 6 Coronal curvature measurement using:** (a) Center of laminae (COL) method in 3-D ultrasound; (b) Cobb method in MRI.

### 3.2.8 3-D Ultrasound Assessments of Vertebral Rotation in the Transverse Plane

#### Center of Laminae (COL) Method

The measurement of vertebral rotation was chosen at the apical level of the curve, which is normally used to predict the progression and evaluate the treatment outcomes [93, 94]. The center of laminae (COL) method has been applied to measure the apical vertebral rotation (AVR) in the 3-D ultrasound images [230, 231]. The two raters identified the centers of laminae manually in the transverse plane of apical vertebral level. The AVR was automatically measured by the angle between the line joining the centers of laminae and the reference horizontal line (scanning couch) by the purpose-design software (Fig. 3.7a).

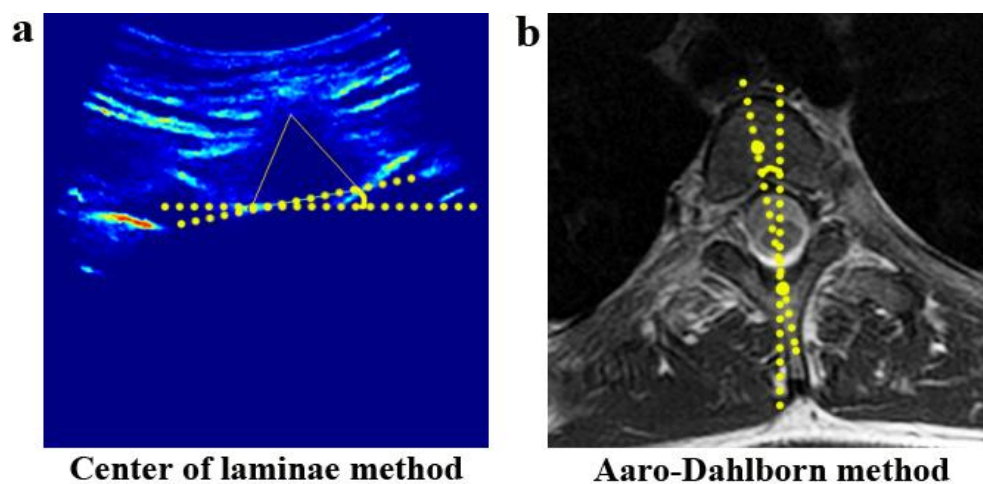


**Figure 3. 7 Apical vertebral rotation (AVR) measurements:** (a) Center of laminae (COL) method in 3-D ultrasound image; (b) Aaro-Dahlborn method in MRI image.

### 3.2.9 3-D Ultrasound Assessments of Kyphotic and Lordotic Angles in the Sagittal Plane

#### Spinous Process Angle (SPA) Method

The spinous process angle (SPA) method was applied to measure the kyphotic and lordotic angles in the 3-D ultrasound images. Firstly, the two raters identified the tips of spinous processes manually at each vertebral level in the transverse planes of 3-D ultrasound images.



Due to the 3-D characteristics of the ultrasound data, the selected tips of spinous processes in the transverse view would be reflected in the corresponding sagittal view. Lines were then drawn automatically by the custom-developed software (MIAS) to join all the tips of spinous processes. Spinous process angle (SPA) is described as the accumulating angle formed by every two lines joining three adjacent spinous processes of a scoliotic spine in the sagittal plane. Thus, the kyphotic angle was automatically calculated by the MIAS software using the SPA method between T1 and T12 vertebrae, while the lordotic angle between L1 and L5 (Fig 3.8 b-c).

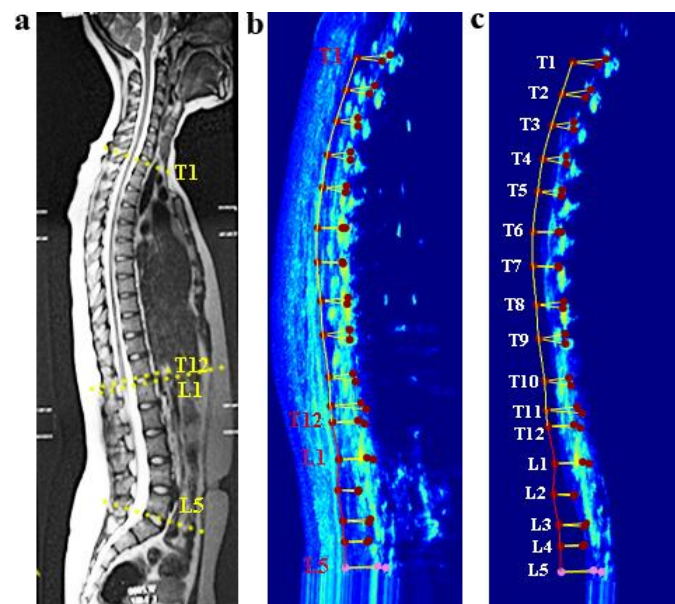


**Figure 3. 8 Kyphotic and lordotic angles measurements:** (a) Cobb method in MRI image; (b-c) Spinous process angle (SPA) method in 3-D ultrasound image.

### 3.2.10 Statistical Analysis

Statistical analyses were performed using the IBM SPSS Statistics Version 21 (IBM, USA). A *p*-value less than 0.05 were considered to be statistically significant. Statistical graphs were made with the GraphPad Prism Version 6.01 software (GraphPad, La Jolla, California, USA).

To assess the intra- and inter-rater reliabilities of 3-D ultrasound measurements, the intra-class correlation coefficient (ICC, [2, k]) with 95% confidence intervals (CI) was calculated. The Currier criteria for evaluating ICC values were adopted [243]: very reliable (0.80–1.0), moderately reliable (0.60–0.79), and questioned reliable (<0.60). In addition, the intra- and inter-rater measurement variations of the 3-D ultrasound method were evaluated using the mean absolute difference (MAD), standard deviation (SD) and standard error of measurement (SEM).

### **3.3 Results**

#### **3.3.1 Anthropometric Information of the Recruited Subjects**

Between January 2014 and November 2015, 40 female subjects were enrolled from the Prince of Wales Hospital, the Chinese University of Hong Kong, to receive the 3-D ultrasound and MRI examinations. Based on the subject inclusion criteria, of the 40 subjects, 16 female subjects with AIS (aged  $14.8 \pm 1.7$  years) were recruited to study the reliability and validity of 3-D ultrasound measurements compared with MRI assessments. The anthropometric information of the recruited subjects were shown in Table 3.1

Of the 16 AIS subjects, 3 had a single thoracic curve, 1 a single lumbar curve, 10 a double curve and 2 a triple curve, producing a total of 30 curves eligible for analysis in this study. The distribution of apical vertebra of these curves was 19 thoracic, 3 thoracolumbar and 8 lumbar levels. The Cobb angles of these curves measured from MRI coronal images ranged from  $10.2^\circ$  to  $68.2^\circ$  and the average value was  $21.7^\circ \pm 15.9^\circ$ .

**Table 3. 1 Anthropometric data of the recruited subjects**

Recruited Subjects (N.)	16
Age (y)	14.8±1.7
Height (m)	1.6±0.1
Weight (Kg)	49.7±4.7
BMI *	19.4±1.6
Menarche (y)	2.5±1.5
Curve Type	
Thoracic curv (N.)	3
Lumbar curve (N.)	1
Double thoracic and lumbar curve (N.)	10
Triple curve (N.)	2

\* BMI: Body Mass Index

### **3.3.2 Reliability of 3-D Ultrasound Assessment of Coronal Curvature in AIS**

To evaluate the intra- and inter-rater reliabilities of 3-D ultrasound measurements, the intra-class correlation coefficient (ICC, [2, k]) with 95% confidence intervals (CI) was calculated. In addition, the intra- and inter-rater variations of 3-D ultrasound measurements was assessed using the mean absolute difference (MAD), standard deviation (SD) and standard error of measurement (SEM).

#### **Intra-Class Correlation: ICC**

The intra- and inter-rater reliabilities for 3-D ultrasound assessments of spinal curvature in the coronal plane were shown in Table 3.2. The intra-rater ICC (2, k) values of the COL method in 3-D ultrasound were 0.997 (0.994-0.998) and 0.993(0.986-0.996) for Rater 1 and Rater 2 respectively. The inter-rater ICC (2, k) value was 0.995 (0.989-0.998). The intra- and inter-rater ICC (2, k) values of the COL method in 3-D ultrasound were greater than 0.9,

which demonstrated high intra- and inter-rater reliabilities in the coronal curvature assessments using 3-D ultrasound.

**Table 3. 2 Intra – and inter- rater reliability of coronal curvature assessments using 3-D ultrasound**

Methods	Observer	Curve, n	ICC [2,k] (95%CI)
3-D ultrasound (COL)	R1	30	0.997 (0.994-0.998)
	R2	30	0.993 (0.986-0.996)
	R1 vs. R2	30	0.995 (0.989-0.998)

COL: Center of laminae;

ICC: Intra-Class Correlation;

95% CI: Confidential Interval.

### **Variations of Measurements**

Table 3.3 shows the intra- and inter-rater variability of coronal curvature measurements using the 3-D ultrasound method. The intra-rater MAD, SD and SEM values were small for the COL method in 3-D ultrasound, which were 0.6°, 0.8° and 0.6° for rater 1, and 0.4°, 1.0° and 0.8° for rater 2, respectively. For the inter-rater variability of 3-D ultrasound measurements, the MAD value ranged from 0.1°-2.8°, the SD from 0.1° to 2.0°; and the SEM from 0.1° to 1.4°. All of these values indicated the small variation between the successive measurements through the 3-D ultrasound method.

**Table 3. 3 Intra – and inter-rater variability of coronal curvature assessments using**

**3-D ultrasound**

Methods	Observer	Curve, n	MAD (°)	SD (°)	SEM (°)
3-D ultrasound (COL)	R1	30	0.6 (0.1-1.3)	0.8 (0.2-1.7)	0.6 (0.2-1.4)
	R2	30	0.7 (0.1-2.1)	1.0 (0.2-2.7)	0.8 (0.1-2.2)
	R1 vs. R2	30	1.2(0.1-2.8)	0.9 (0.1-2.0)	0.6 (0.1-1.4)

COL: Center of Laminae;

MAD: Mean Absolute Difference;

SD: Standard Deviation;

SEM: Standard Error of Measurement.

These results suggested that the COL method in the 3-D ultrasound presented high intra- and inter-rater reliabilities when measuring the coronal curvature in the subjects with AIS in the supine position, compared with the Cobb method in MRI.

### **3.3.3 Reliability of 3-D Ultrasound Assessment of Vertebral Rotation in AIS**

To evaluate the intra- and inter-rater reliabilities of the 3-D ultrasound measurements, the intra-class correlation coefficient (ICC, [2, k]) with 95% confidence intervals (CI) was calculated. In addition, the intra- and inter-rater variations of the 3-D ultrasound measurements was assessed using the mean absolute difference (MAD), standard deviation (SD) and standard error of measurement (SEM).

#### **Intra-Class Correlation: ICC**

Tables 3.4 showed the intra- and inter-rater reliabilities of AVR measurements using the 3-D ultrasound method. The intra-rater ICC (2, k) values of the COL method in 3-D ultrasound were 0.989 (0.979-0.994) and 0.981 (0.966-0.990) for Rater 1 and Rater 2 respectively. The

inter-rater ICC (2, k) value was 0.978 (0.954-0.989). All of these data demonstrated high intra- and inter-rater reliabilities of apical vertebral rotation assessments using 3-D ultrasound.

**Table 3. 4 Intra – and inter-rater reliability of apical vertebral rotation assessments using 3-D ultrasound**

Methods	Observer	Curve, n	ICC [2,k] (95%CI)
3-D ultrasound (COL)	R1	30	0.989 (0.979-0.994)
	R2	30	0.981 (0.966-0.990)
	R1 vs. R2	30	0.978 (0.954-0.989)

COL: Center of laminae;

ICC: Intra-Class Correlation;

95% CI: Confidential Interval.

### **Variations of Measurements**

Table 3.5 shows the variability of vertebral rotation assessments using the 3-D ultrasound method. For the intra-rater variability of the COL method in 3-D ultrasound, the MAD, SD and SEM values were 0.4°, 0.2° and 0.2° for rater 1, and 0.4°, 0.3° and 0.2° for rater 2, respectively. For the inter-rater variability of 3-D ultrasound measurements, the MAD value ranged from 0.0°-3.0°, the SD from 0.0°-2.1° and the SEM from 0.0°-1.5°. All of these indicated that the COL method in 3-D ultrasound presented low variability when assessing the vertebral rotation in the patients with AIS.

**Table 3. 5 Intra -rater variability of apical vertebral rotation assessments using 3-D ultrasound compared with MRI.**

Methods	Observers	Curve, n	MAD (°)	SD (°)	SEM (°)
3-D ultrasound (COL)	R1	30	0.4 (0.1-0.7)	0.2 (0.1-0.5)	0.2 (0.1-0.4)
	R2	30	0.5 (0.1-1.1)	0.3 (0.1-0.7)	0.2 (0.1-0.5)
	R1 vs. R2	30	0.8 (0.0-3.0)	0.6 (0.0-2.1)	0.4 (0.0-1.5)

COL: Center of Laminae;

MAD: Mean Absolute Difference;

SD: Standard Deviation;

SEM: Standard Error of Measurement.

These results suggested that the COL method in 3-D ultrasound presented high intra- and inter-rater reliabilities when measuring the vertebral rotation in the AIS subjects in the supine position, compared with the Aaro-Dahlborn method in MRI.

### **3.3.4 Reliability of Kyphotic/Lordotic Angles Measurements using 3-D Ultrasound in AIS**

To evaluate the intra- and inter-rater reliabilities of the 3-D ultrasound measurements, the intra-class correlation coefficient (ICC, [2, k]) with 95% confidence intervals (CI) was calculated. In addition, the intra- and inter-rater variations of the 3-D ultrasound measurements were assessed using the mean absolute difference (MAD), standard deviation (SD) and standard error of measurement (SEM).

#### **Intra-Class Correlation: ICC**

Tables 3.6 showed the intra- and inter-rater reliabilities of the kyphotic angle measurements using the 3-D ultrasound method. The intra-rater ICC (2, k) values of the SPA method in 3-D ultrasound were 0.963 (0.917-0.986) and 0.931 (0.852-0.973) for Rater 1 and Rater 2

respectively. The inter-rater ICC (2, k) value was 0.946 (0.852-0.981). The intra- and inter-rater ICC (2, k) values of the SPA method in 3-D ultrasound were above 0.9, which demonstrated high reliability of kyphotic angle measurements using the 3-D ultrasound in the patients with AIS.

**Table 3. 6 Intra- and inter-rater reliability of kyphotic angle assessments using 3-D ultrasound**

Methods	Observers	Curve, n	ICC [2,k] (95%CI)
3-D ultrasound (SPA)	R1	16	0.963 (0.917-0.986)
	R2	16	0.931 (0.852-0.973)
	R1 vs. R2	30	0.946 (0.852-0.981)

SPA: Spinous Process Angle;

ICC: Intra-Class Correlation;

95% CI: Confidential Interval.

In addition, the intra- and inter-rater reliabilities of the lordotic angle measurements using the 3-D ultrasound were shown in Table 3.7. The intra-rater ICC (2, k) values of the SPA method in 3-D ultrasound were 0.801 (0.613-0.918) and 0.816 (0.637-0.924) for Rater 1 and Rater 2 respectively. The inter-rater ICC (2, k) value was 0.886 (0.704-0.958). The intra- and inter-rater ICC (2, k) values of the SPA method in 3-D ultrasound were above 0.8, which indicated a high reliable measurement of the lordotic angle using the 3-D ultrasound in the AIS patients.



Table 3. 7 Intra- and inter-rater reliability of lordotic angle assessments using

**3-D ultrasound**

Methods	Observers	Curve, n	ICC [2,k] (95%CI)
3-D ultrasound (SPA)	R1	16	0.801 (0.613-0.918)
	R2	16	0.816 (0.637-0.924)
	R1 vs. R2	30	0.886 (0.704-0.958)

SPA: Spinous Process Angle;

ICC: Intra-Class Correlation;

95% CI: Confidential Interval.

**Variations of Measurements**

Table 3.8 showed the intra- and inter-rater variabilities of the kyphotic angle assessments using the 3-D ultrasound method. For the 3-D ultrasound assessments, the intra-rater MAD value ranged from 0.5°-2.1°, the SD value 0.3°-2.7° and SEM value 0.2°-2.2°. Similarly, the inter-rater MAD value of 3-D ultrasound assessments were within 0.5°-5.2°, the SD value 0.4°-3.6° and SEM value 0.3°-2.6°. These results indicated that the SPA method in 3-D ultrasound presented low intra- and inter-rater variability when assessing the kyphotic angle in the patients with AIS.

**Table 3. 8 Intra- and inter-rater variability of kyphotic angle assessments using 3-D ultrasound**

Methods	Observers	Curve, n	MAD (°)	SD (°)	SEM (°)
3-D ultrasound (SPA)	R1	16	0.9 (0.5-1.5)	0.6 (0.3-0.9)	0.5 (0.2-0.7)
	R2	16	1.2 (0.1-2.1)	1.0 (0.2-2.7)	0.8 (0.1-2.2)
	R1 vs. R2	16	2.2 (0.5-5.2)	1.6 (0.4-3.6)	1.1 (0.3-2.6)

SPA: Spinous Process Angle;

MAD: Mean Absolute Difference;

SD: Standard Deviation;

SEM: Standard Error of Measurement.

Table 3.9 showed the intra- and inter-rater variabilities of the lordotic angle assessments using the 3-D ultrasound in patients with AIS. The range of intra-rater MAD, SD and SEM values was 0.4°-2.5°, 0.2°-1.2° and 0.2°-1.0° respectively, while the inter-rater MAD, SD and SEM values was 0.2°-2.5°, 0.2°-1.8° and 0.1°-1.3°. These results suggested that the SPA method in 3-D ultrasound presented low intra- and inter-rater variability when assessing the lordotic angle in the patients with AIS.

**Table 3. 9 Intra- and inter-rater variability of lordotic angle assessments using 3-D ultrasound**

<b>Methods</b>	<b>Observers</b>	<b>Curve, n</b>	<b>MAD (°)</b>	<b>SD (°)</b>	<b>SEM (°)</b>
3-D ultrasound (SPA)	R1	16	0.9 (0.4-1.2)	0.6 (0.2-1.0)	0.5 (0.2-0.8)
	R2	16	0.9 (0.4-2.5)	0.6 (0.2-1.2)	0.5 (0.2-1.0)
	R1 vs. R2	16	1.2 (0.2-2.5)	0.9 (0.2-1.8)	0.6 (0.1-1.3)

SPA: Spinous Process Angle;

MAD: Mean Absolute Difference;

SD: Standard Deviation;

SEM: Standard Error of Measurement.

These results suggested that the SPA method in 3-D ultrasound presented high intra- and inter-rater reliabilities when measuring the kyphotic and lordotic angles in the AIS subjects in the supine position.

### **3.4 Discussions**

Currently, the application of 3-D ultrasound has been studied in the assessment of coronal curvature in the patients with AIS. The COL method has been proposed by Lou and his colleague in the 3-D ultrasound image and compared with the Cobb method in the

radiographic image. The intra- and inter-rater ICC (2, 1) values of the COL method in 3-D ultrasound were reported to be above 0.80; the SEM less than  $2.8^\circ$  [21]. In the present study, the results were consistent with the previous studies. The intra- and inter-rater ICC (2, k) values of 3-D ultrasound assessment were greater than 0.9; the intra- and inter-rater MAD, SD and SEM were less than  $2.1^\circ$ ,  $2.7^\circ$ , and  $2.2^\circ$  respectively. Besides, the reliability results of 3-D ultrasound measurement in this study were comparable to the intra- and inter-rater statistics of radiographic measurement reported in the literature: MADs ranged from  $1.2^\circ$  to  $7.0^\circ$  [78, 82, 89], and ICCs ranged from 0.88 to 0.99 [82, 91, 242]. This indicated that the reliable measurements can be obtained by the COL method in 3-D ultrasound when measuring the coronal curvature for the patients with AIS.

The feasibility of assessing the vertebral rotation using the proposed 3-D ultrasound method (COL) has been demonstrated in the experiment studies [230, 231]. Three dry vertebrae T7, L1 and L3 with the rotation configuration from  $-30^\circ$  to  $30^\circ$  were scanned using the 3-D ultrasound. The intra- and inter-rater ICC values of the COL method were reported from 0.987 to 0.997; the MAD values were less than  $1.7^\circ$ . The current study showed comparable results to the experiment study. The intra- and inter-rater ICC (2,k) values of 3-D ultrasound measurements were more than 0.9; the MAD, SD and SEM values were less than  $3.0^\circ$ ,  $2.1^\circ$  and  $1.5^\circ$  respectively. The MAD value of the 3-D ultrasound method in this study was larger than that in the experiment studies. This was due to the fact that the ultrasound scanning was more difficult in the patients with AIS than in the dry vertebrae secured in a water-filled container. Moreover, the 3-D ultrasound method presented as reliable assessments as the MRI method in this study. MRI was chosen to be the reference because it enables the straightforward assessment of vertebral rotation in the transverse plane and it would not

expose the subjects to the radiation exposure. These results indicated that the 3-D ultrasound could provide the reliable measurements of vertebral rotation for the patients with AIS.

Based on the characteristics of 3-D ultrasound imaging, this study was conducted to explore the feasibility of using the 3-D ultrasound to measure the kyphotic and lordotic angles in the sagittal plane. The posterior landmarks such as the spinous processes, transverse processes and laminae could be visualized by the ultrasound imaging. Thus, the spinous processes along the thoracic and lumbar could be used to measure the kyphosis and lordosis by means of the accumulating angles. The results have shown that the spinous process angle (SPA) method in 3-D ultrasound presented the high intra- and inter-rater reliabilities when measuring the thoracic kyphosis and lumbar lordosis.

It is noteworthy that some curves or landmarks were missing in some of the 3-D ultrasound images. This resulted in difficult identification of landmarks in the 3-D ultrasound image and inaccurate measurement. There are several possible reasons for the missing landmarks in the 3-D ultrasound images. First, the bad contact between the transducer and subjects' back, especially for a large rib hump, would result in loss of 3-D ultrasound information. In order to ensure a good surface contact, Li et al. designed a silicon sleeve attached to the ultrasound transducer [199]. Therefore, much attention should be paid on how to create a good surface contact between the transducer and subjects' back for 3-D ultrasound scanning in future studies. Second, the thick muscles, in particular of the lumbar region, would cause the 3-D ultrasound signal penetration reduced and lower the resolution of ultrasound images. Third, the vertebral rotation would make it difficult to cover all the information during 3-D ultrasound scanning.

Although the results of this study have demonstrated the reliability of the 3-D ultrasound assessments for scoliotic spine, there are still some limitations. The eligible curves in this study involved a whole range of curve severity of the patients with AIS. However, the severe curves accounted for a small proportion in all the analyzed curves. Therefore, further research is still needed to validate the proposed 3-D ultrasound assessment in a larger sample size. Besides, the semi-automatic program applied in the reconstruction of 3-D ultrasound images, identification of landmarks and angle measurement took around 5 minutes for one trial of 3-D ultrasound measurement and cannot reduce the manual labor cost. Thus, the semi-automatic program used in reconstruction and measurement of 3-D ultrasound images should be upgraded to a fully automatic program so as to reduce the human errors.

### **3.5 Conclusions**

In the present study, the reliability of 3-D ultrasound assessments of the patients with AIS was investigated respectively. The major findings of this study are: (1) The COL method in 3-D ultrasound showed high intra- and inter-rater reliabilities to measure the lateral curvature in the coronal plane and vertebral rotation in the transverse plane. (2) The SPA method in 3-D ultrasound showed high intra- and inter-rater reliabilities to assess the thoracic kyphosis and lumbar lordosis in the sagittal plane.

The radiation-free 3-D ultrasound assessment appeared to be a reliable method for the patients with AIS in the clinical setting. Continuous studies are required to optimize the 3-D ultrasound scanning and measuring procedure, and to further improve the reproducible measurements of 3-D ultrasound. With these efforts, 3-D ultrasound will become a potential option used as an alternative to radiography for screening and routine assessment of scoliosis and other spinal deformities.

## **CHAPTER 4 Validity Study of 3-D Ultrasound Assessments in Patients with Adolescent Idiopathic Scoliosis**

### **4.1 Introduction**

Adolescent idiopathic scoliosis (AIS) is a three-dimensional spinal deformity characterized by lateral curvature and vertebral rotation of spine. It occurs in approximately 3% of adolescents with unknown reasons [1, 2]. Currently, ultrasound has gained considerable attention in the assessment of scoliosis. With the advent of 3-D reconstruction technique, ultrasound imaging has been developed to quantify the 3-D characteristics of scoliotic spine [7-14, 16-18, 221].

Ultrasound imaging has some superior characteristics such as radiation-free, cost effective and easy to operate. The landmarks such as spinous processes, transverse processes and laminae have been identified and used to assess the scoliotic spine [17, 18]. In 1988, the first attempt to use ultrasound to assess the spinal curvature was made by Letts et al., who applied the ultrasonic digitization to identify the spinous process and document the spinal curvature angle using the Ferguson method [197]. Subsequently, in 1989 the possibility of using ultrasound to assess the vertebral rotation has been firstly proposed by Suzuki et al. who identified the spinous processes and laminae in the transverse plane of ultrasound images of each vertebra, and assessed the vertebral rotation directly based on the inclination of the transducer [202].

In the previous study, the center of laminae (COL) method has been proposed to measure the lateral curvature in the coronal plane and vertebral rotation in the transverse plane of 3-D

ultrasound images, while the spinous process angle (SPA) method to estimate the kyphotic and lordotic angles in the sagittal plane. The feasibility and reliability of these proposed 3-D ultrasound methods have been demonstrated in the experimental and clinical studies. Thus, the objective of this study was to further evaluate the validity of application of the proposed 3-D ultrasound methods in the assessments of the subjects with AIS, in comparison with the concurrent MRI methods.

## **4.2 Materials and Methods**

### **4.2.1 Validity Study of 3-D Ultrasound Assessments in AIS**

The feasibility of using 3-D ultrasound to scan and measure the patients with AIS has been investigated under the clinical setting in the previous study. This study was conducted according to the Guidelines for Reporting Reliability and Agreement Studies (GRRAS) [225]. To evaluate the validity of 3-D ultrasound assessments, MRI scan and measure were performed and used as a reference standard. The whole spines of 3-D ultrasound and MRI scans were arranged in the same morning (within 3 hours) in the supine position so as to match the conditions. Before 3-D ultrasound and MRI scanning, a level meter was also used to ensure the anterior superior iliac spines (ASISs) of subjects at horizontal level which was used as a reference for 3-D ultrasound and MRI measurements.

### **4.2.2 Subjects**

The subject selection criteria were as follows: 1) female adolescents; 2) age: 10-18 years; 3) Cobb angle: 10°-80°; 4) no prior surgical treatment; 5) out-of-brace MRI examination of the whole spine on the same morning.

Human ethical approval was granted from both the Human Subjects Ethics Sub-committee of the Hong Kong Polytechnic University and the Joint Chinese University of Hong Kong-New Territories East Cluster Clinical Research Ethics Committee. All the examination procedures were explained and written informed consents were obtained from the subjects and their parents.

#### **4.2.3 Observers**

Two observers with varying experience of ultrasound measurement participated into this study. Observer 1 was a research fellow with approximately 5 years of experience, while Observer 2 a rehabilitative physician with 2 years of experience. Prior to the study, each observer was trained to practice the 3-D ultrasound scanning in the supine and standing positions, and the 3-D ultrasound measurements for at least 10 volunteers.

#### **4.2.4 3-D Ultrasound Scan and Assessments**

##### **3-D Ultrasound Scan in the Supine Position**

The scanning procedure of 3-D ultrasound and image reconstruction has been described in the Chapter 3.

##### **Spinal Curvature Assessment in the Coronal Plane**

Center of Laminae (COL) method has been described in the Chapter 3.

##### **Vertebral Rotation Assessment in the Transverse Plane**

Center of Laminae (COL) method has been described in the Chapter 3.

##### **Thoracic Kyphosis and Lumbar Lordosis Assessment in the Sagittal Plane**



Spinous Process Angle (SPA) method has been described in the Chapter 3.

#### 4.2.5 MRI Scan and Measurements

##### *MRI Scan in the Supine Position*

MRI scan was conducted using a 3.0T MR scanner and a spine array coil (Achieva, Philips Medical Systems, and Netherlands) (Fig 4.1). MRI imaging protocol included sagittal scans of hindbrain and the whole spine from foramen magnum to sacrum, and transverse scans of 5 vertebral levels around the vertebral apex (including the apical vertebra, 2 vertebrae above and below). The above MRI images were obtained using 2D Turbo spin-echo T2 weighted sequence with following parameters: turbo factor=33, TR=4048 milliseconds (ms), TE=120 ms, matrix=312×248, slice thickness=3.5 mm, slice gap=0 mm, field of view= 690 mm, NSA=2. It took at least 30 mins to complete a MRI scan of the full spine. The MRI images would be processed and exported using the DICOM Viewer Version R3.0 SP3 (Philips, Netherland).



**Figure 4. 1 Magnetic resonance imaging (MRI) systems for scoliosis assessments**

All the MRI images were processed by the DICOM Viewer software through adjustment of color gradation, contrast, size, and format. The standard for improving the quality of MRI images was that the landmarks (endplate of vertebral body, pedicles, laminae and spinous processes) along the scoliotic spine could be clearly identified. Then, the apical and upper & lower-end vertebrae were pre-defined in a curve from the coronal view of the MRI image. A central vertical sacral line (CVSL) was drawn passing through the center of the sacrum. Typically, the apical vertebra is most distant from the CVSL, most rotated and deformed, but not tilted. The upper and lower end vertebrae, which are situated close to the CVSL, are most tilted, least deformed and rotated. Moreover, the DICOM Viewer software was used to measure the spinal curvature in the coronal plane, apical vertebral rotation in the transverse plane, thoracic kyphosis and lumbar lordosis in the sagittal plane of MRI images.

### **Spinal Curvature Measurement in the Coronal Plane**

The Cobb method was used to measure the spinal curvature in the coronal plane. The most tilted vertebrae were identified and then two lines are drawn parallel to the superior endplate of the upper-end vertebra and inferior endplate of the lower-end vertebra, the angle between these two lines is the Cobb angle (Fig 4.2b). If there is more than one curve, the procedure was repeated to measure the additional Cobb angle.

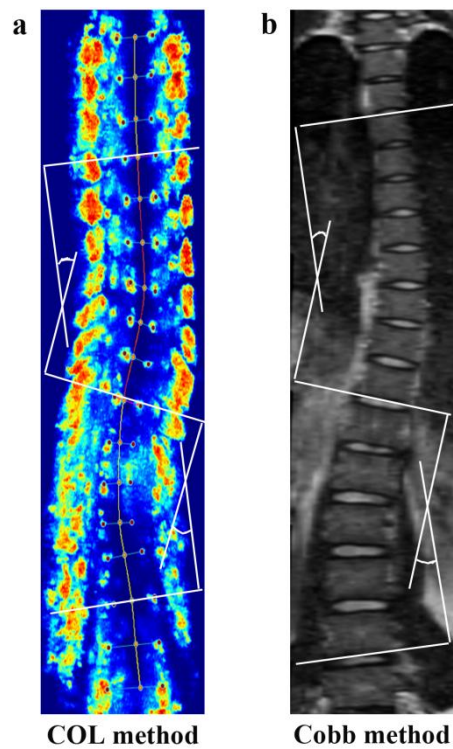


**Figure 4. 2 Coronal curvature measurement using :** (a) Center of laminae (COL) method in 3-D ultrasound; (b) Cobb method in MRI.

**Vertebral Rotation Measurement in the Transverse Plane**

The Aaro-Dahlborn method was applied to measure the apical vertebral rotation (AVR) in the transverse plane [95, 253, 254]. The AVR was calculated by the angle between the line connecting the point at the posterior junction of the two laminae of vertebral arch with the mid-point of vertebral body and the reference line (Fig. 4.3b).

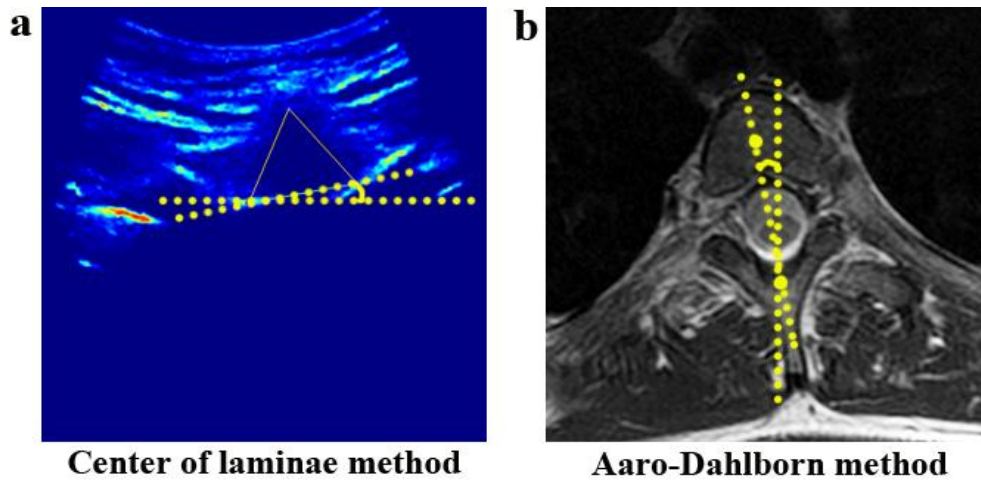


**Figure 4.3 Apical vertebral rotation (AVR) measurements:** (a) Center of laminae (COL) method in 3-D ultrasound image; (b) Aaro-Dahlborn method in MRI image.

#### *Thoracic Kyphosis and Lumbar Lordosis Measurement in the Sagittal Plane*

The spinous process angle (SPA) method was used to measure the kyphotic and lordotic angles in the 3-D ultrasound images. Firstly, the two raters identified the tips of spinous processes manually at each vertebral level in the transverse planes of 3-D ultrasound images. Due to the 3-D characteristics of the ultrasound data, the selected tips of spinous processes in the transverse view would be reflected in the corresponding sagittal view. Lines were then drawn automatically by the custom-developed software (MIAS) to join all the tips of spinous processes. Spinous process angle (SPA) is described as the accumulating angle formed by every two lines joining three adjacent spinous processes of a scoliotic spine in the sagittal plane. Thus, the kyphotic angle was automatically calculated by the MIAS software using the SPA method between T1 and T12 vertebrae, while the lordotic angle between L1 and L5 (Fig 4.4 b-c).

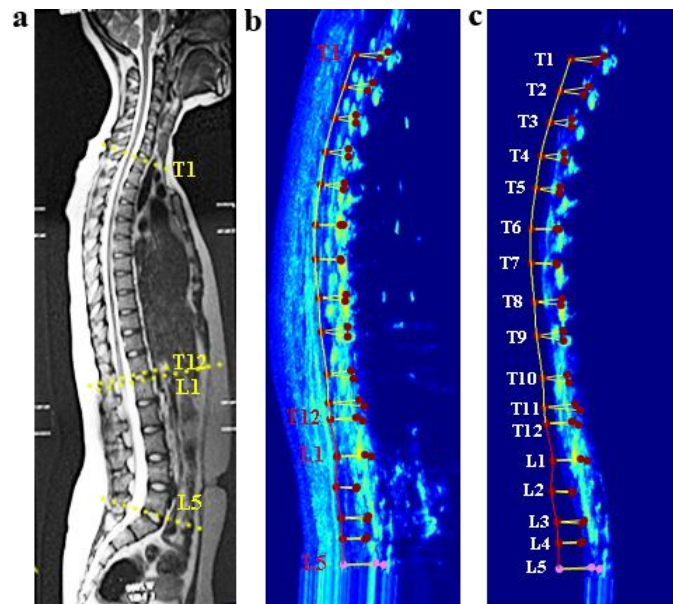


**Figure 4. 4 Kyphotic and lordotic angles measurements:** (a) Cobb method in MRI image;  
 (b-c) Spinous process angle (SPA) method in 3-D ultrasound image.

#### 4.2.6 Statistical Analysis

Statistical analyses were performed using the IBM SPSS Statistics Version 21 (IBM, USA). A *p*-value less than 0.05 were considered to be statistically significant. Statistical graphs were made with GraphPad Prism Version 6.01 software (GraphPad, La Jolla, California, USA).

To evaluate the validity of 3-D ultrasound assessment, the paired Student's *t*-test was used to compare the measurements data obtained from the 3-D ultrasound and MRI methods; the Bland–Altman method was used to examine the agreement between these assessments; Furthermore, the Pearson correlation analysis was applied to evaluate the correlation between the 3-D ultrasound and MRI measurements of scoliotic spine in three-dimensional anatomical planes.

## 4.3 Results

### 4.3.1 Anthropometric Information of the Recruited Subjects

In total, 30 curves from the 16 subjects with AIS were eligible for the validity study of the 3-D ultrasound measurements. The anthropometric information of the recruited subjects has been described in Table 3.1 in the Chapter 3.

### 4.3.2 Validity of 3-D Ultrasound Assessment of Coronal Curvature in AIS

To determine the validity of 3-D ultrasound assessments of spinal curvature in the coronal plane, the comparison of means, the Bland-Altman method and the Pearson correlation analysis were applied between the 3-D ultrasound and MRI measurements in the patients with AIS. Furthermore, the impact of curve magnitude (Cobb angle degrees), variation in selected upper-end vertebra (UEV) and lower-end vertebra (LEV) between the 3-D ultrasound and MRI, as well as the level of apical vertebra on the validity of 3-D ultrasound assessment of coronal curvature were investigated accordingly in the sample categories.

#### Comparison of means

For the entire curve cohort (n=30), the mean value of coronal curvature angle measured by the COL method in 3-D ultrasound was  $21.3^{\circ} \pm 15.1^{\circ}$ , while the average value by the Cobb method in MRI was  $21.7^{\circ} \pm 16.0^{\circ}$ . As shown in Fig 4.5, the curve profiles presented in the coronal plane of 3-D ultrasound images were similar to those of MRI images in AIS patients with mild, moderate and severe curvature angles (Fig. 4.5a-c); the two dashed lines in the scatter plot representing the coronal curvature angle measured by the COL method in 3-D ultrasound versus the Cobb method in MRI respectively were almost identical in the entire curve cohort (Fig 4.5d). Moreover, the Paired *t*-test results showed that there was no significant difference between these two methods under the circumstance of the different

coronal curvature magnitude, variation in selected upper-end vertebra (UEV) and variation in lower-end vertebra (LEV) between the 3-D ultrasound and MRI images (Table 4.1).

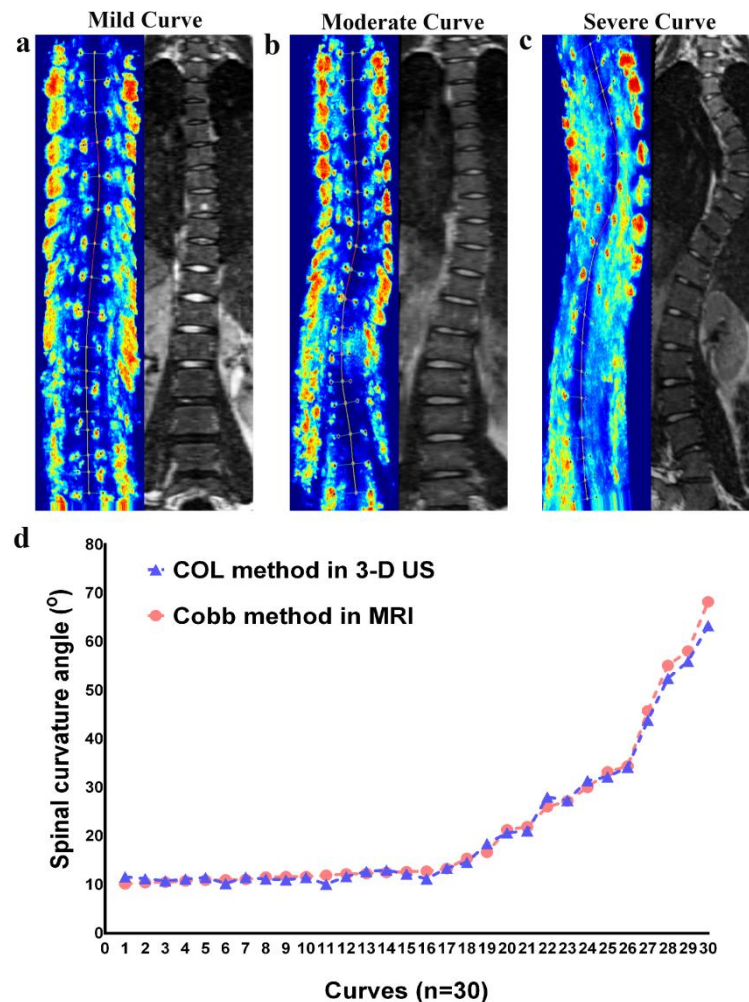


**Figure 4. 5 Comparison of 3-D ultrasound versus MRI measurements for AIS patients with:** (a) Mild curve; (b) Moderate curve; (c) Severe curve; (d) A scatter plot of the COL method in 3-D ultrasound versus the Cobb method in MRI for the entire curve cohort.

**Table 4. 1 Comparison of means of coronal curvature assessments between 3-D ultrasound and MRI methods**

	Curve, n	T-test Sig. (2-tailed)
<b>Cobb Angle Degrees</b>		
10.2~68.2°	30	0.20
10.0~20.0°	19	0.93
20.0~40.0°	7	0.78
<b>Variation in Selected UEV</b>		
variation=0	10	0.23
variation=1	14	0.15
variation=2	6	0.60
<b>Variation in Selected LEV</b>		
variation=0	13	0.37
variation=1	11	0.33
variation=2	6	0.98

UEV: Upper-end vertebra;

LEV: Lower-end vertebra

### **Bland-Altman Method**

The agreement between the COL method in 3-D ultrasound and the Cobb method in MRI was investigated using the Bland–Altman method, which consisted of a scatter plot of the two measurements difference against the average of the two measurements (Fig. 4.6), as well as bias and limits of agreement calculated (Table 4.2). Additional horizontal line represented the mean difference (bias) and the limits of agreement, i.e. the 95% confidence intervals of the measurements ( $\text{mean} \pm 1.96 \times \text{SD}$ ) (Bland and Altman 1995 and 1986). This method is the most popular statistical method for assessing agreement between two methods of clinical measurements [28]. As shown in Figure 4.6, the Bland-Altman plots exhibited good agreement between the 3-D ultrasound and MRI measurements of coronal curvature for the



overall curve cohort (n=30). The corresponding values of Bland-Altman bias, SD of bias and 95% limits of agreement were provided in Table 4.2, where the absolute bias between these two methods was  $0.3^\circ$ , and the 95% limits of agreement was  $-2.4^\circ \sim 3.1^\circ$ .

The impact of different Cobb angles on the agreement between the 3-D ultrasound and MRI measurements was further investigated. As shown in figure 4.6, the samples with  $10.0^\circ \sim 20.0^\circ$  showed lower discrepancy with respect to mean difference than the samples with Cobb angle  $20.0^\circ \sim 40.0^\circ$  (Fig. 4.6b-c). Almost all the measurements clustered around the central lines except the outliers with Cobb angle larger than  $60.0^\circ$ , showing low discrepancy between mean difference and limits of agreement. The absolute bias between these two measurements was  $0.0^\circ$  for the samples with Cobb angle  $10.0^\circ \sim 20.0^\circ$ , compared to  $-0.1^\circ$  for Cobb angle  $20.0^\circ \sim 40.0^\circ$ . Similarly, the 95% limits of agreement were  $-1.8^\circ \sim 1.8^\circ$  and  $-2.4^\circ \sim 2.2^\circ$  for the samples with Cobb angle  $10.0^\circ \sim 20.0^\circ$  and  $20.0^\circ \sim 40.0^\circ$  respectively (Table 4.2). These results indicated that the agreement between the 3-D ultrasound and MRI assessments of coronal curvature could be influenced by the extent of curve magnitude in patients with AIS, especially for the samples with Cobb angle larger than  $60.0^\circ$ .

Furthermore, the impact of variation in selected upper-end vertebra (UEV) and variation in lower-end vertebra (LEV) between the 3-D ultrasound and MRI images were studied. Notably, the samples with variation in selected UEV/LEV (equal to 0) showed lower discrepancy with respect to mean difference than the others with variation in selected UEV/LEV (equal to 1 or 2) (Fig. 4.6d-i). As shown in Table 4.2, the absolute bias between these two measurements was  $-0.4^\circ$  for the samples with variation in selected UEV (equal to 2), the 95% limits of agreement were  $-3.9^\circ \sim 3.1^\circ$ , the absolute difference (7.0) of which was larger than the commonly accepted difference ( $5^\circ$ ) between successive curvature

measurements [29, 30]. Similarly, the absolute bias between these two measurements was  $0.5^\circ$  for the samples with variation in selected UEV (equal to 1r), the 95% limits of agreement were  $-2.7^\circ \sim 3.7^\circ$ , the absolute difference ( $6.4^\circ$ ) of which was still larger than the commonly accepted difference ( $5^\circ$ ). These results suggested that the variation in selected end vertebra between 3-D ultrasound and MRI may decrease the agreement between these two methods. The accurate selection of UEV/LEV in reconstructed 3-D ultrasound images would increase the validity of 3-D ultrasound measurements of coronal curvature in patients with AIS.

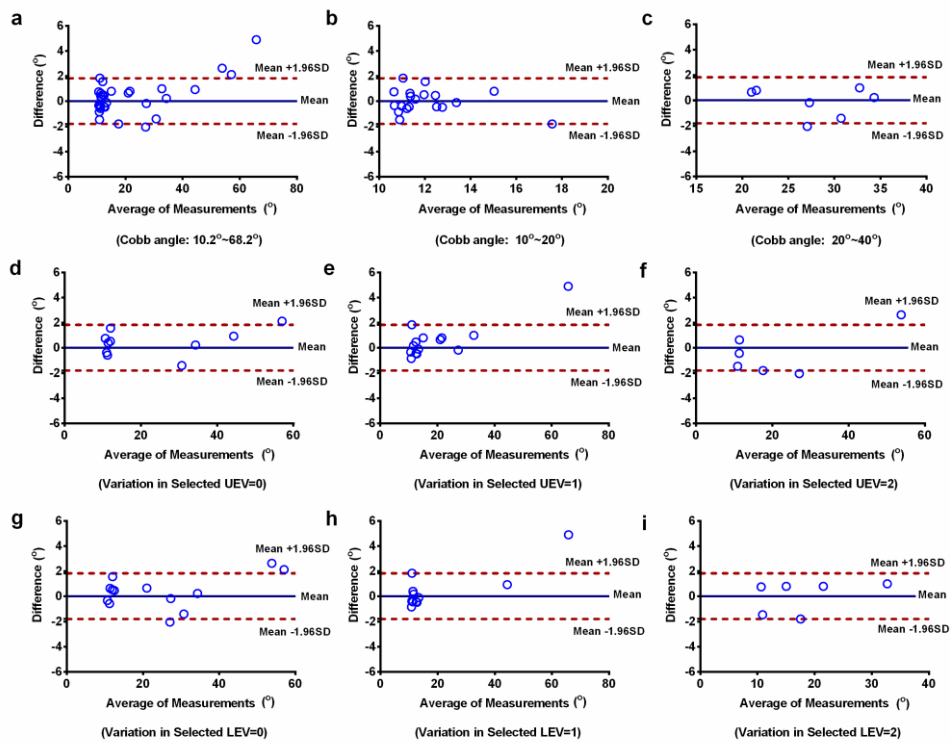


**Figure 4. 6 Bland–Altman plot assessing the agreement of coronal curvature measurements using 3-D ultrasound and MRI methods in the sample categories: (a) Cobb angle:  $10.2^\circ \sim 68.2^\circ$ ; (b) Cobb angle:  $10.0^\circ \sim 20.0^\circ$ ; (c) Cobb angle:  $20.0^\circ \sim 40.0^\circ$ ; (d) Variation in selected UEV=0; (e) Variation in selected UEV=1; (f) Variation in selected UEV=2; (g) Variation in selected LEV=0; (h) Variation in selected LEV=1; (i) Variation in selected LEV=2. The central line represents mean differences (Bias); Upper line shows**

mean+1.96SD and lower line mean-1.96SD. UEV: Upper-end vertebra; LEV: lower-end vertebra.

**Table 4. 2 Agreement of coronal curvature assessments between 3-D ultrasound and**

**MRI methods**

Curve, n	Bland-Altman method			
	Bias	SD of bias	95% Limits of Agreement	
<b>Cobb Angle Degrees</b>				
10.2~68.2°	30	0.3°	1.4°	-2.4° ~ 3.1°
10.0~20.0°	19	0.0°	0.9°	-1.8° ~ 1.8°
20.0~40.0°	7	-0.1°	1.2°	-2.4° ~ 2.2°
<b>Variation in Selected UEV</b>				
variation=0	10	0.4°	1.0°	-1.6° ~ 2.4°
variation=1	14	0.6°	1.4°	-2.2° ~ 3.4°
variation=2	6	-0.4°	1.8°	-3.9° ~ 3.1°
<b>Variation in Selected LEV</b>				
variation=0	13	0.3°	1.3°	-2.2° ~ 2.9°
variation=1	11	0.5°	1.6°	-2.7° ~ 3.7°
variation=2	6	0.0°	1.3°	-2.5° ~ 2.5°

UEV: Upper-end vertebra;

LEV: Lower-end vertebra.

**Pearson Correlation Analysis**

The Pearson correlation analysis was used to assess the correlation between the 3-D ultrasound and MRI methods when measuring the spinal curvature in the patients with AIS. The correlation between the COL method in 3-D ultrasound and the Cobb method in MRI was found to be high for all the sample categories (correlation coefficient  $r > 0.9$ ,  $P < 0.05$ ) (Fig. 4.7 and Table 4.3).

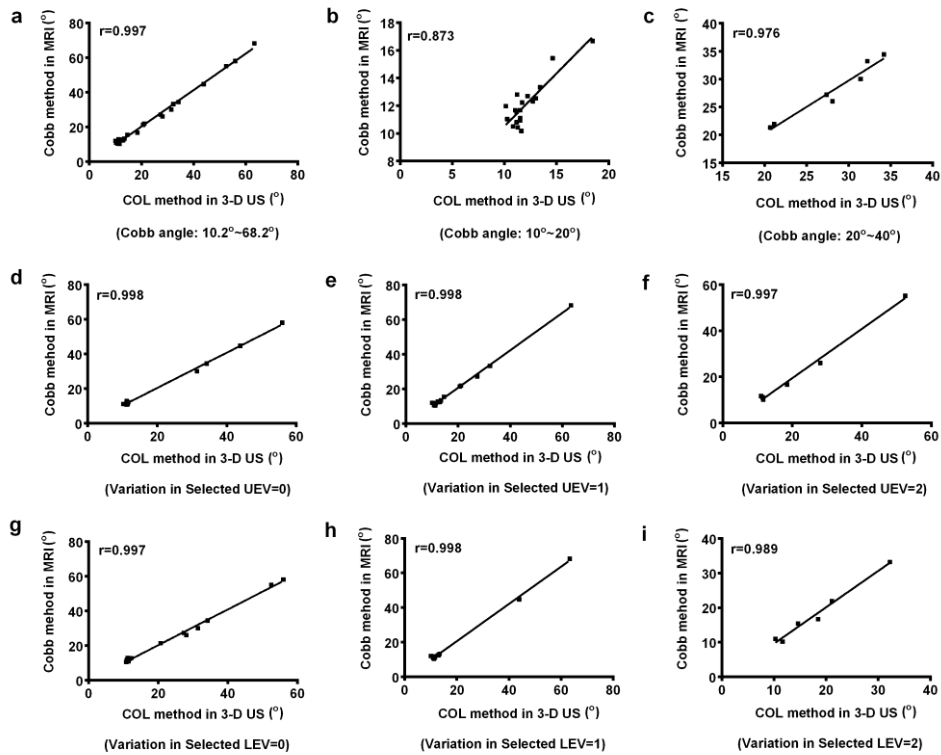


**Figure 4. 7 Correlation of coronal curvature measurements using 3-D ultrasound and MRI methods in the sample categories:** (a) Cobb angle:  $10.2^{\circ}\sim 68.2^{\circ}$ ; (b) Cobb angle:  $10.0^{\circ}\sim 20.0^{\circ}$ ; (c) Cobb angle:  $20.0^{\circ}\sim 40.0^{\circ}$ ; (d) Variation in selected UEV=0; (e) Variation in selected UEV=1; (f) Variation in selected UEV=2; (g) Variation in selected LEV=0; (h) Variation in selected LEV=1; (i) Variation in selected LEV=2. UEV: Upper-end vertebra; LEV: lower-end vertebra.

**Table 4. 3 Pearson correlation analyses of coronal curvature assessments between 3-D ultrasound and MRI methods**

	Curve, n	correlation coefficient (r.)
<b>Cobb Angle Degrees</b>		
10.2~68.2°	30	0.997
10.0~20.0°	19	0.873
20.0~40.0°	7	0.976
<b>Variation in Selected UEV</b>		
variation=0	10	0.998
variation=1	14	0.998
variation=2	6	0.997
<b>Variation in Selected LEV</b>		
variation=0	13	0.997
variation=1	11	0.998
variation=2	6	0.989

UEV: Upper-end vertebra;

LEV: Lower-end vertebra.

Taken together, the validity of the 3-D ultrasound assessment of spinal curvature in the coronal plane was demonstrated by comparison with the MRI measurement in the supine position.

#### **4.3.3 Validity of 3-D Ultrasound Assessments of Vertebral Rotation in AIS**

To determine the validity of 3-D ultrasound assessments of vertebral rotation in the transverse plane, the comparison of means, the Bland-Altman method and the Pearson correlation analysis were applied between the 3-D ultrasound and MRI measurements in the patients with AIS. Furthermore, the impact of apical vertebral rotation degrees, variation in selected apical vertebra between the 3-D ultrasound and MRI images, as well as the level of

apical vertebra on the validity of 3-D ultrasound assessment of vertebral rotation were investigated accordingly in the sample categories.

### **Comparison of means**

For the entire curve cohort (n=30), the mean value of vertebral rotation (AVR) measured by the COL method in 3-D ultrasound was  $7.7^{\circ} \pm 5.7^{\circ}$  while the average value by the Aaro-Dahlborn method in MRI was  $7.5^{\circ} \pm 5.2^{\circ}$ . Figure 4.8 shows three scatter plots of vertebral rotation (AVR) measurements using the 3-D ultrasound versus the MRI methods in the categorized samples. The mean absolute difference between these two methods were  $0.3^{\circ} \pm 0.3^{\circ}$ ,  $0.5^{\circ} \pm 0.3^{\circ}$  and  $1.0^{\circ} \pm 1.1^{\circ}$  for the samples with AVR of  $0.0^{\circ} \sim 5.0^{\circ}$ ,  $5.0^{\circ} \sim 10.0^{\circ}$ , and  $>10.0^{\circ}$  respectively. The paired Student's *t*-test results showed that there was no significant difference between these two methods, regardless of different vertebral rotation degrees, variation in selected apical vertebra between the 3-D ultrasound and MRI images, and various level of apical vertebra (Table 4.4).

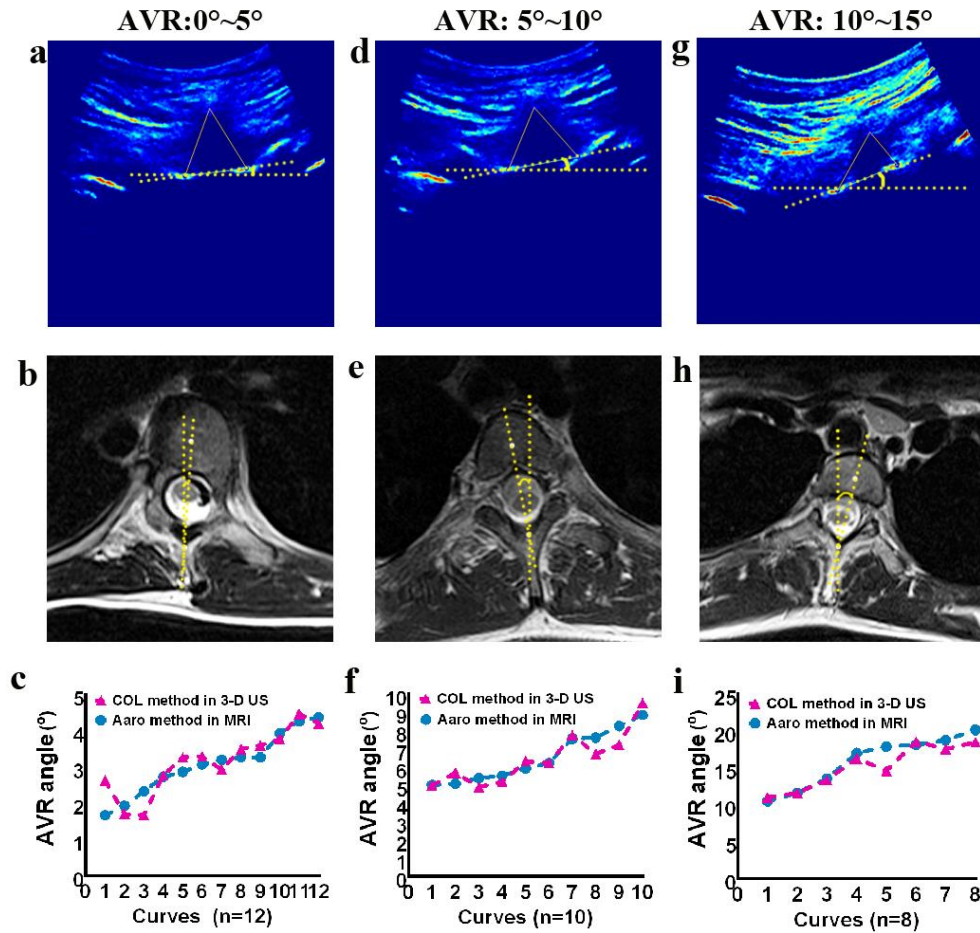


**Figure 4. 8 Comparison of measurements of apical vertebral rotation using 3-D ultrasound versus MRI methods in the sample categories: (a) ~ (c) AVR: 0.0°~5.0°; (d) ~ (f) AVR: 5.0°~10.0°; (g) ~ (i) AVR: >10.0°. AVR: apical vertebral rotation; COL: center of laminae; 3-D US: 3-D ultrasound.**

**Table 4. 4 Comparison of means of apical vertebral rotation assessments between 3-D ultrasound and MRI methods**

	Curve, n	T-test Sig. (2-tailed)
<b>AVR Degrees</b>		
0.0°~5.0°	12	0.54
5.0°~10.0°	10	0.63
>10.0°	8	0.13
Total	30	0.18
<b>Variation in Selected Apical Vertebra</b>		
variation=0	12	0.64
variation=1	12	0.28
variation=2	6	0.50
<b>Level of Apical Vertebra</b>		
T1-T4	4	0.34
T5-T8	7	0.13
T9-T12	9	0.62
L1-L5	9	0.67

AVR: apical vertebral rotation.

### **Bland-Altman Method**

The agreement between the 3-D ultrasound and MRI measurements was investigated using the Bland–Altman method. Of this method, the Bland–Altman plot showed the average of the two measurements (*x-axis*) against the difference between the two measurements (*y-axis*). Additional horizontal line represented the mean difference (bias) and the limits of agreement, i.e. the 95% confidence intervals of the measurements ( $\text{mean} \pm 1.96 \times \text{SD}$ ) (Bland and Altman 1995 and 1986). As shown in Figure 4.9, the Bland-Altman plots exhibited good agreement between the 3-D ultrasound and MRI measurements of vertebral rotation for the overall curve



cohort (n=30). The absolute bias between these two methods was  $0.2^\circ$ , and the 95% limits of agreement was  $-1.4^\circ \sim 1.8^\circ$  (Table 4.5).

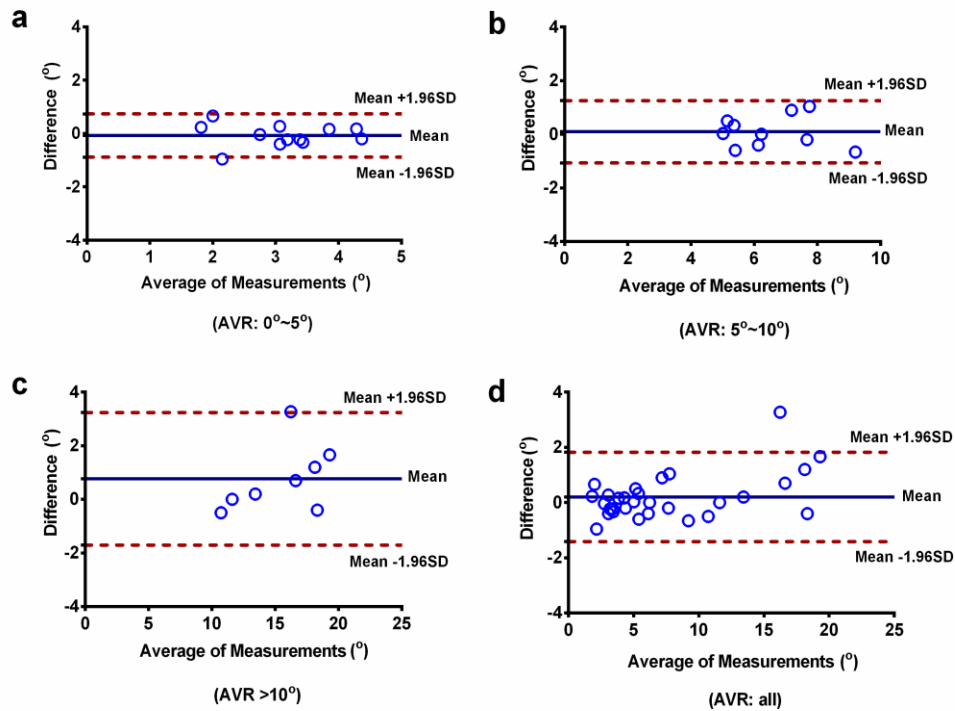


**Figure 4. 9** Bland–Altman plot assessing the agreement of apical vertebral rotation measurements using 3-D ultrasound versus MRI methods in the sample categories: (a) AVR:  $0.0^\circ \sim 5.0^\circ$ ; (b) AVR:  $5.0^\circ \sim 10.0^\circ$ ; (c) AVR:  $>10.0^\circ$ ; (d) the entire curve cohort. The central line represents mean differences (Bias); Upper line shows mean+1.96SD and lower line mean-1.96SD. AVR: apical vertebral rotation.

**Table 4. 5 Evaluation of agreement of apical vertebral rotation assessments between 3-D ultrasound and MRI methods**

Curve, n	Bland-Altman Method			
	Bias	SD of bias	95% Limits of Agreement	
<b>AVR Degrees</b>				
0.0°~5.0°	12	-0.1°	0.4°	-0.9° ~ 0.7°
5.0°~10.0°	10	0.1°	0.6°	-1.1° ~ 1.3°
>10.0°	8	0.8°	1.3°	-1.7° ~ 3.2°
Total	30	0.2°	0.8°	-1.4° ~ 1.8°
<b>Variation in Selected Apical Vertebra</b>				
variation=0	12	0.1°	0.7°	-1.3° ~ 1.5°
variation=1	12	0.4°	1.1°	-1.8° ~ 2.5°
variation=2	6	0.1°	0.4°	-0.6° ~ 0.8°
<b>Level of Apical Vertebra</b>				
T1-T4	4	-0.3°	0.5°	-1.4° ~ 0.7°
T5-T8	7	0.8°	1.2°	-1.6° ~ 3.2°
T9-T12	9	0.1°	0.7°	-1.2° ~ 1.4°
L1-L5	9	0.1°	0.6°	-1.0° ~ 1.2°

AVR: apical vertebral rotation.

The impact of different apical vertebral rotation (AVR) degrees on the agreement between the 3-D ultrasound and MRI measurements was further investigated. As shown in figure 4.3, the samples with AVR 0.0° ~ 5.0° showed lower discrepancy than the others with AVR 5.0° ~ 10.0° and >10.0° (Fig. 4.10 a-c). The samples with AVR 0.0° ~ 5.0°, 5.0° ~ 10.0° and >10.0° have the corresponding values of the absolute bias -0.1°, 0.1° and 0.8°, the 95% limits of agreement -0.9°~0.7°, -1.1°~1.3° and -1.7°~3.2° (Table 4.5). These results indicated that the validity of 3-D ultrasound measurement of vertebral rotation could be influenced when the extent of the rotation of the vertebra would be more than 10°.

Furthermore, the impact of variation in selected apical vertebra between the 3-D ultrasound and MRI images was studied. Notably, the samples with no variation showed lower discrepancy than the samples with variation (equal to 1), but larger than the samples with variation (equal to 2) (Fig. 4.10). Correspondingly, the least absolute bias and 95% limits of agreement were  $0.1^\circ$  and  $-0.6^\circ \sim 0.8^\circ$  for the samples with variation in selected apical vertebra (equal to 2) (Table 4.5). The reason for this may be due to the small proportion of the samples with variation in selected apical vertebra (equal to 2) for analyzed in this study.

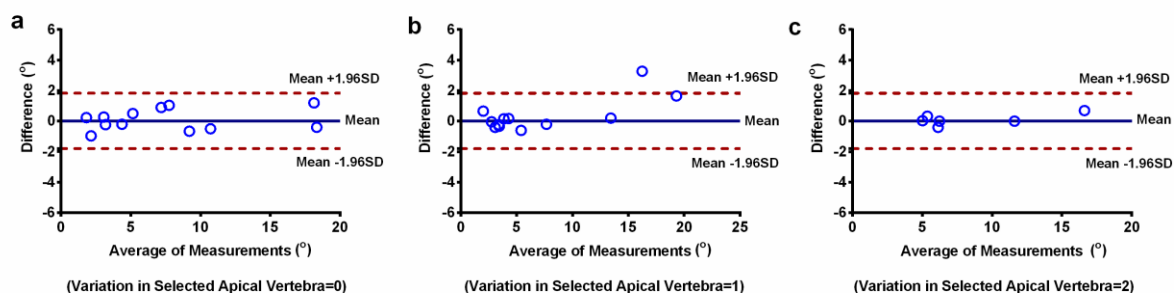


**Figure 4. 10 Bland–Altman plot assessing the agreement of apical vertebral rotation measurements using 3-D ultrasound versus MRI methods in the sample categories: (a) Variation in SAV =0; (b) Variation in SAV=1; (c) Variation in SAV=2. The central line represents mean differences (Bias); Upper line shows mean+1.96SD and lower line mean-1.96SD. AVR: apical vertebral rotation; SAV: selected apical vertebra.**

In addition, the impact of the level of apical vertebra on the validity of 3-D ultrasound measurements of vertebral rotation was investigated. As shown in Figure 4.11, the samples with level of apical vertebra in T5-T8 presented larger discrepancy than the others. The corresponding values of the absolute bias were  $0.3^\circ$ ,  $0.8^\circ$ ,  $0.1^\circ$  and  $0.1^\circ$  for the samples with level of apical vertebra in T1-T4, T5-T8, T9-T12 and L1-L5 respectively. Similarly, the 95%

limits of agreement were  $-1.4^{\circ} \sim 0.7^{\circ}$ ,  $-1.6^{\circ} \sim 3.2^{\circ}$ ,  $-1.2^{\circ} \sim 1.4^{\circ}$  and  $-1.0^{\circ} \sim 1.2^{\circ}$  for the samples with the above mentioned levels of apical vertebra (Table 4.5).

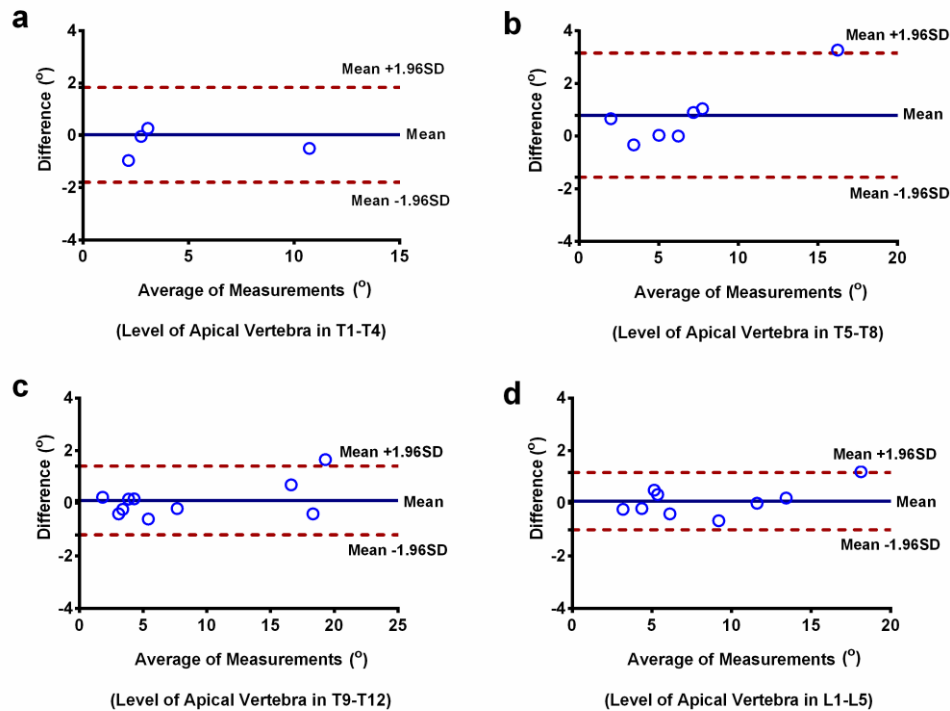


**Figure 4. 11 Bland–Altman plot assessing the agreement of apical vertebral rotation measurements using 3-D ultrasound versus MRI methods in the sample categories: (a) Level of apical vertebra in T1-T4; (b) Level of apical vertebra in T5-T8; (c) Level of apical vertebra in T9-T12; (d) Level of apical vertebra in L1-L5. The central line represents mean differences (Bias); Upper line shows mean+1.96SD and lower line mean-1.96SD. AVR: apical vertebral rotation.**

**Pearson Correlation Analysis**

The Pearson correlation analysis was used to assess the correlation between the 3-D ultrasound and MRI methods when measuring the vertebral rotation in the patients with AIS. The correlation coefficient ( $r$ ) in all the sample categories was greater than 0.8 ( $P < 0.05$ ),

indicating a high correlation between the 3-D ultrasound and MRI assessments of vertebral rotation (Table 4.6). The different vertebral rotation degrees, variation in selected apical vertebra between the 3-D ultrasound and MRI images, and various level of apical vertebra did not have effect on the Pearson correlation analysis between the 3-D ultrasound and MRI assessments (Figure 4.12-4.14).

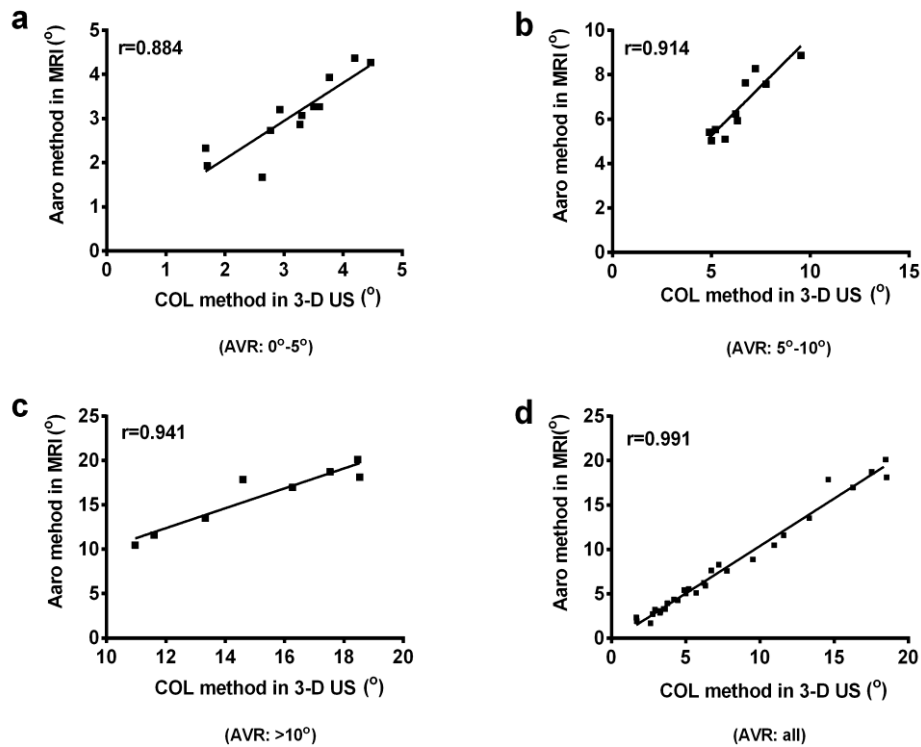


**Figure 4. 12 Correlation of apical vertebral rotation measurements using 3-D ultrasound versus MRI methods in the sample categories: (a) AVR: 0.0°~5.0°; (b) AVR: 5.0°~10.0°; (c) AVR: >10.0°; (d) the entire curve cohort. AVR: apical vertebral rotation; COL: center of laminar; 3-D US: 3-D ultrasound.**

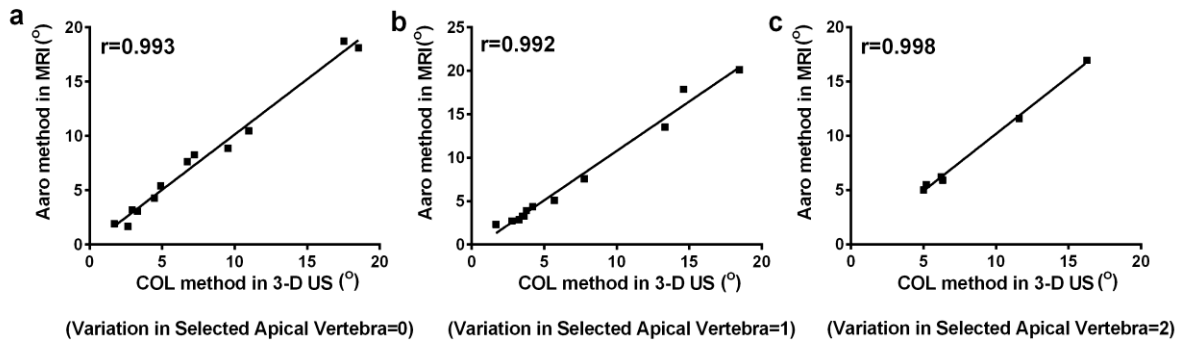


**Figure 4. 13 Correlation of apical vertebral rotation measurements using 3-D ultrasound versus MRI methods in the sample categories: (a) Variation in SAV =0; (b) Variation in SAV=1; (c) Variation in SAV=2. AVR: apical vertebral rotation; COL: center of laminar; 3-D US: 3-D ultrasound; SAV: selected apical vertebra.**

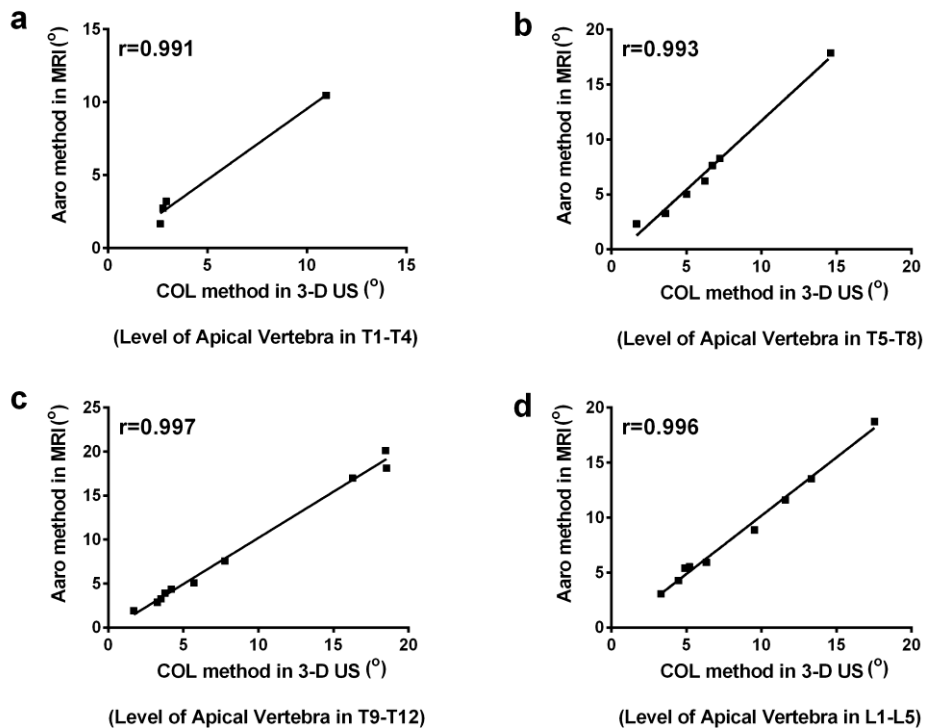


**Figure 4. 14 Correlation of apical vertebral rotation measurements using 3-D ultrasound versus MRI methods in the sample categories: (a) Level of apical vertebra in T1-T4; (b) Level of apical vertebra in T5-T8; (c) Level of apical vertebra in T9-T12; (d) Level of apical vertebra in L1-L5.**

Level of apical vertebra in L1-L5. AVR: apical vertebral rotation; COL: center of laminar; 3-D US: 3-D ultrasound.

**Table 4. 6 Pearson correlation analysis of apical vertebral rotation assessments between 3-D ultrasound and MRI methods**

	Curve, n	Pearson correlation coefficient (r.)
<b>AVR Degrees</b>		
0.0°~5.0°	12	0.884
5.0°~10.0°	10	0.914
>10.0°	8	0.941
Total	30	0.991
<b>Variation in Selected Apical Vertebra</b>		
variation=0	12	0.993
variation=1	12	0.992
variation=2	6	0.998
<b>Level of Apical Vertebra</b>		
T1-T4	4	0.991
T5-T8	7	0.993
T9-T12	9	0.997
L1-L5	9	0.996

AVR: apical vertebral rotation.

Taken together, the validity of the 3-D ultrasound measurements of vertebral rotation in the transverse plane was confirmed with the MRI measurements in patients with AIS.

#### **4.3.4 Validity of 3-D Ultrasound Assessment of Kyphotic/Lordotic Angles in AIS**

To determine the validity of 3-D ultrasound assessments of kyphosis and lordosis in the sagittal plane, the comparison of means, the Bland-Altman method and the Pearson

correlation analysis were applied between the 3-D ultrasound and MRI measurements in the patients with AIS.

**Comparison of Means**

For the entire cohort (n=16), the mean value of kyphotic angle measured by the SPA method in 3-D ultrasound was  $31.0^{\circ} \pm 6.6^{\circ}$  while the average value by the Cobb method in MRI was  $30.8^{\circ} \pm 7.1^{\circ}$ . The paired Student’s *t*-test showed that there was no significant difference between these two methods in the entire cohort. Interestingly, the statistical difference between the 3-D ultrasound and MRI assessments existed significantly when the kyphosis angles were within  $10.0^{\circ} \sim 30.0^{\circ}$  (Table 4.7).

**Table 4. 7 Comparison of means of kyphotic angle assessments between 3-D ultrasound and MRI methods**

Parameter	Range	Curve, n	T-test Sig. (2-tailed)
Kyphotic angle (T1-T12)	10.0°~30.0°	8	<i>p</i> <0.05
	30.0°~50.0°	8	0.18
	Total	16	0.65

However, for the entire cohort (n=16), the mean value of lordotic angle measured by the SPA method in 3-D ultrasound was  $18.8^{\circ} \pm 2.9^{\circ}$  while the average value by the Cobb method in MRI was  $31.6^{\circ} \pm 8.5^{\circ}$ . The significant difference was found between these two methods by the paired Student’s *t*-test in the entire cohort (Table 4.8).

**Table 4. 8 Comparison of means of lordotic angle assessments between 3-D ultrasound and MRI methods**

Parameter	Range	Curve, n	T-test Sig. (2-tailed)
-----------	-------	----------	------------------------



Lordotic angle (L1-L5)	10.0°~30.0°	8	$p<0.01$
	30.0°~50.0°	8	$p<0.01$
	Total	16	$p<0.01$

### **Bland-Altman Method**

The agreement of kyphosis measurements between the 3-D ultrasound and MRI was investigated using the Bland–Altman method. Of this method, the Bland–Altman plot showed the average of the two measurements (*x-axis*) against the difference between the two measurements (*y-axis*). Additional horizontal line represented the mean difference (bias) and the limits of agreement, i.e. the 95% confidence intervals of the measurements ( $\text{mean} \pm 1.96 \times \text{SD}$ ). As shown in Figure 4.15, the Bland-Altman plots exhibited good agreement between the 3-D ultrasound and MRI measurements of the thoracic kyphotic angle for the overall cohort (n=16). The absolute bias between these two methods was  $-0.2^\circ$ , and the 95% limits of agreement was  $-2.1^\circ \sim 3.7^\circ$  (Table 4.9).

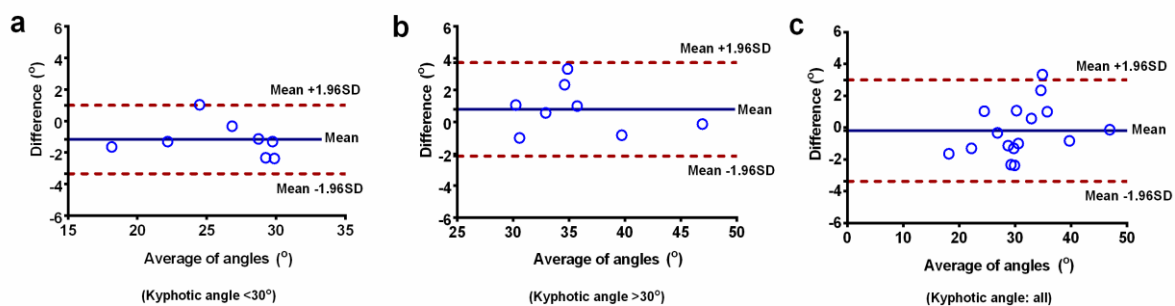


**Figure 4. 15 Bland–Altman plot assessing the agreement of kyphotic angle measurements using 3-D ultrasound versus MRI methods in the sample categories: (a) Kyphotic angle  $<30^\circ$ ; (b) Kyphotic angle  $>30^\circ$ ; (c) the entire curve cohort. The central line represents mean differences (Bias); Upper line shows  $\text{mean}+1.96\text{SD}$  and lower line  $\text{mean}-1.96\text{SD}$ .**

**Table 4.9 Agreement of kyphotic angle assessments between 3-D ultrasound and MRI method**

Parameter	Range	Curve, n	Bland-Altman method		
			Bias	SD of bias	95% Limits of Agreement
Kyphotic angle (T1-T12)	10.0°~30.0°	8	-1.2°	1.1°	-3.3° ~ 1.0°
	30.0°~50.0°	8	0.8°	1.5°	-3.3° ~ 1.0°
	Total	16	-0.2°	1.6°	-2.1° ~ 3.7°

However, the Bland-Altman plots exhibited poor agreement between the 3-D ultrasound and MRI measurements of the lumbar lordotic angle for the overall cohort (n=16) (Figure 4.16). The absolute bias between these two methods was 12.8°, and the 95% limits of agreement was -1.3°~26.9° (Table 4.10). Moreover, the greater the lumbar lordosis angle (30.0°~50.0°) is, the lower the agreement between the 3-D ultrasound and MRI measurements.

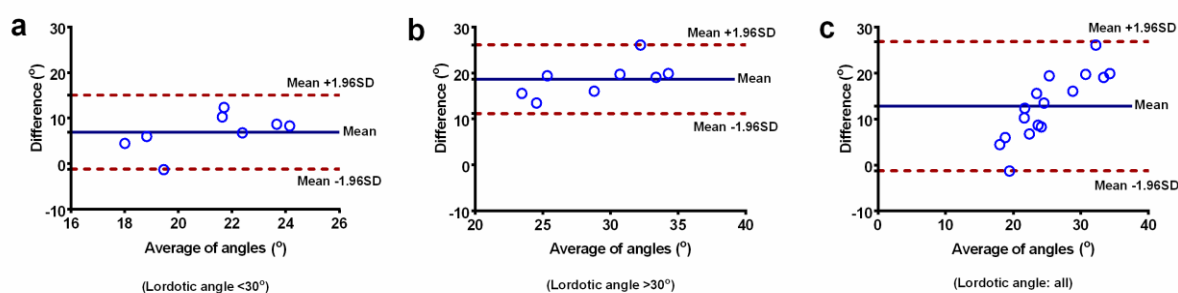


**Figure 4.16 Bland–Altman plot assessing the agreement of lordotic angle measurements using 3-D ultrasound versus MRI methods in the sample categories: (a) Lordotic angle <30°; (b) Lordotic angle >30°; (c) the entire curve cohort. The central line represents mean differences (Bias); Upper line shows mean+1.96SD and lower line mean-1.96SD.**

**Table 4. 10 Agreement of lordotic angle assessments between 3-D ultrasound and MRI methods**

Parameter	Range	Curve, n	Bland-Altman method		
			Bias	SD of bias	95% Limits of Agreement
Lordotic angle (L1-L5)	10.0°~30.0°	8	6.9°	4.1°	-1.2° ~ 15.1°
	30.0°~50.0°	8	18.7°	3.8°	11.2° ~ 26.2°
	Total	16	12.8°	7.2°	-1.3° ~ 26.9°

These results indicated that there was agreement between the 3-D ultrasound method (SPA) and MRI method (Cobb) when measuring the thoracic kyphosis rather than the lumbar lordosis in the patients with AIS.

**Pearson Correlation Analysis**

The Pearson correlation analysis was used to assess the correlation between the 3-D ultrasound and MRI methods when measuring the thoracic kyphosis and lumbar lordosis in the patients with AIS. The correlation coefficient (r) was greater than 0.9 (P<0.05) for the kyphotic angle measurements between these two methods (Table 4.11). Moreover, the correlation between the 3-D ultrasound and MRI assessments of the thoracic kyphosis was not affected by the degree of thoracic kyphotic angle (Figure 4.17).

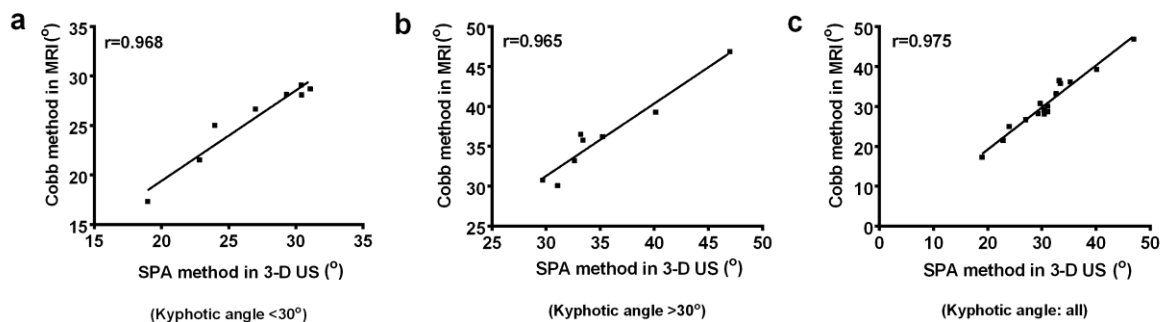


**Figure 4. 17 Correlation of kyphotic angle measurements using 3-D ultrasound versus MRI methods in the sample categories: (a) Kyphotic angle <30°; (b) Kyphotic angle >30°; (c) the entire curve cohort. SPA: spinous process angle; 3-D US: 3-D ultrasound.**

**Table 4. 11 Pearson correlation analysis of kyphotic angle assessments between 3-D ultrasound and MRI methods**

Parameter	Range	Curve, n	Pearson correlation coefficient ( <i>r</i> .)
Kyphotic angle (T1-T12)	10.0°~30.0°	8	0.968
	30.0°~50.0°	8	0.965
	Total	16	0.975

As shown in Figure 4.18, however, the correlation of lumbar lordosis measurements between the 3-D ultrasound and MRI methods was low, with the Pearson correlation coefficient (*r*) ranged from 0.103 to 0.753 (Table 4.12). These results suggested that the 3-D ultrasound measurement of lumbar lordosis was not correlated with the MRI assessment in the patients with AIS.

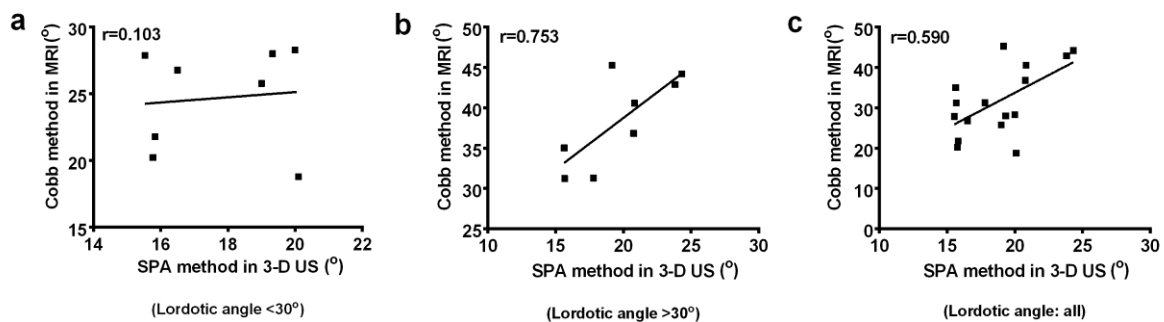


**Figure 4. 18 Correlation of lordotic angle measurements using 3-D ultrasound versus MRI methods in the sample categories:** (a) Lordotic angle <30°; (b) Lordotic angle >30°; (c) the entire curve cohort. SPA: spinous process angle; 3-D US: 3-D ultrasound.

**Table 4. 12 Pearson correlation analysis of lordotic angle assessments between 3-D ultrasound and MRI methods**

Parameter	Range	Curve, n	Pearson correlation coefficient ( <i>r.</i> )
Lordotic angle (L1-L5)	10.0°~30.0°	8	0.103
	30.0°~50.0°	8	0.753
	Total	16	0.590

In summary, the validity of the 3-D ultrasound method (SPA) in the sagittal plane was confirmed with the MRI method (Cobb) when measuring the thoracic kyphosis but not the lumbar lordosis for the patients with AIS.

## 4.4 Discussions

### 4.4.1 Validity Study of 3-D Ultrasound Assessment of Coronal Curvature in AIS

Nowadays, the radiographic assessment of scoliotic spine continues to be the most widely used method in a scoliosis clinic. In standing posterior-anterior radiographs, the spinal curvature can be assessed with the Cobb method, which was adopted by the Scoliosis Research Society (SRS) as the standard reference method to diagnose and monitor AIS [3].

On the basis of the reliability results, the validity of the COL method in 3-D ultrasound was investigated. In the previous studies, Lou et al. reported that the difference between spinal curvature angles measured using the COL method in ultrasound and the Cobb method in radiograph ranged from 0.2° to 1.4°; the correlation between these two methods was high for

mild and moderate AIS patients. This study showed comparable results to the previous studies when MRI was chosen to be the reference. MRI can provide a clear 3-D image of the scoliotic spine without radiation exposure [146], which is similar to ultrasound. Our study demonstrated that the coronal curvature measured by 3-D ultrasound showed no significant difference but strong correlation with MRI in the supine position.

In addition, the validity of ultrasound assessment was investigated by the Bland-Altman method, which is the most popular statistical method for assessing agreement between two methods of clinical measurements [248]. In this method, the 95% limits of agreement are the estimates of values, which mean 95% of differences between two methods will lie between these limits. The larger the 95% limits of agreement are, the more discrepancy between the two methods will be. Currently, the variation within  $5.0^\circ$  between successive curvature measurements has been considered to be acceptable clinical error [249, 250]. Therefore, it is postulated that the accuracy of the COL method of 3-D ultrasound will be validated if the 95% limits of agreement are within  $5.0^\circ$  between the 3-D ultrasound and MRI assessments. In the present study, 95% limits of agreement were reasonably narrow, not extending over the acceptable clinical error ( $5.0^\circ$ ) in most cases. These results demonstrated the validity of the COL method in 3-D ultrasound when measuring spinal curvature in the coronal plane. However, the curve magnitude of Cobb angle more than  $60^\circ$  or the variation in selected UEV/LEV (equal to 1 or 2) between the 3-D ultrasound and MRI images enlarged the 95% limits of agreement ( $> 5.0^\circ$ ). It appears that the severe scoliotic curve and end-vertebra selection error may influence the agreement between the 3-D ultrasound and MRI assessments, leading to the inaccurate measurement of coronal curvature using 3-D ultrasound. The possible reasons for these maybe the lower resolution of 3-D ultrasound images obtained from the difficult scanning of the severe curve, the lack of experience of

observers, as well as the changed posture of subjects from 3-D ultrasound to MRI scanning. Therefore, future studies are required to investigate how to enhance the resolution of 3-D ultrasound images, standardize the 3-D ultrasound scanning and measurement procedure, and reduce the end-vertebra selection error, in order to improve the validity of 3-D ultrasound measurement of coronal curvature in the patients with AIS.

#### **4.4.2 Validity Study of 3-D Ultrasound Assessment of Vertebral Rotation in AIS**

Several methods have been proposed to assess the vertebral rotation using radiographic images, based on the position of the projected landmarks in relation to the vertebral body [57, 95]. However, the measurements taken from the radiographic images only represent a projected rotation, which are not directly measured in the transverse plane. Furthermore, the frequent exposure to radiation has been of primary concern for the scoliotic patients [6]. Compared with the radiographic assessments, computed tomography (CT) and magnetic resonance imaging (MRI) both enable visualization of the transverse plane of the vertebra for the measurements of the vertebral rotation [3, 57]. The CT / MRI scans and measurements can provide the 3-D information of the spinal structure, thus they are clinically applicable for both preoperative and postoperative assessments of vertebral rotation [146, 252]. However, CT exposes the patients to more radiation than the standard radiographs and MRI examinations are often time-consuming and expensive. Therefore, it is not feasible to use CT / MRI in mass screening and frequent monitoring for scoliosis, such as the measurements of lateral curvature and vertebral rotation.

The posterior structure of vertebrae could be displayed by ultrasound imaging in the transverse plane. Similar to CT / MRI, ultrasound imaging can visualize and measure the vertebral rotation in the transverse plane of scoliotic spine [202, 230, 231]. In this study, the

validity of the 3-D ultrasound on vertebral rotation measurements has been demonstrated in the patients with AIS under the clinical setting. The COL method in 3-D ultrasound has been verified with the Aaro-Dahlborn method in MRI.

An important parameter in determining the validity of the new method of measurement is the agreement with a standard method. A recent systematic review concluded that the Bland-Altman method, correlation coefficient and comparison of means were the most common statistical methods used to measure the agreement in relevant studies [248]. In the current study, the validity of the 3-D ultrasound assessment of vertebral rotation has been demonstrated by these statistical methods. The results of comparison of means indicated that the difference between the 3-D ultrasound and MRI measurements seemed to be enlarged ( $0.3^{\circ}\pm 0.3^{\circ}$ ,  $0.5^{\circ}\pm 0.3^{\circ}$  and  $1.0^{\circ}\pm 1.1^{\circ}$ ) with the AVR degrees increased ( $0.0^{\circ} \sim 5.0^{\circ}$ ,  $5.0^{\circ} \sim 10.0^{\circ}$  and  $>10.0^{\circ}$ ). This observation was also supported from the Bland-Altman method, which clearly showed that the 95% limits of agreement ( $-0.9^{\circ} \sim 0.7^{\circ}$ ,  $-1.1^{\circ} \sim 1.3^{\circ}$  and  $-1.7^{\circ} \sim 3.2^{\circ}$ ) were extended with the increase of AVR degrees ( $0.0^{\circ} \sim 5.0^{\circ}$ ,  $5.0^{\circ} \sim 10.0^{\circ}$  and  $>10.0^{\circ}$ ). These observations suggested that the measurement errors of vertebral rotation using the 3-D ultrasound may be related with the extent of the rotation of the vertebra. Based on the theory of ultrasound imaging, the increase of vertebral rotation would have a tendency to make the spinous process block the ultrasound signals echoed from laminae, leading to the inadequate imaging of laminae and the inaccurate assessments of COL methods. Moreover, the large rib humps associated with the severe vertebral rotation would make it difficult to maintain a good surface contact between the ultrasound transducer and subject's back during the ultrasound scanning. Therefore, future studies are required to investigate how to improve the accuracy of 3-D ultrasound assessment, in particular, of the large rotation angle of vertebrae in the patients with AIS.



It is noticeable that the variation in selected apical vertebra (equal to 2) did not decrease the agreement between these two methods compared with the samples with no variation and variation (equal to 1). This may be due to the lower sample size (n=6) in the samples with variation in selected apical vertebra (equal to 2) relatively to the other two samples (both n=12).

Besides, the extent of rotation of the vertebra, variation in selected apical vertebra between the 3-D ultrasound and MRI images, and different levels of apical vertebra did not affect the correlation between the 3-D ultrasound and MRI measurements of vertebral rotation in the transverse plane. Contrary to the results obtained from the Bland-Altman method, the correlation coefficient (r) between these two methods for the samples with AVR of  $0.0^{\circ} \sim 5.0^{\circ}$  was lower than the samples with AVR of  $5.0^{\circ} \sim 10.0^{\circ}$  and  $>10.0^{\circ}$ . This might be due to the fact that the correlation coefficient does not perfectly represent the agreement between two variables. Above all, this study provided the preliminary evidence to support the validity of vertebral rotation measurements using the 3-D ultrasound in comparison with the MRI measurements in the transverse plane. Continuous studies with large sample size to further validate the 3-D ultrasound measurements of vertebral rotation in the patients with AIS will be necessary.

#### **4.4.3 Validity Study of 3-D Ultrasound Assessment of Kyphotic/Lordotic Angles in AIS**

The thoracic kyphosis is defined as the angle between the superior end-plate of T4 and the inferior end-plate of T12; while the lumbar lordosis is the angle between the inferior end-plate of T12 and the superior end-plate of S1 [3, 74]. The thoracic kyphosis and lordosis angles can be measured using the Cobb method in the sagittal plane of radiograph or MRI,

with the reliability ICC value ranged from 0.83 to 0.92 [74]. However, the Cobb method reflects only the inclination between the endplates of upper-end and lower-end vertebrae, rather than the actual 3-D characteristics of the kyphotic and lordotic angles from the sagittal view [74].

The 3-D ultrasound imaging could allow the radiation-free visualization of the coronal curvature and the vertebral rotation in the patients with AIS. However, it is still unknown whether to use the 3-D ultrasound to measure the thoracic kyphosis and lumbar lordosis of scoliotic spine in the sagittal plane. The spinous process angle (SPA) method has been proposed to measure the kyphotic and lordotic angles in the sagittal plane of 3-D ultrasound images [198, 199]. Specially, this method is based on the posterior structure of vertebrae along the curvature in the sagittal plane, compared with the Cobb method in radiograph.

Based on the characteristics of 3-D ultrasound imaging, the kyphotic and lordotic angles were estimated using the 3-D ultrasound method by means of the accumulating angles in the sagittal plane. The results have shown that the spinous process angle (SPA) method in 3-D ultrasound presented the high intra- and inter-rater reliabilities when measuring the thoracic kyphosis and lumbar lordosis. However, the validity of 3-D ultrasound method (SPA) was not verified in this study, especially for the lumbar lordotic angle measurement. The lumbar lordotic angle degrees obtained from the 3-D ultrasound and MRI methods were found neither to be in agreement nor correlated in the patients with AIS.

The inconsistency between the 3-D ultrasound and MRI measurements may be related to the different characteristics of these two methods. In fact, the kyphotic angle measured by the Cobb method only reflects the degree of tilt between the upper endplate of T1 and the lower

endplate of T12 in the sagittal plane, which is similar to the lordotic angle measurement between the upper endplate of L1 and the lower endplate of L5. In contrast, SPA method needs to calculate the sum of the angles formed between the two lines from three adjacent spinous processes from T1 to T12, and from L1 to L5 in the sagittal plane of 3-D ultrasound images as the angles of thoracic kyphosis and lumbar lordosis, respectively. Besides, the Cobb method plays emphasis on the structural features of the anterior vertebral body, while the SPA method on the sequential changes in the posterior part of the vertebrae, such as the spinal spinous processes of scoliotic spine [74].

Although the results of this study have not demonstrated the validity of SPA method in 3-D ultrasound, this method has shown its own advantages in the measurements of thoracic kyphosis and lumbar lordosis in the sagittal plane. Therefore, further research is still needed to validate the proposed 3-D ultrasound assessments with regard to the definition of kyphotic and lordotic angles in the sagittal profile and is conducted in a larger sample size.

#### **4.4.4 Limitation of Study**

Even though the eligible curves in this study involved a whole range of curve severity (from 10.2° to 68.2°) of the patients with AIS, the sample size and proportion of the severe curves was relatively small. Thus, further research is still required to evaluate the reliability of the proposed 3-D ultrasound assessment in a larger sample size. Furthermore, the quality of the 3-D reconstructed ultrasound images largely depends on the experience and scanning skills of the operator, which may affect the reliability and accuracy of the ultrasound assessments. Therefore, it is necessary to develop more advanced techniques that could facilitate the automatic ultrasound scanning. As well, the semi-automatic program used in reconstruction

and assessment of 3-D ultrasound images should be upgraded to a fully automatic program so as to reduce the human errors.

#### **4.4.5 Future Application of 3-D Ultrasound Assessments**

These results established the potential application of 3-D ultrasound as a clinical tool in the assessment of coronal curvature for the patients with AIS. Hence, it is feasible to propose and apply 3-D ultrasound method to assess the scoliotic spine, perform the school screening, and monitor the curve progression of AIS. On the basis of 3-D ultrasound assessments, continuous studies are deserved to monitor and assist the rehabilitation treatments for AIS. However, the 3-D ultrasound technology cannot be used on the subjects who have had spinal surgery with implants on the laminae, as well as possible laminar decortications and/or resection of the spinous processes. Metal implants inside the body make strong ultrasound reflections that may block the imaging of the required landmarks on the vertebra.

#### **4.5 Conclusion**

The major findings of this study were: (1) Compared with the Cobb method in MRI, the validity of the COL method in 3-D ultrasound on coronal curvature measurement has been demonstrated in the patients with AIS under the clinical setting. When the degree of scoliotic curve is more than  $60.0^\circ$ , the validity of 3-D ultrasound will be affected. (2) Compared with the Aaro-Dahlborn method in MRI, the validity of the COL method in 3-D ultrasound on vertebral rotation measurements has been demonstrated in the patients with AIS under the clinical setting. The increase of vertebral rotation would have a tendency to affect the accuracy of 3-D ultrasound assessments, in particular, of the large rotation angle of vertebrae in the patients with AIS. (3) Compared with the Cobb method in MRI, the validity of the SPA

method in 3-D ultrasound in the sagittal curvature measurements has not been demonstrated in the patients with AIS under the clinical setting.

In this study, the validity of 3-D ultrasound assessments has been verified, including the spinal curvature in the coronal plane (COL method); vertebral rotation in the transverses plane (COL method); kyphosis other than lordosis in the sagittal plane (SPA method). The 3-D ultrasound has the potential to offer a reliable and valid assessment for the patients with AIS under the clinical setting. A large sample size is required to further validate the proposed 3-D ultrasound method in the future studies. On the basis of the 3-D ultrasound assessments, continuous studies are deserved to monitor and assist the rehabilitation treatments for the patients with AIS in a non-invasive approach.

# **CHAPTER 5 Supine versus Standing Change of Coronal Curvature and Vertebral Rotation of 3-D Ultrasound Measurements in Adolescent Idiopathic Scoliosis**

## **5.1 Introduction**

Adolescent idiopathic scoliosis (AIS) presents with lateral and rotational deformities of spine. Due to the gravitational effect, spinal orientation between the standing and supine positions may change their corresponding lateral curvatures and vertebral rotations [262-265]. However, less is known about how the gravitational loading influences the coronal curvature and vertebral rotation in the patients with AIS.

While the majority of clinical assessments of scoliotic spine are performed on the standing radiographs, supine imaging modalities such as CT or MRI are used in the certain cases and can provide the valuable additional information on the difference in the scoliotic curve geometry between the supine and standing positions. Understanding this difference also gives researchers and clinicians the guidelines when interpreting the supine imaging modalities (such as CT or MRI) where a standing plane radiographic measure may not be available [148, 264-266].

Recent studies have shown that the curve magnitudes assessed on the supine MRI images would underestimate that measured on the standing radiographs, indicating the important biomechanical role of gravitational loading on the coronal curvature of scoliotic spine [148, 265, 266]. Moreover, Cobb angle measured from the supine MRI showed a strong positive correlation with that from the standing radiographs for structural or nonstructural curves, and

this correlation was not influenced by the patient age or body mass index [148, 265, 266]. However, the magnitudes of the coronal curvature changes between the supine and standing positions have been obtained from the different imaging modalities. Thus, it is advocated for the same imaging modality to be applied between the supine and standing positions, providing the relatively more realistic variation of the lateral curvature caused by the gravitational loading in the patients with AIS.

With respect to the rotation of vertebrae, previous research has investigated the effect of gravitational loading on the axial vertebral rotation in the normal subjects [267]. However, little is known about how the scoliotic axial deformity changes with the gravitational loading on the spine and how this subsequently affects the overall spinal deformity. It is necessary to understand the biomechanics of gravitational loading on the lateral curvature as well as the vertebral rotation in the assessments of scoliosis patients, which could be used as the measurements of spinal flexibility [264, 268] and assisted for the procedures of surgical and orthotic treatments [269, 270].

In summary, the purpose of this study is to investigate the gravitational effect on the changes of coronal curvature and vertebral rotation between the standing and supine postures using the same imaging modality, 3-D radiation-free ultrasound, in the patients with AIS. A further objective was to analyze the relevant factors to these changes and the correlation of 3-D ultrasound measurements between the supine *versus* standing positions in the patients with AIS.

## **5.2 Materials and Methods**

### **5.2.1 Subjects**

The subject selection criteria were as follows: 1) female adolescents; 2) age: 10-18 years; 3) Cobb angle: 10°-80°; 4) no prior surgical treatment; 5) out-of-brace MRI examination of the whole spine on the same morning.

Sixteen female subjects with AIS (aged  $15.4 \pm 2.6$  years) were recruited from the local scoliosis clinic. Human ethical approval was granted from both the Human Subjects Ethics Sub-committee of the Hong Kong Polytechnic University and the Joint Chinese University of Hong Kong-New Territories East Cluster Clinical Research Ethics Committee. All the examination procedures were explained and written informed consents were obtained from the subjects and their parents.

### **5.2.2 3-D Ultrasound System**

The 3-D ultrasound scan was performed with a 3-D SonixTABLET ultrasound unit (Analogic, Massachusetts, USA), consisting of a C5-2/60 convex transducer, SonixGPS and a 3D Guidance device (driveBAY, Ascension Ltd., USA). The related programs and parameters have been described in the Chapter 3.

### **5.2.3 Observers**

Same as described in the Chapter 3.

### **5.2.4 3-D Ultrasound Scan in the Supine / Standing Positions**

Ultrasound scanning was performed continuously along the coronal plane from C7 to S1, with the subjects in the standing and supine positions, respectively. After 3 times scanning



(with no breaks in between) in each position, the 3-D ultrasound reconstructed images were created and the two raters measured the spinal curvature and vertebral rotation independently in 3 trials each with one week interval. The time required was about 3 minutes for the 3-D ultrasound measurements.

### **3-D Ultrasound Scan in the Supine Position**

Same as described in the Chapter 3 (Figure 5.1a).

### **3-D Ultrasound Scan in the Standing Position**

The subjects were instructed to stand upright with the feet at shoulder width and the eyes looking at a horizontal steadfast object. The spinous processes from C7 to S1 were palpated and the general trend of coronal curvature was marked on the subjects' back by a water soluble marker. Ultrasound scanning was conducted continuously along the region of scoliotic spine from C7 to S1 (Figure 5.1b). Similar to the ultrasound scanning in the supine position, it also took less than 1 min to complete a full scan.

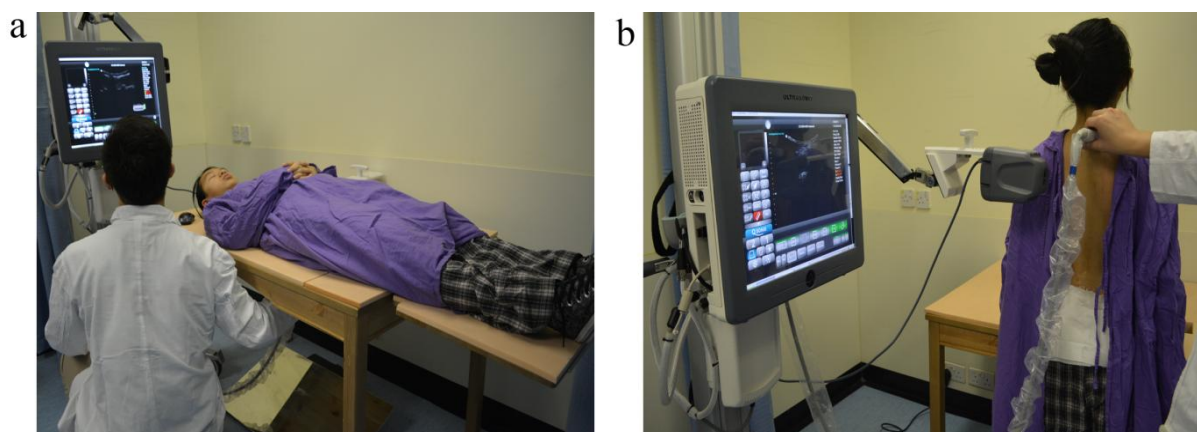


**Figure 5. 1 3-D Ultrasound Scanning in the Supine (a) and Standing (b) Positions.**

### **5.2.5 3-D Ultrasound Assessments of Patients with AIS**

#### **Spinal Curvature in the Coronal Plane**

Same as described in the Chapter 3.

#### **Vertebral Rotation in the Transverse Plane**

Same as described in the Chapter 4.

### **5.2.6 Statistical Analysis**

Statistical analyses were performed using the IBM SPSS Statistics Version 21 (IBM, USA). A *p*-value less than 0.05 were considered to be statistically significant. Statistical graphs were made with GraphPad Prism Version 6.01 software (GraphPad, La Jolla, California, USA).

The difference of lateral curvature and vertebral rotation measurements between the supine and standing positions was presented as means  $\pm$  SD. Multi-linear regression was used to analyze the factors related to the supine *versus* standing changes of lateral curvature and vertebral rotation in the patients with AIS. The dependent variable was assigned as the coronal curvature degree in the supine position, the coronal curvature degree in the standing position, the vertebral rotation degree in the supine position, the vertebral rotation degree in the standing position, as well as the variation in selected upper-end vertebra (UEV), the lower-end vertebra (LEV), and the apical vertebra between supine *versus* standing positions. In addition, Pearson correlation analysis was used to investigate the possible correlation between standing and supine postures in the two clinical parameters: coronal curvature angles and vertebral rotation angles, respectively.

## 5.3 Results

### 5.3.1 Comparison of 3-D Ultrasound Measurements in Supine versus Standing Positions

The average of the 3 times data measured by the rater 1 was used in the present study. The difference of lateral curvature and vertebral rotation measurements between the supine *versus* standing positions were presented as means  $\pm$  SD.

#### Average Difference of Coronal Curvature Angle

The 3-D ultrasound measurements of coronal curvature angle in the supine and standing positions were shown in Figure 5.2. For the entire curve cohort (n=30), the range of coronal curvature angle measured by the COL method in 3-D ultrasound was 10.1°~63.3° in the supine position, while 12.0°~69.9° in the standing position. The average difference of coronal curvature angle between these two positions was 4.1° $\pm$ 2.0°, the range was between 1.9° and 11.7°. As shown in Table 5.1, the mean value of supine *versus* standing change of the lateral curvature was 3.0° $\pm$ 0.8°, 5.1° $\pm$ 1.3° to 7.0° $\pm$ 3.3° for the samples with supine COL value at the range of 10.0°-20.0°, 20.0°-40.0°, and >40.0° respectively.

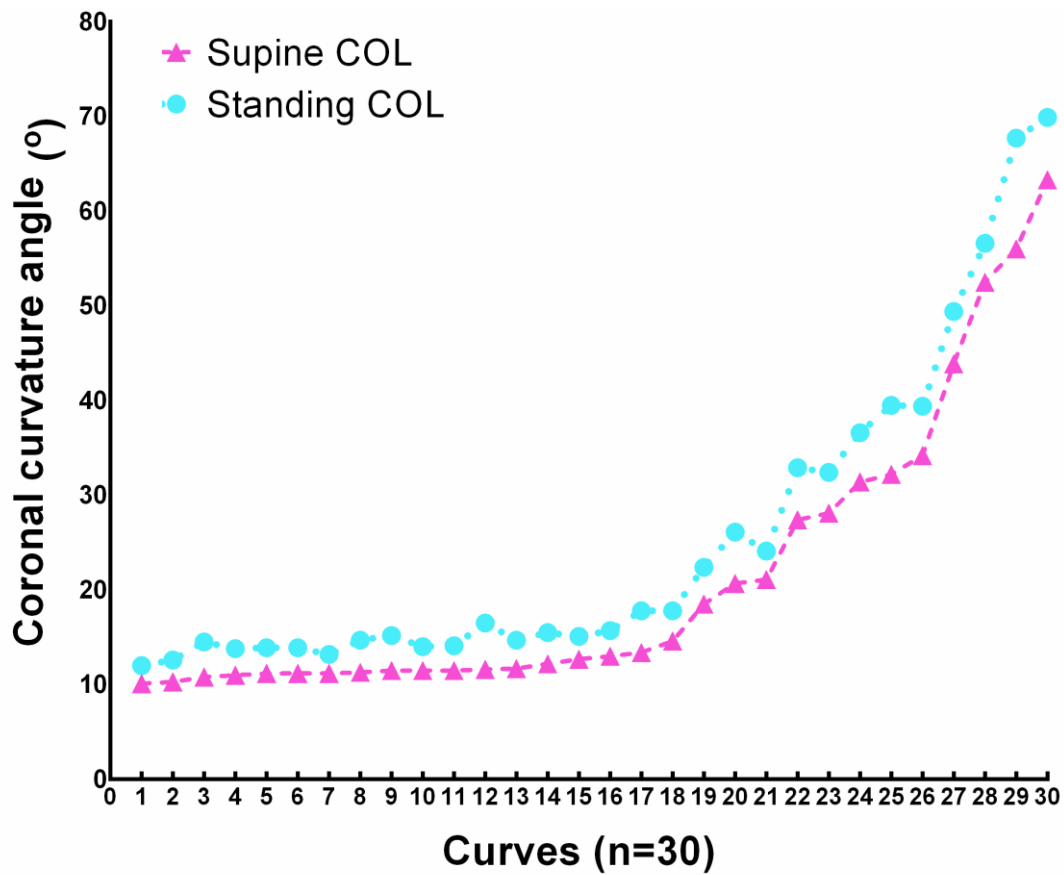


**Figure 5. 2 Comparison of coronal curvature measurements using 3-D ultrasound between supine versus standing positions in patients with AIS**

**Table 5. 1 Average difference of coronal curvature angle between supine versus standing positions using 3-D ultrasound measurements in AIS**

Method	Coronal Curvature Angle (Supine)	Supine versus Standing		
		Curve, n	Average difference	Range
3-D ultrasound (COL)	10.0°-20.0°	19	3.0°±0.8°	1.9°~4.9°
	20.0°-40.0°	7	5.1°±1.3°	3.0°~7.3°
	>40.0°	4	7.0°±3.3°	4.1°~11.7°
	Total	30	4.1°±2.0°	1.9°~11.7°

COL: Center of Laminae.

### **Average Difference of Vertebral Rotation Angle**

The 3-D ultrasound assessments of vertebral rotation angle in the supine and standing positions were shown in Figure 5.3. For the entire curve cohort (n=30), the range of vertebral rotation angle measured by the COL method in 3-D ultrasound was 1.7°~18.7° in the supine position, while 3.1°~24.3° in the standing position. The average difference of vertebral rotation angle between these two positions was 2.1°±1.2°, the range was between 0.0° and 5.9°. As shown in Table 6.2, the mean value of supine *versus* standing change of the vertebral rotation was 2.0°±0.6°、 1.2°±1.0°、 3.2°±1.4° for the samples with supine COL value at the range of 0.0°~5.0°、 5.0°~10.0°、 >10.0° respectively. Interestingly, the vertebral rotation angle within the 0.0°~5.0° was found to have greater supine *versus* standing change than that within the 5.0°~10.0°. The reason may be due to that the vertebra with lower rotation angle would be more susceptible to the change of posture during the 3-D ultrasound scanning and measure.

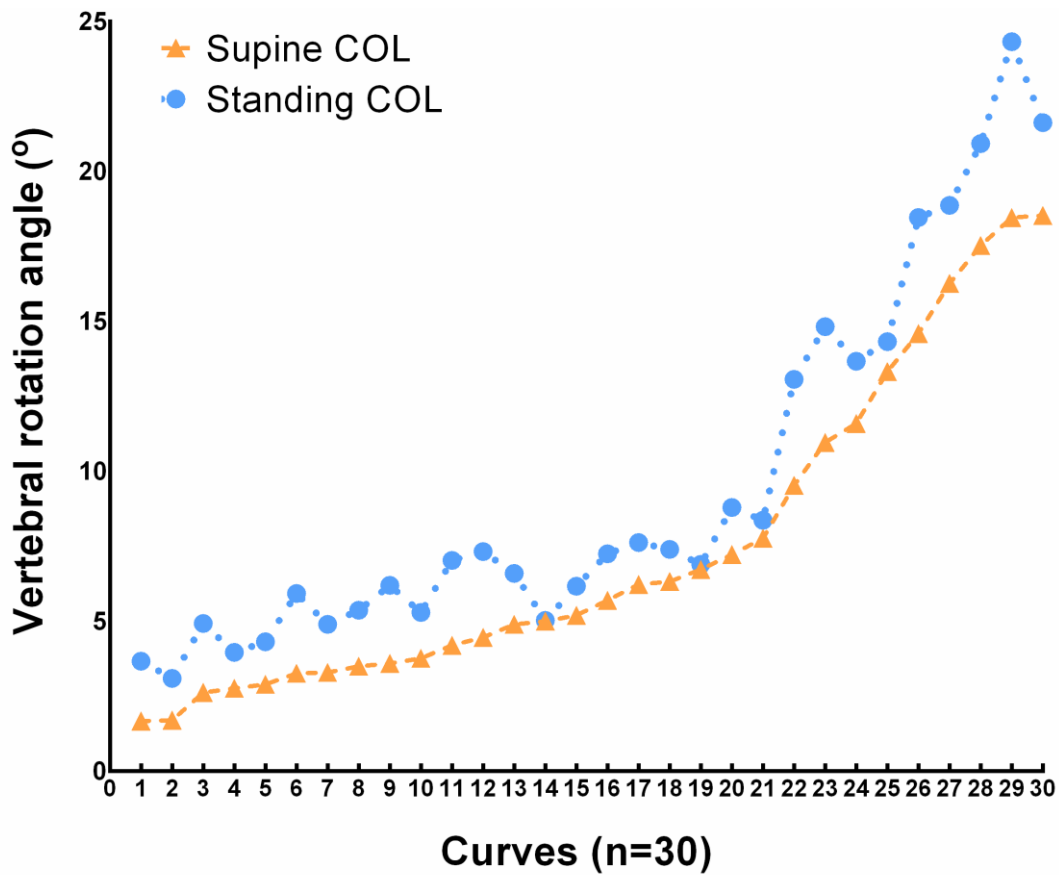


Figure 5. 3 Comparison of vertebral rotation measurements using 3-D ultrasound between supine and standing positions in patients with AIS.

Table 5. 2 Average difference of coronal curvature angle between supine versus standing positions using 3-D ultrasound measurements in AIS

Method	Vertebral Rotation Angle (Supine)	Supine versus Standing		
		Curve, n	Average difference	Range
3-D ultrasound (COL)	0.0°~5.0°	13	2.0°±0.6°	1.2°~2.9°
	5.0°~10.0°	9	1.2°±1.0°	0.0°~3.5°
	>10.0°	8	3.2°±1.4°	1.0°~5.9°
	Total	30	2.1°±1.2°	0.0°~5.9°

COL: Center of Laminae.

### **5.3.2 Relevant Factors to 3-D Ultrasound Measurement Difference in Supine versus Standing Positions**

Further research was conducted to investigate the potential factors to the change of lateral curvature and vertebral rotation from supine to standing positions. Multi-linear regression was used to analyze whether there was a relationship between the mean supine *versus* standing change of 3-D ultrasound measurements and the possible variables, including the coronal curvature degree in supine, coronal curvature degree in standing, vertebral rotation degree in supine, vertebral rotation degree in standing, as well as variation in selected upper-end vertebra (UEV), lower-end vertebra (LEV), and apical vertebra between the supine and standing positions.

#### **Relevant Factors to Coronal Curvature Difference in Supine versus Standing Positions**

As shown in Table 5.3, multi-linear regression revealed a statistically significant relationship between the mean change of the coronal curvature from supine to standing positions and three of the candidate independent variables: coronal curvature angle in the supine position ( $p < 0.001$ ), coronal curvature angle in the standing position ( $p < 0.001$ ) and variation in selected upper-end vertebra between these two positions ( $p = 0.03$ ).

**Table 5. 3 Multiple linear regression of coronal curvature difference in supine versus standing positions.**

Dependent variable	Independent variable	Unstandardized Coefficients		Standardized Coefficients	t	Sig.
		Beta	Std. Error	Beta		
Coronal Curvature Difference (Supine <i>versus</i> Standing)	Coronal Curvature Angle (Supine)	-1.00	0.01	-7.54	-144.25	0.00
	Coronal Curvature Angle (Standing)	1.00	0.01	8.32	162.66	0.00
	Vertebral Rotation Angle (Supine)	0.00	0.00	-0.01	-0.86	0.40
	Vertebral Rotation Angle (Standing)	0.00	0.00	0.00	0.47	0.64
	Variations in Selected UEV	-0.03	0.01	-0.01	-2.30	0.03
	Variations in Selected LEV	-0.01	0.01	0.00	-0.59	0.56

The statistical data are obtained from IBM SPSS 21.0 software.

UEV: Upper-end Vertebra

LEV: Lower-end Vertebra

**Relevant Factors to Vertebral Rotation Difference in Supine versus Standing Positions**

Similarly, multi-linear regression revealed a statistically significant relationship between the mean change of the vertebral rotation from supine to standing positions and the candidate independent variables: vertebral rotation angle in the supine position ( $p < 0.001$ ) and vertebral rotation angle in the standing position ( $p < 0.001$ ) (Table 5.4).

To sum up, the changes of coronal curvature and vertebral rotation between the supine to standing positions were related to the coronal curvature and vertebral rotation angles itself. It is postulated that the effect of the gravitational loading on the spine might be depended on the lateral curvature and vertebral rotation degrees of scoliotic spine.



**Table 5. 4 Multiple linear regression of vertebral rotation difference in supine versus standing positions.**

Dependent variable	Independent variable	Unstandardized Coefficients		Standardized Coefficients	t	Sig.
		Beta	Std. Error	Beta		
Vertebral Rotation Difference (Supine <i>versus</i> Standing)	Vertebral Rotation Angle (Supine)	-1.00	0.01	-4.22	-185.43	0.00
	Vertebral Rotation Angle (Standing)	1.00	0.01	4.86	203.92	0.00
	Coronal Curvature Angle (Supine)	0.00	0.00	-0.02	-0.46	0.65
	Coronal Curvature Angle (Standing)	0.00	0.00	0.02	0.30	0.76
	Variation in Selected Apical Vertebra	-0.01	0.01	0.00	-0.81	0.42

The statistical data are obtained from IBM SPSS 21.0 software.

### 5.3.3 Correlation of 3-D Ultrasound Measures between Supine and Standing Positions

Pearson correlation analysis was used to investigate the possible correlation between the standing and supine postures in the two clinical parameters: coronal curvature angles and vertebral rotation angles, respectively.

#### **Correlation of Coronal Curvature Measurements between Supine and Standing Positions**

The graphic representation of the Pearson's correlation analysis showed a strong positive correlation of the coronal curvature measurements between the supine and standing positions, with the Pearson correlation coefficient (r) equal to 0.997 (Table 5.5). The derived formula for converting the coronal curvature angle measured by the 3-D ultrasound from supine to

standing positions was  $y=1.1008x+1.9049$ , where y and x represented the coronal curvature angle measured in the standing and supine positions, respectively (Figure 5.4).

**Table 5.5 Pearson correlation coefficient (r) between supine and standing positions**

Measurement	Sample no. (Curves)	Pearson Correlation Coefficient (r)
Coronal curvature angle	30	0.997
Vertebral rotation angle	30	0.985

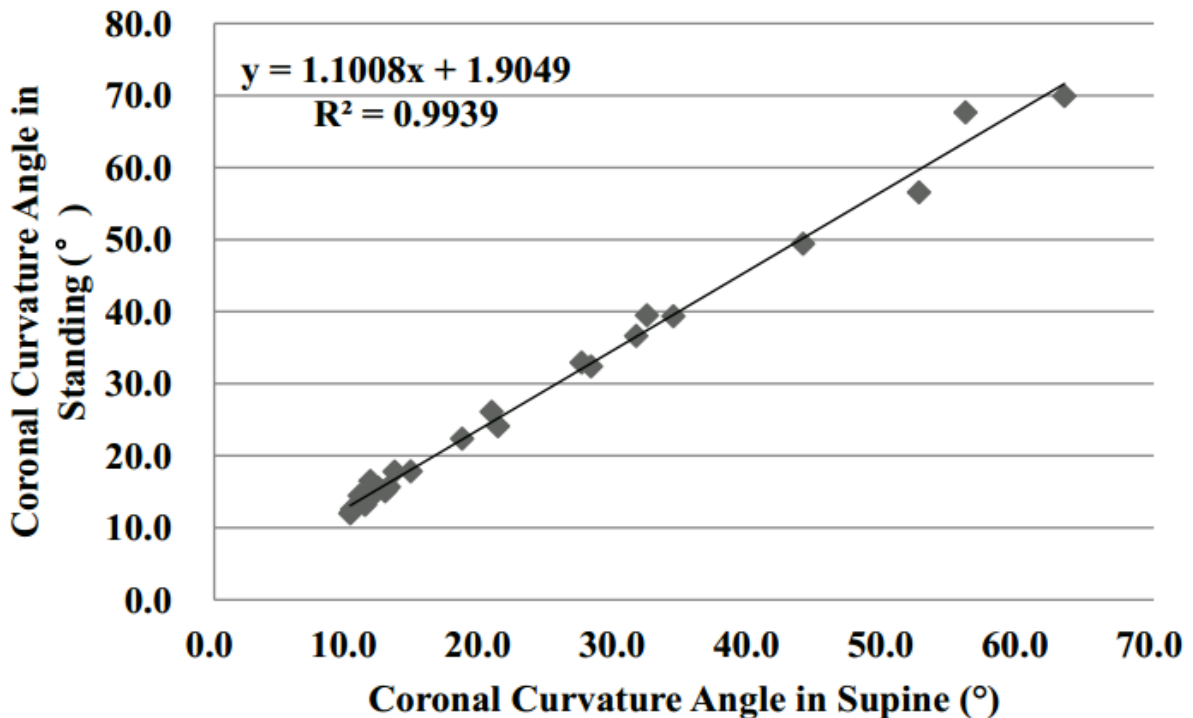


**Figure 5.4 Correlation of coronal curvature measurements using 3-D ultrasound between supine and standing positions in patients with AIS.**

**Correlation of Vertebral Rotation Measurements using 3-D Ultrasound**

Similarly, a strong positive correlation of vertebral rotation measurements between the supine and standing positions has been also demonstrated by the Pearson’s correlation analysis, where the Pearson correlation coefficient (r) was equal to 0.985 (Table 5.5). The formula

could be derived as  $y=1.1318x+1.1039$  for converting the vertebral rotation angle measured by 3-D ultrasound from supine to standing positions, where y and x represented the vertebral rotation angle measured in the standing and supine positions, respectively (Figure 5.5).

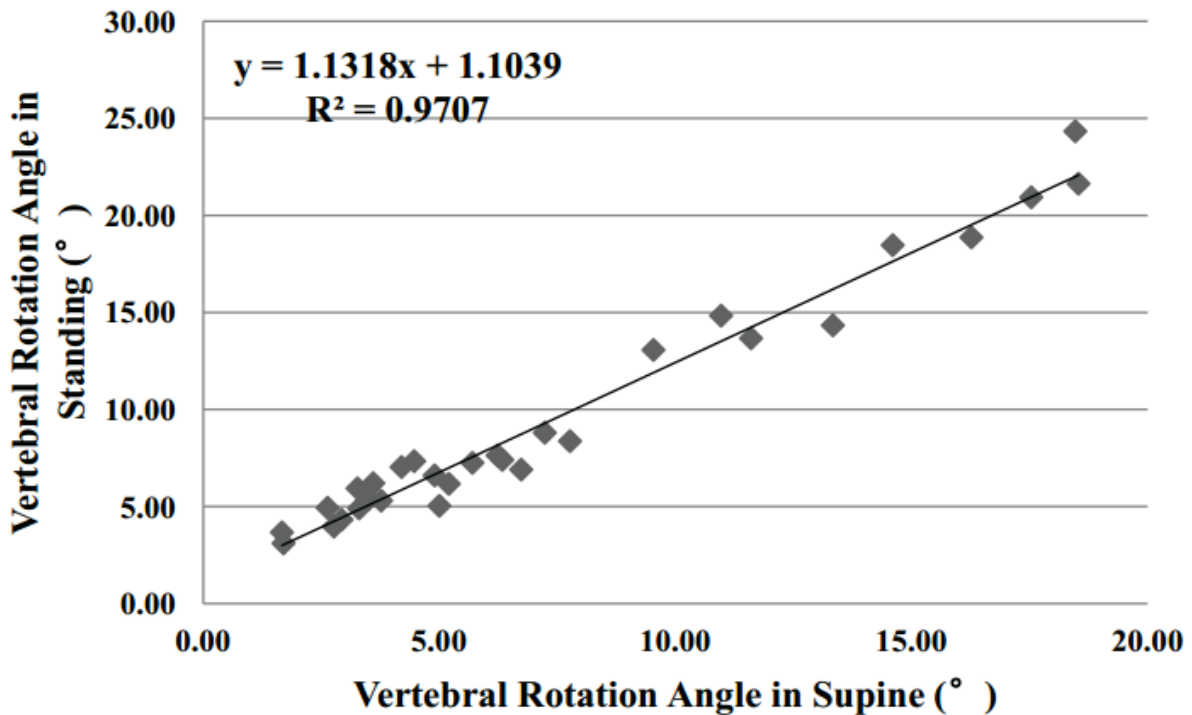


**Figure 5. 5 Correlation of vertebral rotation measurements using 3-D ultrasound between supine and standing positions in patients with AIS.**

## 5.4 Discussions

In the current clinical practice of scoliosis, the majority of assessments are undertaken in the standing radiographs. Meanwhile, the supine imaging modalities such as CT or MRI can provide the important information of the 3-D characteristics of the scoliotic spine, thus they are clinically applicable for both preoperative and postoperative assessments of lateral curvature and vertebral rotation [146, 252]. It is essential for the researchers and clinicians specialized on the spinal deformity to understand the supine *versus* standing postural

differences when interpreting the assessment data provided by the supine imaging modalities (such as CT or MRI) where a standing (plane radiographic) measure may not be available [148, 264-266, 271]. Currently, the supine *versus* standing differences of the coronal curvature have been investigated in the patients with AIS.

In addition to the change in the lateral curvature, the postures from supine to standing is also likely to cause the differences in the vertebral rotation (particularly some de-rotation of the rib hump is likely to occur during the supine scanning) [272]. Thus, the primary aim of this study was to identify the supine *versus* standing changes of both the coronal curvature and vertebral rotation using the same imaging modality, 3-D ultrasound, in the patients with AIS. The range of coronal curvature change was between  $1.9^{\circ}$  and  $11.7^{\circ}$ , while the vertebral rotation between  $0.0^{\circ}$  and  $5.9^{\circ}$ . The results obtained in the current study were comparable to the previous studies performed by Zetterberg et al. [267] and Torell et al. [262], in which the coronal curvature change was within  $6.1^{\circ} \sim 9.0^{\circ}$  in the radiographic measurements during the postural changes. However, the postural change of lateral curvature found in this study was lower than the  $11.4^{\circ} \sim 16.3^{\circ}$  reported in the Yazici et al. [263] and Keenen et al.'s [264] studies. It is obvious that in the previous studies, the coronal curvature was measured using the CT in the supine position and the radiograph in the standing position, but not the same imaging modality as performed in the current study. Taken together, the magnitudes of coronal curvature and vertebral rotation change measured in this study expanded the knowledge of the postural differences when comparing the supine to standing images of the patients with scoliotic spine.

Furthermore, the secondary purpose of this study was to determine whether any variables were linked to the supine *versus* standing changes of the coronal curvature and vertebral

rotation. The magnitude of coronal curvature and the variation in selected upper-end vertebra (UEV) between these two postures were found to be significantly associated with the coronal curvature change, while the magnitude of vertebral rotation was linked to the vertebral rotation change during the postural difference. From a biomechanical perspective, the patients with a larger coronal curvature angle have greater moments acting on their spine due to the gravitational loading, so it is intuitive that the supine *versus* standing change of coronal curvature would be related to the curve magnitude. In addition, the vertebral rotation has been reported to be coupled with the lateral curvature in the scoliotic spine. Interestingly, the supine *versus* standing difference of coronal curvature was also found to be associated with the selection of upper-end vertebra (UEV) rather than the lower-end vertebra (LEV) between the two postures. However, this was not consistent with the previous study, in which the pre-selection of vertebral endplates was reported to have no clinically significant effect on the coronal curvature change between the supine and standing positions. The reason may be due to the different method used to select the end vertebrae in the 3-D ultrasound images compared with that in the CT or radiographic images. Overall, these results suggest that the variation of selected end-vertebra between the two postures still need to be taken into account when interpreting the supine to standing change of the coronal curvature in the patients with AIS.

Besides, the present study suggests that the supine to standing change of coronal curvature and vertebral rotation could be further investigated as an alternative flexibility measure for the scoliotic spine, especially for the cases when additional imaging is undesirable or not available [264, 268]. A current method for assessing the spinal flexibility is the use of fulcrum bending radiographs. To predict the curve correct ability, the fulcrum is deliberately placed against the rib corresponding to the apex of the curve, in which the effect of muscle

activation would be reduced. By contrast, the supine to standing change of coronal curvature and vertebral rotation can be considered as a globalized loading where factors such as increasing gravitational loading at lower vertebral levels and muscle activation could play a significant role.

Based on the positive correlations between the two postures demonstrated by the Pearson's' correlation analysis, the formula have been derived for converting the coronal curvature and vertebral rotation angles measured by 3-D ultrasound in the supine position to those in the standing position respectively. The eligible curves in this study involved a whole range of curve severity (from 10.2° to 68.2°) of the patients with AIS, but the proportion of the severe curves was relatively small. Thus, it is required to validate this formula with regard to the changes of coronal curvature and vertebral rotation between the supine and standing positions in a larger sample size.

## **5.5 Conclusions**

The major findings of this study were: (1) the supine *versus* standing change of coronal curvature measured by the 3-D ultrasound is within 1.9°~11.7°; while the vertebral rotation changes within 0.0°~5.9°; (2) the magnitude of coronal curvature and the selection of upper-end vertebra between the two postures have clinically significant effect on the coronal curvature change measured by the 3-D ultrasound; (3) the difference of vertebral rotation of the 3-D ultrasound measurements between the two positions tends to increase with the severity of scoliotic spine; (4) there is a high correlation of the 3-D ultrasound measurements of lateral curvature and vertebral rotation between the supine and standing positions.

The feasibility of using the 3-D ultrasound to assess the supine *versus* standing change of coronal curvature and vertebral rotation in the patients with AIS has been demonstrated in this study. The difference of the clinical parameters between the two positions tends to increase with the severity of AIS. Supine to standing change of coronal curvature and vertebral rotation could be regarded as a useful alternative measure of spinal flexibility in the patients with AIS. Further studies on the 3-D changes of AIS using the 3-D ultrasound are deserved in a large sample size.

## CHAPTER 6 Conclusions and Recommendations

### 6.1 Conclusions

An accurate 3-D assessment is crucial to facilitate the diagnosis of scoliotic deformation and optimize the treatment strategies [3, 24]. In the routine clinical practice, the radiographic assessments are performed throughout the course of treatments for the patients with AIS [1, 2]. However, the frequent exposure to radiation has been of primary concern and the radiographic assessments of scoliotic spine are limited in the coronal and sagittal planes [6].

Ultrasound, a non-invasive imaging technique, has currently gained considerable attention in the assessment of scoliosis. The development of the 3-D ultrasound system can enable the 3-D reconstruction of vertebral images and facilitate the measurement of scoliotic spine in various anatomical planes that could not be accomplished previously [7-14, 16-18, 221]. Spinous processes, laminae and transverse processes can be visualized and used as the landmarks to measure the lateral curvature and vertebral rotation in the coronal and transverse planes of the 3-D ultrasound images in the phantom experiments [10, 12, 17, 18, 21, 199, 224]. However, the studies using 3-D ultrasound to evaluate the scoliosis in the clinical setting, as well as in the different scanning positions are limited. Thus, the primary objective of this study was to explore the possibility of using the proposed 3-D ultrasound methods to measure the spinal curvature in the coronal plane, vertebral rotation in the transverse plane and kyphosis/lordosis in the sagittal plane in the subjects with AIS under the clinical setting, and to evaluate its reliability and validity with the concurrent MRI method. In addition, the second purpose of this study is to investigate the gravitational effect on the changes of the coronal curvature and vertebral rotation between the supine *versus* standing postures using the 3-D ultrasound in the patients with AIS.



In the present study, the center of laminae (COL) method in 3-D ultrasound presented high intra- and inter-rater reliabilities to measure the spinal curvature in the coronal plane and the vertebral rotation in the transverse plane, while the spinous process angle (SPA) method showed high intra- and inter-rater reliabilities to assess the kyphotic and lordotic angles in the sagittal plane. Compared with the MRI assessments, the validity of the COL method in 3-D ultrasound on the measurements of coronal curvature and vertebral rotation has been demonstrated through the comparison of means, Bland-Altman method and Pearson correlation analysis. Moreover, the SPA method has found to be valid for the kyphotic angle but not the lordotic angle assessments in the patients with AIS under the clinical setting.

The feasibility of application of 3-D ultrasound to assess the supine *versus* standing difference of coronal curvature and vertebral rotation in AIS has been demonstrated in this study. The difference of the clinical parameters between the two positions tends to increase with the severity of AIS.

## **6.2 Recommendations**

Continuous studies are required to optimize the 3-D ultrasound scanning and measuring procedure, and to further validate the 3-D ultrasound measurements in a large sample size. With these efforts, 3-D ultrasound will become a potential option used as an alternative to radiography for screening and routine assessment of scoliosis and other spinal deformities.

Supine to standing change of coronal curvature and vertebral rotation could be regarded as a useful alternative measure of spinal flexibility in patients with AIS. Further studies on the 3-D changes of AIS using the 3-D ultrasound are deserved in a large sample size.

## APPENDICES

### APPENDIX A -- CONSENT TO PARTICIPATE IN RESEARCH

#### CONSENT TO PARTICIPATE IN RESEARCH

Project Title: Validation of the Clinical Application of Non-invasive 3-D Ultrasound and Automation Method in Assessing the Cobb Angle and Vertebral Rotation in Adolescent Idiopathic Scoliosis

I \_\_\_\_\_ hereby consent to participate in the captioned research conducted by Dr. Tsz-ping LAM (Assistant Professor of the Department of Orthopaedics & Traumatology, The Chinese University of Hong Kong) and Dr. Man-sang Wong (Associate Professor of the Interdisciplinary Division of Biomedical Engineering, The Hong Kong Polytechnic University), and assisted-conducted by PhD candidate WANG Qian.

I understand that the information obtained from this research may be used in future research and published. However, my right to privacy will be retained, i.e. my personal details will not be revealed.

The procedure as set out in the attached information sheet has been fully explained. I understand the benefit and risks involved. My participation in the project is voluntary.

I acknowledge that I have the right to question any part of the procedure and can withdraw at any time without penalty of any kind.

If you would like more information about this study, please contact Dr. Man-sang WONG at 2766-7680.

Name of participant: \_\_\_\_\_

Signature of participant: \_\_\_\_\_

Date: \_\_\_\_\_

Name of researcher: \_\_\_\_\_

Signature of researcher: \_\_\_\_\_

Date: \_\_\_\_\_

Name of supervisor: \_\_\_\_\_

Signature of supervisor: \_\_\_\_\_

Date: \_\_\_\_\_

## APPENDIX B -- CONSENT TO PARTICIPATE IN RESEARCH

### (CHINESE VERSION)

#### 參與研究同意書

項目名稱：

關於非侵入性的三維超聲和自動影像識別技術用於評估青少年特發性脊椎側彎患者的科氏角度和椎體旋轉度的臨床應用驗證

本人 \_\_\_\_\_ 特此同意參加由香港中文大學矯形外科及創傷學系 林子平 助理教授和香港理工大學生物醫學工程跨領域學部 黃文生 副教授負責執行及加以說明，並且將由 黃文生 副教授的博士研究生 王謙 來協助執行。

我理解此研究所獲得的資料可用於未來的研究和學術交流。然而我有權保護自己的隱私，我的個人資料將不能被洩漏。

我對所附資料的有關步驟已經得到充分的解釋。我是自願參加與這項研究。

我理解我有權在研究過程中提出問題，並可在任何時候決定退出研究而不會受到任何不正常的待遇或責任追究。

參加者姓名： \_\_\_\_\_

參加者簽名： \_\_\_\_\_

日期： \_\_\_\_\_

研究人員姓名： \_\_\_\_\_

研究人員簽名： \_\_\_\_\_

日期： \_\_\_\_\_

導師姓名： \_\_\_\_\_

導師簽名： \_\_\_\_\_

日期： \_\_\_\_\_

## APPENDIX C -- INFORMATION SHEET

### INFORMATION SHEET

Project Title: Validation of the Clinical Application of Non-invasive 3-D Ultrasound and Automation Method in Assessing the Cobb Angle and Vertebral Rotation in Adolescent Idiopathic Scoliosis

You are invited to participate in a study conducted by Dr. Tsz-ping LAM, Assistant Professor of the Department of Orthopaedics and Traumatology, The Chinese University of Hong Kong and Dr. Man-sang Wong, Associate Professor of the Interdisciplinary Division of Biomedical Engineering, The Hong Kong Polytechnic University. WANG Qian, who is a PhD candidate of Dr. Man-sang Wong, will be the assistant in this study.

The aim of this study is trying to apply clinical ultrasound technique in assessing spinal deformities of the patients with adolescent idiopathic scoliosis in a non-invasive approach. The 3-D clinical ultrasound consists of an ultrasound system and a 3-D add-on system. The 3-D of the ultrasound probe will be recorded by using electro-magnetic wave signal which is safe for human. The scoliotic spine images obtained from the clinical ultrasound technique will be compared with that taken from the Magnetic Resonance Imaging Method (including coronal, sagittal and transverse planes).

Subjects can withdraw from the study at anytime without affecting their continuous treatment.

The results of this study can contribute in scientific practice of assessment and orthotic intervention and form a data base for further developments of orthotic treatment protocol for adolescent idiopathic scoliosis.

All information related to you will remain confidential, and will be identifiable by codes only known to the researcher. Subjects are at minimum risk with this study. Minimal risk means that the risks of harm anticipated in the proposed research are not greater considering probability and magnitude, than those ordinarily encountered in daily life.

You have every right to withdraw from the study before or during the measurement without penalty of any kind.

If you have any complaints about the conduct of this research study, please do not hesitate to contact Miss Ivy CHAU, Secretary of the Human Subjects Ethics Sub-Committee of The Hong Kong Polytechnic University in person or in writing (c/o Room M1303, Human Resources Office of the Hong Kong Polytechnic University) or the Joint Chinese University of Hong Kong - New Territories East Cluster Clinical Research Ethics Committee (Tel. No.: 2632 ).

If you would like more information about this study, please contact Dr. Man-sang WONG at 2766-7680. Thank you for your interest in participating in this study.

Principal Investigator: Dr. Tsz-ping LAM  
Co-investigator: Dr. Man-sang WONG

## APPENDIX D -- INFORMATION SHEET (CHINESE VERSION)

### 項目名稱:

關於非侵入性的三維超聲和自動影像識別技術用於評估青少年特發性脊椎側彎患者的科氏角度和椎體旋轉度的臨床應用驗證

誠邀閣下參加由香港中文大學矯形外科及創傷學系 林子平 助理教授和香港理工大學生物醫學工程跨領域學部 黃文生 副教授負責執行的研究項目。此項目將由 黃文生 副教授的博士研究生 王謙 來協助執行。

此研究的目標是使用三維臨床超聲和影像自動識別技術來評估青春期的特發性脊柱側彎病人的脊柱情況。閣下只需要在傳統的磁共振影像檢查當天接受一項簡單的三維臨床超聲檢查。三維臨床超聲是在普通臨床超聲的儀器上配置三維定位系統用於追蹤超聲掃描的探頭在三維空間中的位置，從而把二維的超聲圖像重建成為三維的圖像。此設備中的三維定位系統是用電磁波信號進行追蹤和重建的，系統中所用的信號對人體無害。分別由臨床超聲儀器和磁共振影像儀器獲得的三維脊柱圖片將會被用來進行對比（包括冠狀面、橫切面和矢狀面三個平面上的比較）。

所有的參加者都有權在任何時候選擇退出此項目，並且不影響其後續的治療。臨床超聲波檢查已經使用多年，到目前為止還沒有出現任何安全問題報告，因此在測試的過程中將不會令閣下有任何不必要的不適。

此研究得出的結果可在矯形器的治療科學運用做出貢獻及能形成一個數據庫以便研究人員進一步研發能更好的治療青春期的特發性脊柱側彎的矯形器。

凡有關閣下的資料均會保密，一切資料的編碼只有研究人員知道。

閣下享有充分的權利在研究開始之前或之後決定退出這項研究，而不會受到任何對閣下不正常的待遇或責任追究。

如果閣下有任何對這項研究的不滿，請隨時親自或寫信聯絡香港理工大學-人事倫理委員會秘書 周艾維（地址：香港理工大學人力資源辦公室 M1303 室轉交）或聯絡香港中文大學-新界東醫院聯網臨床研究倫理席委員會（電話：2632- ）。)

如果閣下想獲得更多有關這項研究的資料，請與 黃文生 副教授聯絡，辦公室電話：2766-7680。

謝謝 閣下參與這項研究。

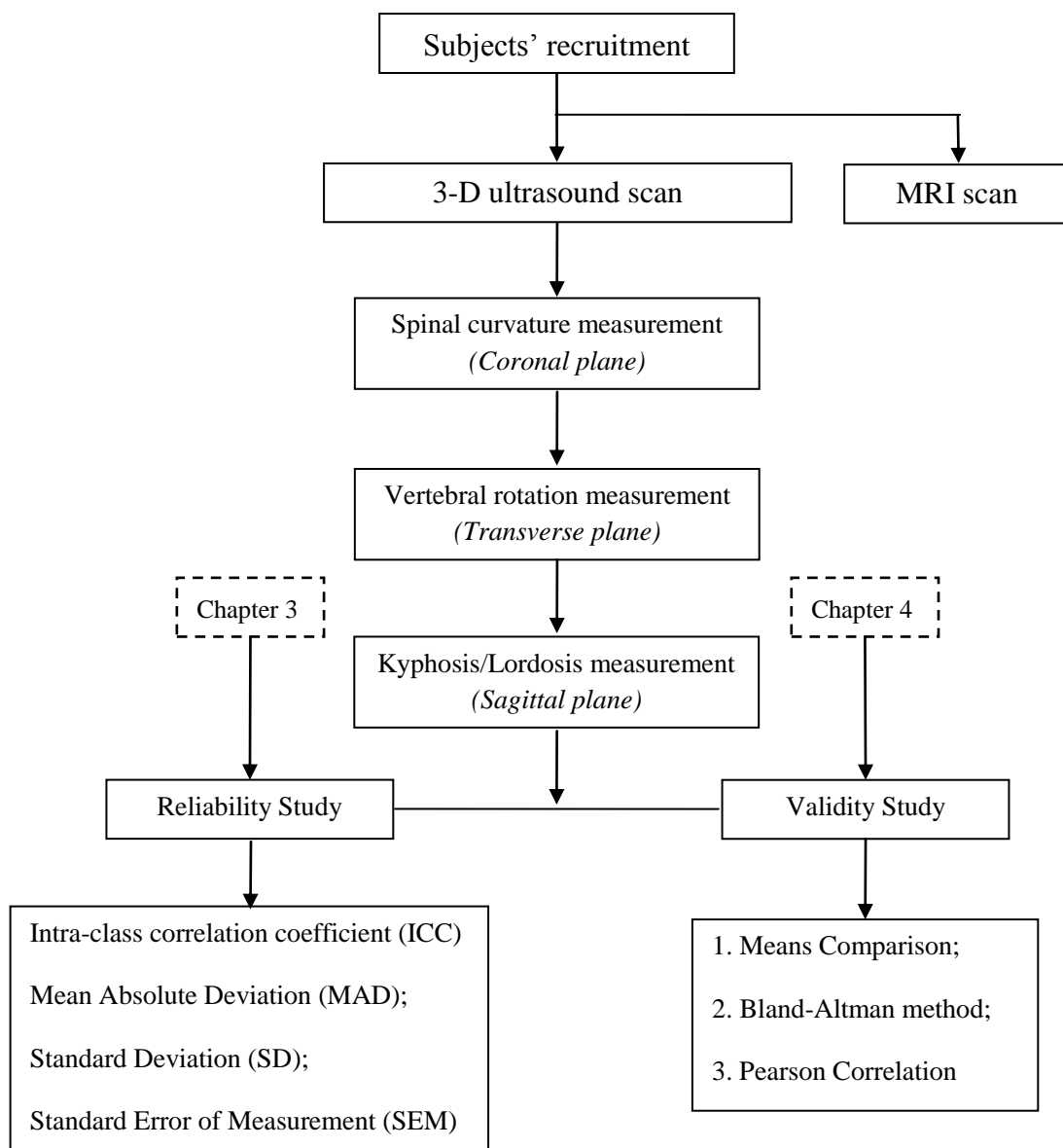
首席調查員：林子平 助理教授

聯合調查員：黃文生 副教授

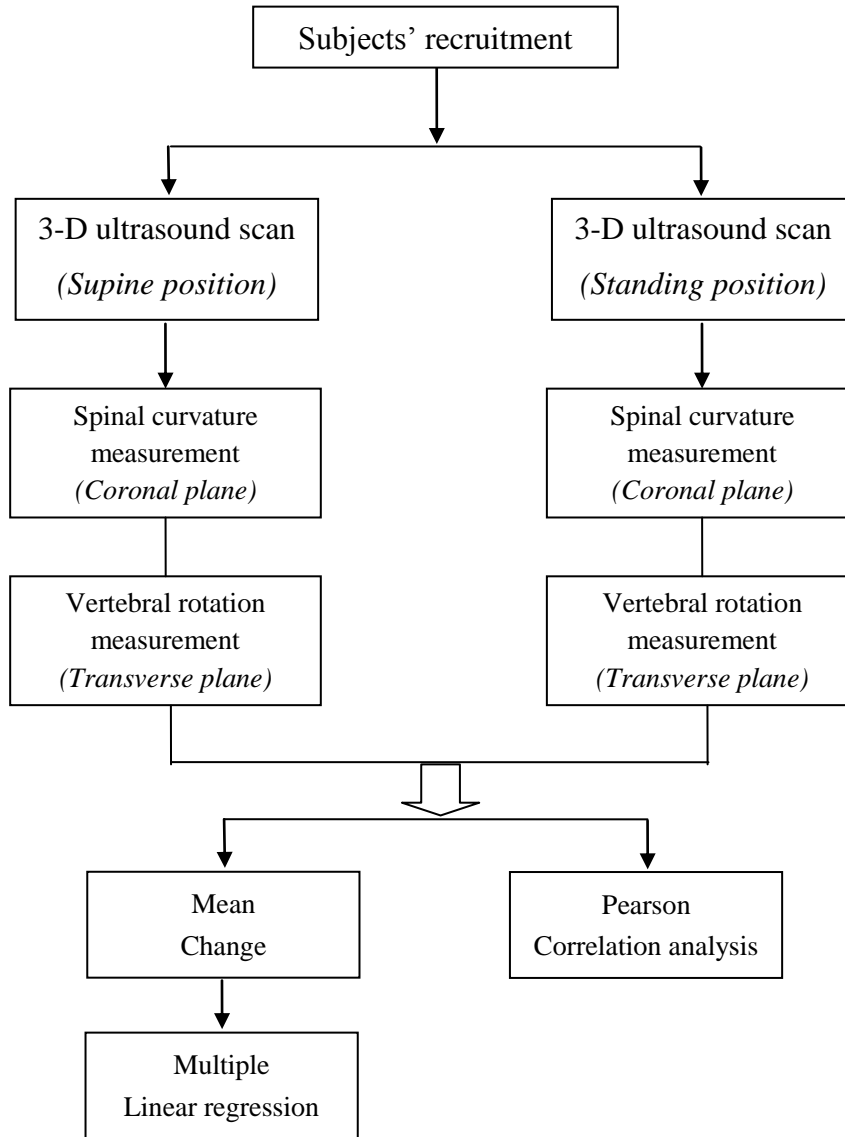
## APPENDIX E -- PROJECT PROTOCOL

### Project Title: Three dimensional Assessments of Adolescent Idiopathic Scoliosis using Three-dimensional Ultrasound

#### Study Protocol of Chapter 3 and 4



## Study Protocol of Chapter 5



## REFERENCES

1. Hresko MT: **Idiopathic Scoliosis in Adolescents**. *New England Journal of Medicine* 2013, **368**(9):834-841.
2. Weinstein SL, Dolan LA, Cheng JC, Danielsson A, Morcuende JA: **Adolescent idiopathic scoliosis**. *The Lancet* 2008, **371**(9623):1527-1537.
3. Kotwicki T: **Evaluation of scoliosis today: examination, X-rays and beyond**. *Disabil Rehabil* 2008, **30**(10):742-751.
4. Presciutti SM, Karukanda T, Lee M: **Management decisions for adolescent idiopathic scoliosis significantly affect patient radiation exposure**. *The spine journal : official journal of the North American Spine Society* 2014, **14**(9):1984-1990.
5. Pace N, Ricci L, Negrini S: **A comparison approach to explain risks related to X-ray imaging for scoliosis, 2012 SOSORT award winner**. *Scoliosis* 2013, **8**(1):1-11.
6. Knott P, Pappo E, Cameron M, Demauroy J, Rivard C, Kotwicki T, Zaina F, Wynne J, Stikeleather L, Bettany-Saltikov J *et al*: **SOSORT 2012 consensus paper: reducing x-ray exposure in pediatric patients with scoliosis**. *Scoliosis* 2014, **9**:4.
7. Vo QN, Lou EH, Le LH: **Reconstruction of a scoliotic spine using a three-dimensional medical ultrasound system**. *Scoliosis* 2015, **10**(Suppl 1):P17.
8. Vo Q, Lou E, Le LH, Huynh L: **Investigation of the Optimal Freehand Three-Dimensional Ultrasound Configuration to Image Scoliosis: An In-vitro Study**. In: *5th International Conference on Biomedical Engineering in Vietnam: 2015*; Springer; 2015: 163-166.
9. Nguyen DV, Vo QN, Le LH, Lou EHM: **Validation of 3D surface reconstruction of vertebrae and spinal column using 3D ultrasound data – A pilot study**. *Medical Engineering & Physics* 2015, **37**(2):239-244.



10. Cheung C-WJ, Zhou G-Q, Law S-Y, Lai K-L, Jiang W-W, Zheng Y-P: **Freehand three-dimensional ultrasound system for assessment of scoliosis.** *Journal of Orthopaedic Translation* 2015, **3**(3):123-133.
11. Cheung C, Zhou G, Law S, Mak T, Lai K, Zheng Y: **Ultrasound Volume Projection Imaging for Assessment of Scoliosis.** *Medical Imaging, IEEE Transactions on* 2015, **34**(8):1760 - 1768.
12. Cheung CW, Law SY, Zheng YP: **Development of 3-D ultrasound system for assessment of adolescent idiopathic scoliosis (AIS): And system validation.** *Conf Proc IEEE Eng Med Biol Soc* 2013, **2013**:6474-6477.
13. Zheng Y-P: **3D Ultrasound Imaging for Assessment of Scoliosis.** *The Spine Journal* 2012, **12**(9):S164.
14. Purnama KE, Wilkinson MH, Veldhuizen AG, van Ooijen PM, Lubbers J, Burgerhof JG, Sardjono TA, Verkerke GJ: **A framework for human spine imaging using a freehand 3D ultrasound system.** *Technology and Health Care* 2010, **18**(1):1-17.
15. Cheung C-WJ, Zheng Y: **Development of 3-D Ultrasound System for Assessment of Adolescent Idiopathic Scoliosis (AIS).** In: *6th World Congress of Biomechanics. Volume 31*, edn.; 2010: 584-587.
16. Purnama IKE, Wilkinson MHF, Veldhuizen AG, van Ooijen PMA, Sardjono TA, Lubbers J, Verkerke GJ: **Following Scoliosis Progression in the Spine using Ultrasound Imaging.** In: *World Congress on Medical Physics and Biomedical Engineering, Vol 25, Pt 2 - Diagnostic Imaging. Volume 25*, edn.; 2009: 600-602.
17. Chen W, Le LH, Lou EH: **Ultrasound Imaging of Spinal Vertebrae to Study Scoliosis.** *Open Journal of Acoustics* 2012, **2**(3):95-103.
18. Chen W, Lou EH, Le LH: **Using ultrasound imaging to identify landmarks in vertebra models to assess spinal deformity.** In: *Engineering in Medicine and*

- Biology Society, EMBC, 2011 Annual International Conference of the IEEE: 2011: IEEE; 2011: 8495-8498.*
19. Zheng R, Chan AC, Chen W, Hill DL, Le LH, Hedden D, Moreau M, Mahood J, Southon S, Lou E: **Intra-and Inter-rater Reliability of Coronal Curvature Measurement for Adolescent Idiopathic Scoliosis Using Ultrasonic Imaging Method—A Pilot Study.** *Spine Deformity* 2015, **3**(2):151-158.
  20. Young M, Hill DL, Zheng R, Lou E: **Reliability and accuracy of ultrasound measurements with and without the aid of previous radiographs in adolescent idiopathic scoliosis (AIS).** *European Spine Journal* 2015:1-7.
  21. Chen W, Lou EH, Zhang PQ, Le LH, Hill D: **Reliability of assessing the coronal curvature of children with scoliosis by using ultrasound images.** *Journal of children's orthopaedics* 2013, **7**(6):521-529.
  22. CG K, FH N, JA C, CAG M: **Nett's atlas of human anatomy for CPT (current procedural terminology) coding. 2nd Edition.** *American Medical Association* 2009.
  23. HN H, SR G, RA B, FJ E, GR B, SW W: **Rothman-Simeone, the spine 4th Edition.** *WB Saunders Inc, USA* 1999.
  24. Negrini S, Aulisa AG, Aulisa L, Circo AB, de Mauroy JC, Durmala J, Grivas TB, Knott P, Kotwicki T, Maruyama T: **2011 SOSORT guidelines: orthopaedic and rehabilitation treatment of idiopathic scoliosis during growth.** *Scoliosis* 2012, **7**(3):1.
  25. Dayer R, Haumont T, Belaieff W, Lascombes P: **Idiopathic scoliosis: etiological concepts and hypotheses.** *J Child Orthop* 2013, **7**(1):11-16.
  26. Schlosser TP, van der Heijden GJ, Versteeg AL, Castelein RM: **How 'idiopathic' is adolescent idiopathic scoliosis? A systematic review on associated abnormalities.** *PloS one* 2014, **9**(5):e97461.

27. Zhang H, Guo C, Tang M, Liu S, Li J, Guo Q, Chen L, Zhu Y, Zhao S: **Prevalence of scoliosis among primary and middle school students in Mainland China: a systematic review and meta-analysis.** *Spine (Phila Pa 1976)* 2015, **40**(1):41-49.
28. Fong DY, Cheung KM, Wong YW, Wan YY, Lee CF, Lam TP, Cheng JC, Ng BK, Luk KD: **A population-based cohort study of 394,401 children followed for 10 years exhibits sustained effectiveness of scoliosis screening.** *The spine journal : official journal of the North American Spine Society* 2015, **15**(5):825-833.
29. Horne JP, Flannery R, Usman S: **Adolescent idiopathic scoliosis: diagnosis and management.** *Am Fam Physician* 2014, **89**(3):193-198.
30. Kotwicki T, Chowanska J, Kinel E, Czaprowski D, Tomaszewski M, Janusz P: **Optimal management of idiopathic scoliosis in adolescence.** *Adolescent health, medicine and therapeutics* 2013, **4**:59-73.
31. Weinstein S, Ponseti I: **Curve progression in idiopathic scoliosis.** *The Journal of bone and joint surgery American volume* 1983, **65**(4):447-455.
32. Zhang Y, Yang Y, Dang X, Zhao L, Ren J, Zhang L, Sun J: **Factors relating to curve progression in female patients with adolescent idiopathic scoliosis treated with a brace.** *Eur Spine J* 2015, **24**(2):244-248.
33. Weinstein SL, Zavala DC, Ponseti IV: **Idiopathic scoliosis: long-term follow-up and prognosis in untreated patients.** *The Journal of bone and joint surgery American volume* 1981, **63**(5):702-712.
34. Beausejour M, Goulet L, Parent S, Feldman DE, Turgeon I, Roy-Beaudry M, Sosa JF, Labelle H: **The effectiveness of scoliosis screening programs: methods for systematic review and expert panel recommendations formulation.** *Scoliosis* 2013, **8**(1):12.

35. Labelle H, Richards SB, De Kleuver M, Grivas TB, Luk KD, Wong HK, Thometz J, Beausejour M, Turgeon I, Fong DY: **Screening for adolescent idiopathic scoliosis: an information statement by the scoliosis research society international task force.** *Scoliosis* 2013, **8**:17.
36. Leone A, Aulisa A, Perisano C, Re T, Galli M: **Advantages of a two-step procedure for school-based scoliosis screening.** *La Radiologia medica* 2010, **115**(2):238-245.
37. Lee CF, Fong DY, Cheung KM, Cheng JC, Ng BK, Lam TP, Mak KH, Yip PS, Luk KD: **Referral criteria for school scoliosis screening: assessment and recommendations based on a large longitudinally followed cohort.** *Spine (Phila Pa 1976)* 2010, **35**(25):E1492-1498.
38. Plaszewski M, Bettany-Saltikov J: **Are current scoliosis school screening recommendations evidence-based and up to date? A best evidence synthesis umbrella review.** *Eur Spine J* 2014, **23**(12):2572-2585.
39. Plaszewski M, Nowobilski R, Kowalski P, Cieslinski M: **Screening for scoliosis: different countries' perspectives and evidence-based health care.** *International journal of rehabilitation research Internationale Zeitschrift fur Rehabilitationsforschung Revue internationale de recherches de readaptation* 2012, **35**(1):13-19.
40. Grivas TB, Hresko MT, Labelle H, Price N, Kotwicki T, Maruyama T: **The pendulum swings back to scoliosis screening: screening policies for early detection and treatment of idiopathic scoliosis - current concepts and recommendations.** *Scoliosis* 2013, **8**(1):16.
41. Ueno M, Takaso M, Nakazawa T, Imura T, Saito W, Shintani R, Uchida K, Fukuda M, Takahashi K, Ohtori S *et al*: **A 5-year epidemiological study on the prevalence rate of idiopathic scoliosis in Tokyo: school screening of more than 250,000 children.**

- Journal of orthopaedic science : official journal of the Japanese Orthopaedic Association* 2011, **16**(1):1-6.
42. Suh SW, Modi HN, Yang JH, Hong JY: **Idiopathic scoliosis in Korean schoolchildren: a prospective screening study of over 1 million children.** *Eur Spine J* 2011, **20**(7):1087-1094.
  43. Adobor RD, Rimeslatten S, Steen H, Brox JI: **School screening and point prevalence of adolescent idiopathic scoliosis in 4000 Norwegian children aged 12 years.** *Scoliosis* 2011, **6**(1):23.
  44. Luk KD, Lee CF, Cheung KM, Cheng JC, Ng BK, Lam TP, Mak KH, Yip PS, Fong DY: **Clinical effectiveness of school screening for adolescent idiopathic scoliosis: a large population-based retrospective cohort study.** *Spine (Phila Pa 1976)* 2010, **35**(17):1607-1614.
  45. Fong DY, Lee CF, Cheung KM, Cheng JC, Ng BK, Lam TP, Mak KH, Yip PS, Luk KD: **A meta-analysis of the clinical effectiveness of school scoliosis screening.** *Spine (Phila Pa 1976)* 2010, **35**(10):1061-1071.
  46. Korovessis PG: **Scoliometer is useful instrument with high reliability and repeatability.** *Spine* 1999, **24**(3):307-308.
  47. Korovessis PG, Stamatakis MV: **Prediction of scoliotic cobb angle with the use of the scoliometer.** *Spine* 1996, **21**(14):1661-1666.
  48. Fabio Z, Stefano N, Salvatore A: **TRACE (Trunk Aesthetic Clinical Evaluation), a routine clinical tool to evaluate aesthetics in scoliosis patients: development from the Aesthetic Index (AI) and repeatability.** *Scoliosis and spinal disorders* 2009, **4**(1):3.
  49. Bago J, Sanchez-Raya J, Perez-Grueso FJ, Climent JM: **The Trunk Appearance Perception Scale (TAPS): a new tool to evaluate subjective impression of trunk**

- deformity in patients with idiopathic scoliosis.** *Scoliosis and spinal disorders* 2010, **5**(1):1-9.
50. Aulisa AG, Guzzanti V, Perisano C, Marzetti E, Specchia A, Galli M, Giordano M, Aulisa L: **Determination of quality of life in adolescents with idiopathic scoliosis subjected to conservative treatment.** *Scoliosis and spinal disorders* 2010, **5**(1):21.
51. Asher M, Min LS, Burton D, Manna B: **The reliability and concurrent validity of the scoliosis research society-22 patient questionnaire for idiopathic scoliosis.** *Spine* 2003, **28**(1):63-69.
52. Asher M, Min LS, Burton D, Manna B: **Scoliosis research society-22 patient questionnaire: responsiveness to change associated with surgical treatment.** *Spine* 2003, **28**(1):70.
53. Asher M, Min LS, Burton D, Manna B: **Discrimination validity of the scoliosis research society-22 patient questionnaire: relationship to idiopathic scoliosis curve pattern and curve size.** *Spine* 2003, **28**(1):74-78.
54. Vasiliadis E, Grivas TB, Gkoltsiou K: **Development and preliminary validation of Brace Questionnaire (BrQ): a new instrument for measuring quality of life of brace treated scoliotics.** *Scoliosis and spinal disorders* 2006, **1**(1):1-8.
55. Kotwicki T, Kinel E, Stryła W, Szulc A: **Estimation of the stress related to conservative scoliosis therapy: an analysis based on BSSQ questionnaires.** *Scoliosis and spinal disorders* 2007, **2**(1):1-6.
56. Botenshelmus C, Klein R, Stephan C: **The reliability of the Bad Sobernheim Stress Questionnaire (BSSQbrace) in adolescents with scoliosis during brace treatment.** *Scoliosis and spinal disorders* 2006, **1**(1):22.

57. Lam GC, Hill DL, Le LH, Raso JV, Lou EH: **Vertebral rotation measurement: a summary and comparison of common radiographic and CT methods.** *Scoliosis* 2008, **3**(1):1-16.
58. Bettany-Saltikov J, Parent E, Romano M, Villagrasa M, Negrini S: **Physiotherapeutic scoliosis-specific exercises for adolescents with idiopathic scoliosis.** *European journal of physical and rehabilitation medicine* 2014, **50**(1):111-121.
59. Romano M, Minozzi S, Zaina F, Saltikov JB, Chockalingam N, Kotwicki T, Hennes AM, Negrini S: **Exercises for adolescent idiopathic scoliosis: a Cochrane systematic review.** *Spine (Phila Pa 1976)* 2013, **38**(14):E883-893.
60. Mordecai SC, Dabke HV: **Efficacy of exercise therapy for the treatment of adolescent idiopathic scoliosis: a review of the literature.** *Eur Spine J* 2012, **21**(3):382-389.
61. Negrini S, Minozzi S, Bettany-Saltikov J, Chockalingam N, Grivas TB, Kotwicki T, Maruyama T, Romano M, Zaina F: **Braces for idiopathic scoliosis in adolescents.** *Cochrane Database of Systematic Reviews* 2015, **6**.
62. Stokes OM, Luk KD: **The current status of bracing for patients with adolescent idiopathic scoliosis.** *The bone & joint journal* 2013, **95-b**(10):1308-1316.
63. Zaina F, De Mauroy JC, Grivas T, Hresko MT, Kotwizki T, Maruyama T, Price N, Rigo M, Stikeleather L, Wynne J *et al*: **Bracing for scoliosis in 2014: state of the art.** *European journal of physical and rehabilitation medicine* 2014, **50**(1):93-110.
64. Weinstein SL, Dolan LA, Wright JG, Dobbs MB: **Effects of bracing in adolescents with idiopathic scoliosis.** *New England Journal of Medicine* 2013, **369**(16):1512-1521.

65. Bettany-Saltikov J, Weiss HR, Chockalingam N, Taranu R, Srinivas S, Hogg J, Whittaker V, Kalyan RV, Arnell T: **Surgical versus non-surgical interventions in people with adolescent idiopathic scoliosis.** *The Cochrane database of systematic reviews* 2015, **4**:Cd010663.
66. Olgun ZD, Yazici M: **Posterior instrumentation and fusion.** *J Child Orthop* 2013, **7**(1):69-76.
67. Helenius I: **Anterior surgery for adolescent idiopathic scoliosis.** *J Child Orthop* 2013, **7**(1):63-68.
68. Franic M, Kujundzic Tiljak M, Pozar M, Romic D, Mimica M, Petrak J, Ivankovic D, Pecina M: **Anterior versus posterior approach in 3D correction of adolescent idiopathic thoracic scoliosis: a meta-analysis.** *Orthopaedics & traumatology, surgery & research : OTSR* 2012, **98**(7):795-802.
69. Lykissas MG, Jain VV, Nathan ST, Pawar V, Eismann EA, Sturm PF, Crawford AH: **Mid- to long-term outcomes in adolescent idiopathic scoliosis after instrumented posterior spinal fusion: a meta-analysis.** *Spine (Phila Pa 1976)* 2013, **38**(2):E113-119.
70. Ledonio CG, Polly DW, Jr., Vitale MG, Wang Q, Richards BS: **Pediatric pedicle screws: comparative effectiveness and safety: a systematic literature review from the Scoliosis Research Society and the Pediatric Orthopaedic Society of North America task force.** *The Journal of bone and joint surgery American volume* 2011, **93**(13):1227-1234.
71. Suk SI, Kim JH, Kim SS, Lim DJ: **Pedicle screw instrumentation in adolescent idiopathic scoliosis (AIS).** *Eur Spine J* 2012, **21**(1):13-22.



72. Malfair D, Flemming AK, Dvorak MF, Munk PL, Vertinsky AT, Heran MK, Graeb DA: **Radiographic evaluation of scoliosis: review.** *American Journal of Roentgenology* 2010, **194**(3\_supplement):S8-S22.
73. Kim H, Kim HS, Moon ES, Yoon CS, Chung TS, Song HT, Suh JS, Lee YH, Kim S: **Scoliosis imaging: what radiologists should know.** *Radiographics* 2010, **30**(7):1823-1842.
74. Vrtovec T, Pernuš F, Likar B: **A review of methods for quantitative evaluation of spinal curvature.** *European Spine Journal* 2009, **18**(5):593-607.
75. Dang NR, Moreau MJ, Hill DL, Mahood JK, Raso J: **Intra-observer reproducibility and interobserver reliability of the radiographic parameters in the Spinal Deformity Study Group's AIS Radiographic Measurement Manual.** *Spine (Phila Pa 1976)* 2005, **30**(9):1064-1069.
76. Kuklo TR, Potter BK, Polly Jr DW, O'Brien MF, Schroeder TM, Lenke LG: **Reliability analysis for manual adolescent idiopathic scoliosis measurements.** *Spine* 2005, **30**(4):444-454.
77. De Carvalho A, Vialle R, Thomsen L, Amzallag J, Cluzel G, le Pointe HD, Mary P: **Reliability analysis for manual measurement of coronal plane deformity in adolescent scoliosis. Are 30 x 90 cm plain films better than digitized small films?** *Eur Spine J* 2007, **16**(10):1615-1620.
78. Gstoettner M, Sekyra K, Walochnik N, Winter P, Wachter R, Bach CM: **Inter-and intraobserver reliability assessment of the Cobb angle: manual versus digital measurement tools.** *European Spine Journal* 2007, **16**(10):1587-1592.
79. Gupta MC, Wijesekera S, Sossan A, Martin L, Vogel LC, Boakes JL, Lerman JA, McDonald CM, Betz RR: **Reliability of radiographic parameters in neuromuscular scoliosis.** *Spine (Phila Pa 1976)* 2007, **32**(6):691-695.

80. Allen S, Parent E, Khorasani M, Hill D, Lou E, Raso J: **Validity and reliability of active shape models for the estimation of Cobb angle in patients with adolescent idiopathic scoliosis.** *Journal of Digital Imaging* 2008, **21**(2):208-218.
81. Mok JM, Berven SH, Diab M, Hackbarth M, Hu SS, Deviren V: **Comparison of observer variation in conventional and three digital radiographic methods used in the evaluation of patients with adolescent idiopathic scoliosis.** *Spine (Phila Pa 1976)* 2008, **33**(6):681-686.
82. Tanure MC, Pinheiro AP, Oliveira AS: **Reliability assessment of Cobb angle measurements using manual and digital methods.** *The spine journal : official journal of the North American Spine Society* 2010, **10**(9):769-774.
83. Facanha-Filho FA, Winter RB, Lonstein JE, Koop S, Novacheck T, L'Heureux E, Noren CA: **Measurement accuracy in congenital scoliosis.** *The Journal of Bone & Joint Surgery* 2001, **83**(1):42-42.
84. Kuklo TR, Potter BK, O'Brien MF, Schroeder TM, Lenke LG, Polly Jr DW, Group SDS: **Reliability analysis for digital adolescent idiopathic scoliosis measurements.** *Journal of spinal disorders & techniques* 2005, **18**(2):152-159.
85. Chockalingam N, Dangerfield PH, Giakas G, Cochrane T, Dorgan JC: **Computer-assisted Cobb measurement of scoliosis.** *European Spine Journal* 2002, **11**(4):353-357.
86. Zhang J, Lou E, Hill DL, Raso JV, Wang Y, Le LH, Shi X: **Computer-aided assessment of scoliosis on posteroanterior radiographs.** *Medical & biological engineering & computing* 2010, **48**(2):185-195.
87. Kuklo TR, Potter BK, Schroeder TM, O'Brien MF: **Comparison of manual and digital measurements in adolescent idiopathic scoliosis.** *Spine* 2006, **31**(11):1240-1246.

88. Srinivasalu S, Modi HN, Smehta S, Suh SW, Chen T, Murun T: **Cobb angle measurement of scoliosis using computer measurement of digitally acquired radiographs-intraobserver and interobserver variability.** *Asian spine journal* 2008, **2**(2):90-93.
89. Mehta SS, Modi HN, Srinivasalu S, Chen T, Suh SW, Yang JH, Song HR: **Interobserver and intraobserver reliability of Cobb angle measurement: endplate versus pedicle as bony landmarks for measurement: a statistical analysis.** *Journal of pediatric orthopedics* 2009, **29**(7):749-754.
90. Aubin CE, Bellefleur C, Joncas J, de Lanauze D, Kadoury S, Blanke K, Parent S, Labelle H: **Reliability and accuracy analysis of a new semiautomatic radiographic measurement software in adult scoliosis.** *Spine (Phila Pa 1976)* 2011, **36**(12):E780-790.
91. Chan AC, Morrison DG, Nguyen DV, Hill DL, Parent E, Lou EH: **Intra-and Interobserver Reliability of the Cobb Angle–Vertebral Rotation Angle–Spinous Process Angle for Adolescent Idiopathic Scoliosis.** *Spine Deformity* 2014, **2**(3):168-175.
92. Stokes IA, Aronsson DD: **Computer-assisted algorithms improve reliability of King classification and Cobb angle measurement of scoliosis.** *Spine (Phila Pa 1976)* 2006, **31**(6):665-670.
93. Di Silvestre M, Lolli F, Bakaloudis G, Maredi E, Vommaro F, Pastorelli F: **Apical vertebral derotation in the posterior treatment of adolescent idiopathic scoliosis: myth or reality?** *European Spine Journal* 2013, **22**(2):313-323.
94. Cui G, Watanabe K, Nishiwaki Y, Hosogane N, Tsuji T, Ishii K, Nakamura M, Toyama Y, Chiba K, Matsumoto M: **Loss of apical vertebral derotation in adolescent idiopathic scoliosis: 2-year follow-up using multi-planar**

- reconstruction computed tomography.** *European Spine Journal* 2012, **21**(6):1111-1120.
95. Vrtovec T, Pernuš F, Likar B: **A review of methods for quantitative evaluation of axial vertebral rotation.** *European Spine Journal* 2009, **18**(8):1079-1090.
96. Abul-Kasim K, Karlsson MK, Hasserijs R, Ohlin A: **Measurement of vertebral rotation in adolescent idiopathic scoliosis with low-dose CT in prone position - method description and reliability analysis.** *Scoliosis* 2010, **5**(1):1-4.
97. Cheh G, Lenke LG, Lehman Jr RA, Kim YJ, Nunley R, Bridwell KH: **The reliability of preoperative supine radiographs to predict the amount of curve flexibility in adolescent idiopathic scoliosis.** *Spine* 2007, **32**(24):2668-2672.
98. Clamp JA, Andrews JR, Grevitt MP: **A study of the radiologic predictors of curve flexibility in adolescent idiopathic scoliosis.** *Journal of spinal disorders & techniques* 2008, **21**(3):213-215.
99. Davis BJ, Gadgil A, Trivedi J, Ahmed el NB: **Traction radiography performed under general anesthetic: a new technique for assessing idiopathic scoliosis curves.** *Spine (Phila Pa 1976)* 2004, **29**(21):2466-2470.
100. Hamzaoglu A, Talu U, Tezer M, Mirzanli C, Domanic U, Goksan SB: **Assessment of curve flexibility in adolescent idiopathic scoliosis.** *Spine (Phila Pa 1976)* 2005, **30**(14):1637-1642.
101. Ibrahim T, Gabbar OA, El-Abed K, Hutchinson MJ, Nelson IW: **The value of radiographs obtained during forced traction under general anaesthesia in predicting flexibility in idiopathic scoliosis with Cobb angles exceeding 60 degree.** *J Bone Joint Surg Br* 2008, **90**(11):1473-1476.
102. Liu RW, Teng AL, Armstrong DG, Poe-Kochert C, Son-Hing JP, Thompson GH: **Comparison of supine bending, push-prone, and traction under general**

- anesthesia radiographs in predicting curve flexibility and postoperative correction in adolescent idiopathic scoliosis.** *Spine (Phila Pa 1976)* 2010, **35(4):416-422.**
103. Li J, Hwang S, Wang F, Chen Z, Wu H, Li B, Wei X, Zhu X, Li M: **An innovative fulcrum-bending radiographical technique to assess curve flexibility in patients with adolescent idiopathic scoliosis.** *Spine (Phila Pa 1976)* 2013, **38(24):E1527-1532.**
104. Omidi-Kashani F, Hasankhani EG, Moradi A, Toossi KZ, Nojomi M: **Modified fulcrum bending radiography: A new combined technique that may reflect scoliotic curve flexibility better than other conventional methods.** *J Orthop* 2013, **10(4):172-176.**
105. Cheung KM, Natarajan D, Samartzis D, Wong Y-W, Cheung W-Y, Luk KD: **Predictability of the fulcrum bending radiograph in scoliosis correction with alternate-level pedicle screw fixation.** *The Journal of Bone & Joint Surgery* 2010, **92(1):169-176.**
106. Li J, Dumonski ML, Samartzis D, Hong J, He S, Zhu X, Wang C, Vaccaro AR, Albert TJ, Li M: **Coronal deformity correction in adolescent idiopathic scoliosis patients using the fulcrum-bending radiograph: a prospective comparative analysis of the proximal thoracic, main thoracic, and thoracolumbar/lumbar curves.** *European Spine Journal* 2011, **20(1):105-111.**
107. Basques BA, Long WD, 3rd, Golinvaux NS, Bohl DD, Samuel AM, Lukasiewicz AM, Webb ML, Grauer JN: **Poor visualization limits diagnosis of proximal junctional kyphosis in adolescent idiopathic scoliosis.** *The spine journal : official journal of the North American Spine Society* 2015, **12(6):53-62.**

108. Jr PD, Kilkelly FX, Mchale KA, Asplund LM, Mulligan M, Chang AS: **Measurement of lumbar lordosis. Evaluation of intraobserver, interobserver, and technique variability.** *Spine* 1996, **21**(13):1530.
109. Izatt MT, Adam CJ, Verzin EJ, Labrom RD, Askin GN: **CT and radiographic analysis of sagittal profile changes following thoracoscopic anterior scoliosis surgery.** *Scoliosis* 2012, **7**(1):15.
110. Janssen MM, Vincken KL, van Raak SM, Vrtovec T, Kemp B, Viergever MA, Bartels LW, Castelein RM: **Sagittal spinal profile and spinopelvic balance in parents of scoliotic children.** *The spine journal : official journal of the North American Spine Society* 2013, **13**(12):1789-1800.
111. Boulay C, Tardieu C, Hecquet J, Benaim C, Mitulescu A, Marty C, Prat-Pradal D, Legaye J, Duval-Beaupère G, Pélissier J: **Anatomical reliability of two fundamental radiological and clinical pelvic parameters: incidence and thickness.** *European Journal of Orthopaedic Surgery & Traumatology* 2005, **15**(3):197-204.
112. Boulay C, Tardieu C, Hecquet J, Benaim C, Mouilleseaux B, Marty C, Prat-Pradal D, Legaye J, Duval-Beaupère G, Pélissier J: **Sagittal alignment of spine and pelvis regulated by pelvic incidence: standard values and prediction of lordosis.** *European Spine Journal* 2006, **15**(4):415-422.
113. Le HJ, Aunoble S, Philippe L, Nicolas P: **Pelvic parameters: origin and significance.** *European Spine Journal* 2011, **20**(5):564-571.
114. Risser JC: **The Classic: The Iliac Apophysis: An Invaluable Sign in the Management of Scoliosis.** *Clinical Orthopaedics and Related Research* 2010, **468**(3):646-653.

115. Bitan FD, Veliskakis KP, Campbell BC: **Differences in the Risser grading systems in the United States and France.** *Clinical Orthopaedics & Related Research* 2005, **436**(436):190-195.
116. He J-W, Yan Z-H, Liu J, Yu Z-K, Wang X-Y, Bai G-H, Ye X-J, Zhang X: **Accuracy and repeatability of a new method for measuring scoliosis curvature.** *Spine* 2009, **34**(9):E323-E329.
117. He JW, Bai GH, Ye XJ, Liu K, Yan ZH, Zhang X, Wang XY, Huang YX, Yu ZK: **A comparative study of axis-line-distance technique and Cobb method on assessing the curative effect on scoliosis.** *Eur Spine J* 2012, **21**(6):1075-1081.
118. Liu RW, Yaszay B, Glaser D, Bastrom TP, Newton PO: **A method for assessing axial vertebral rotation based on differential rod curvature on the lateral radiograph.** *Spine (Phila Pa 1976)* 2012, **37**(18):E1120-1125.
119. Gold M, Dombek M, Miller PE, Emans JB, Glotzbecker MP: **Prediction of thoracic dimensions and spine length on the basis of individual pelvic dimensions: validation of the use of pelvic inlet width obtained by radiographs compared with computed tomography.** *Spine* 2014, **39**(1):74-80.
120. Noh DK, Lee NG, You JH: **A novel spinal kinematic analysis using X-ray imaging and vicon motion analysis: a case study.** *Biomed Mater Eng* 2014, **24**(1):593-598.
121. Gille O, Champain N, Benchikh-El-Fegoun A, Vital J-M, Skalli W: **Reliability of 3D reconstruction of the spine of mild scoliotic patients.** *Spine* 2007, **32**(5):568-573.
122. Grenier S, Parent S, Cheriet F: **Personalized 3D reconstruction of the rib cage for clinical assessment of trunk deformities.** *Med Eng Phys* 2013, **35**(11):1651-1658.
123. Glaser DA, Doan J, Newton PO: **Comparison of 3-dimensional spinal reconstruction accuracy: biplanar radiographs with EOS versus computed tomography.** *Spine (Phila Pa 1976)* 2012, **37**(16):1391-1397.

124. Kadoury S, Cheriet F, Laporte C, Labelle H: **A versatile 3D reconstruction system of the spine and pelvis for clinical assessment of spinal deformities.** *Med Biol Eng Comput* 2007, **45**(6):591-602.
125. Courvoisier A, Drevelle X, Dubousset J, Skalli W: **Transverse plane 3D analysis of mild scoliosis.** *Eur Spine J* 2013, **22**(11):2427-2432.
126. Courvoisier A, Drevelle X, Vialle R, Dubousset J, Skalli W: **3D analysis of brace treatment in idiopathic scoliosis.** *Eur Spine J* 2013, **22**(11):2449-2455.
127. Humbert L, De Guise J, Aubert B, Godbout B, Skalli W: **3D reconstruction of the spine from biplanar X-rays using parametric models based on transversal and longitudinal inferences.** *Medical engineering & physics* 2009, **31**(6):681-687.
128. Somoskeoy S, Tunyogi-Csapo M, Bogyo C, Illes T: **Accuracy and reliability of coronal and sagittal spinal curvature data based on patient-specific three-dimensional models created by the EOS 2D/3D imaging system.** *The spine journal : official journal of the North American Spine Society* 2012, **12**(11):1052-1059.
129. Sabourin M, Jolivet E, Miladi L, Wicart P, Rampal V, Skalli W: **Three-dimensional stereoradiographic modeling of rib cage before and after spinal growing rod procedures in early-onset scoliosis.** *Clinical biomechanics (Bristol, Avon)* 2010, **25**(4):284-291.
130. Ilharreborde B, Dubousset J, Skalli W, Mazda K: **Spinal penetration index assessment in adolescent idiopathic scoliosis using EOS low-dose biplanar stereoradiography.** *Eur Spine J* 2013, **22**(11):2438-2444.
131. Moura DC, Boisvert J, Barbosa JG, Labelle H, Tavares JM: **Fast 3D reconstruction of the spine from biplanar radiographs using a deformable articulated model.** *Med Eng Phys* 2011, **33**(8):924-933.



132. Ilharreborde B, Steffen JS, Nectoux E, Vital JM, Mazda K, Skalli W, Obeid I: **Angle measurement reproducibility using EOS three-dimensional reconstructions in adolescent idiopathic scoliosis treated by posterior instrumentation.** *Spine (Phila Pa 1976)* 2011, **36**(20):E1306-1313.
133. Kotwicki T, Napiontek M: **Intravertebral deformation in idiopathic scoliosis: a transverse plane computer tomographic study.** *Journal of Pediatric Orthopaedics* 2008, **28**(2):225-229.
134. Göçen S, Aksu MG, Baktiroglu L, Özcan Ö: **Evaluation of computed tomographic methods to measure vertebral rotation in adolescent idiopathic scoliosis: an intraobserver and interobserver analysis.** *Journal of Spinal Disorders & Techniques* 1998, **11**(3):210-214.
135. Gocen S, Havitcioglu H, Alici E: **A new method to measure vertebral rotation from CT scans.** *Eur Spine J* 1999, **8**(4):261-265.
136. Forsberg D, Lundstrom C, Andersson M, Vavruch L, Tropp H, Knutsson H: **Fully automatic measurements of axial vertebral rotation for assessment of spinal deformity in idiopathic scoliosis.** *Phys Med Biol* 2013, **58**(6):1775-1787.
137. Doi T, Kido S, Kuwashima U, Tono O, Tarukado K, Harimaya K, Matsumoto Y, Kawaguchi K, Iwamoto Y: **A new method for measuring torsional deformity in scoliosis.** *Scoliosis* 2011, **6**(1):1-7.
138. Adam CJ, Izatt MT, Harvey JR, Askin GN: **Variability in Cobb angle measurements using reformatted computerized tomography scans.** *Spine (Phila Pa 1976)* 2005, **30**(14):1664-1669.
139. Gstoettner M, Lechner R, Glodny B, Thaler M, Bach CM: **Inter- and intraobserver reliability assessment of computed tomographic 3D measurement of pedicles in**

- scoliosis and size matching with pedicle screws.** *European Spine Journal* 2011, **20**(10):1771-1779.
140. Kuraishi S, Takahashi J, Hirabayashi H, Hashidate H, Ogihara N, Mukaiyama K, Kato H: **Pedicle morphology using computed tomography-based navigation system in adolescent idiopathic scoliosis.** *J Spinal Disord Tech* 2013, **26**(1):22-28.
141. Adam CJ, Cargill SC, Askin GN: **Computed tomographic-based volumetric reconstruction of the pulmonary system in scoliosis: trends in lung volume and lung volume asymmetry with spinal curve severity.** *Journal of pediatric orthopedics* 2007, **27**(6):677-681.
142. Chun EM, Suh SW, Modi HN, Kang EY, Hong SJ, Song HR: **The change in ratio of convex and concave lung volume in adolescent idiopathic scoliosis: a 3D CT scan based cross sectional study of effect of severity of curve on convex and concave lung volumes in 99 cases.** *Eur Spine J* 2008, **17**(2):224-229.
143. Yu WS, Chan KY, Yu FW, Yeung HY, Ng BK, Lee KM, Lam TP, Cheng JC: **Abnormal bone quality versus low bone mineral density in adolescent idiopathic scoliosis: a case-control study with in vivo high-resolution peripheral quantitative computed tomography.** *The spine journal : official journal of the North American Spine Society* 2013, **13**(11):1493-1499.
144. Fu G, Yoshihara H, Kawakami N, Goto M, Tsuji T, Ohara T, Imagama S: **Microcomputed tomographic evaluation of vertebral microarchitecture in pinealectomized scoliosis chickens.** *Journal of pediatric orthopedics Part B* 2011, **20**(6):382-388.
145. Abul-Kasim K, Overgaard A, Maly P, Ohlin A, Gunnarsson M, Sundgren PC: **Low-dose helical computed tomography (CT) in the perioperative workup of adolescent idiopathic scoliosis.** *European radiology* 2009, **19**(3):610-618.

146. Lee MC, Solomito M, Patel A: **Supine magnetic resonance imaging Cobb measurements for idiopathic scoliosis are linearly related to measurements from standing plain radiographs.** *Spine (Phila Pa 1976)* 2013, **38**(11):E656-661.
147. Wang F, Sun X, Mao S, Liu Z, Qiao J, Zhu F, Zhu Z, Qiu Y: **MR Imaging May Serve as a Valid Alternative to Standing Radiography in Evaluating the Sagittal Alignment of the Upper Thoracic Spine.** *J Spinal Disord Tech* 2013, **30**(3):124-128.
148. Wessberg P, Danielson BI, Willén J: **Comparison of Cobb angles in idiopathic scoliosis on standing radiographs and supine axially loaded MRI.** *Spine* 2006, **31**(26):3039-3044.
149. Little JP, Izatt MT, Labrom RD, Askin GN, Adam CJ: **Investigating the change in three dimensional deformity for idiopathic scoliosis using axially loaded MRI.** *Clinical biomechanics (Bristol, Avon)* 2012, **27**(5):415-421.
150. Diefenbach C, Lonner BS, Auerbach JD, Bharucha N, Dean LE: **Is radiation-free diagnostic monitoring of adolescent idiopathic scoliosis feasible using upright positional magnetic resonance imaging?** *Spine (Phila Pa 1976)* 2013, **38**(7):576-580.
151. Diab M, Landman Z, Lubicky J, Dormans J, Erickson M, Richards BS: **Use and outcome of MRI in the surgical treatment of adolescent idiopathic scoliosis.** *Spine* 2011, **36**(8):667-671.
152. Liljenqvist UR, Allkemper T, Hackenberg L, Link TM, Steinbeck J, Halm HF: **Analysis of vertebral morphology in idiopathic scoliosis with use of magnetic resonance imaging and multiplanar reconstruction.** *The Journal of Bone & Joint Surgery* 2002, **84**(3):359-368.
153. Parent S, Labelle H, Skalli W, de Guise J: **Thoracic pedicle morphometry in vertebrae from scoliotic spines.** *Spine* 2004, **29**(3):239-248.

154. Rajwani T, Bagnall KM, Lambert R, Videman T, Kautz J, Moreau M, Mahood J, Raso VJ, Bhargava R: **Using magnetic resonance imaging to characterize pedicle asymmetry in both normal patients and patients with adolescent idiopathic scoliosis.** *Spine (Phila Pa 1976)* 2004, **29**(7):E145-152.
155. Çatan H, Buluç L, Anık Y, Ayyıldız E, Şarlak AY: **Pedicle morphology of the thoracic spine in preadolescent idiopathic scoliosis: magnetic resonance supported analysis.** *European Spine Journal* 2007, **16**(8):1203-1208.
156. Kotani T, Minami S, Takahashi K, Isobe K, Nakata Y, Takaso M, Inoue M, Maruta T, Akazawa T, Ueda T *et al*: **An analysis of chest wall and diaphragm motions in patients with idiopathic scoliosis using dynamic breathing MRI.** *Spine (Phila Pa 1976)* 2004, **29**(3):298-302.
157. Chu WC, Li AM, Ng BK, Chan DF, Lam TP, Lam WW, Cheng JC: **Dynamic magnetic resonance imaging in assessing lung volumes, chest wall, and diaphragm motions in adolescent idiopathic scoliosis versus normal controls.** *Spine (Phila Pa 1976)* 2006, **31**(19):2243-2249.
158. Chu WC, Ng BK, Li AM, Lam TP, Lam WW, Cheng JC: **Dynamic magnetic resonance imaging in assessing lung function in adolescent idiopathic scoliosis: a pilot study of comparison before and after posterior spinal fusion.** *J Orthop Surg Res* 2007, **2**:1-7.
159. Violas P, Estivalezes E, Pedrono A, de Gauzy JS, Sevely A, Swider P: **A method to investigate intervertebral disc morphology from MRI in early idiopathic scoliosis: a preliminary evaluation in a group of 14 patients.** *Magn Reson Imaging* 2005, **23**(3):475-479.

160. Buttermann GR, Mullin WJ: **Pain and disability correlated with disc degeneration via magnetic resonance imaging in scoliosis patients.** *Eur Spine J* 2008, **17**(2):240-249.
161. Gervais J, Perie D, Parent S, Labelle H, Aubin CE: **MRI signal distribution within the intervertebral disc as a biomarker of adolescent idiopathic scoliosis and spondylolisthesis.** *BMC Musculoskelet Disord* 2012, **13**:239-249.
162. Dohn P, Vialle R, Thevenin-Lemoine C, Balu M, Lenoir T, Abelin K: **Assessing the rotation of the spinal cord in idiopathic scoliosis: a preliminary report of MRI feasibility.** *Childs Nerv Syst* 2009, **25**(4):479-483.
163. Birchall D, Hughes D, Gregson B, Williamson B: **Demonstration of vertebral and disc mechanical torsion in adolescent idiopathic scoliosis using three-dimensional MR imaging.** *Eur Spine J* 2005, **14**(2):123-129.
164. Stokes IA, Moreland MS: **Concordance of back surface asymmetry and spine shape in idiopathic scoliosis.** *Spine* 1989, **14**(1):73-78.
165. Goldberg CJ, Kaliszer M, Moore DP, Fogarty EE, Dowling FE: **Surface topography, Cobb angles, and cosmetic change in scoliosis.** *Spine* 2001, **26**(4):E55-E63.
166. Turner-Smith AR, Harris JD, Houghton GR, Jefferson RJ: **A method for analysis of back shape in scoliosis.** *Journal of biomechanics* 1988, **21**(6):497-509.
167. Oxborrow N: **Assessing the child with scoliosis: the role of surface topography.** *Archives of disease in childhood* 2000, **83**(5):453-455.
168. Thometz J, Lamdan R, Liu X, Lyon R: **Relationship between Quantec measurement and Cobb angle in patients with idiopathic scoliosis.** *Journal of Pediatric Orthopaedics* 2000, **20**(4):512-516.

169. Frerich JM, Hertzler K, Knott P, Mardjetko S: **Comparison of radiographic and surface topography measurements in adolescents with idiopathic scoliosis.** *Open Orthop J* 2012, **6**(1):261-265.
170. Mangone M, Raimondi P, Paoloni M, Pellanera S, Di Michele A, Di Renzo S, Vanadia M, Dimaggio M, Murgia M, Santilli V: **Vertebral rotation in adolescent idiopathic scoliosis calculated by radiograph and back surface analysis-based methods: correlation between the Raimondi method and rasterstereography.** *Eur Spine J* 2013, **22**(2):367-371.
171. Ajemba P, Durdle N, Hill D, Raso J: **Classifying torso deformity in scoliosis using orthogonal maps of the torso.** 2007, **45**(6):575-584.
172. Ajemba PO, Durdle NG, Hill DL, James Raso V: **Validating an imaging and analysis system for assessing torso deformities.** *Computers in biology and medicine* 2008, **38**(3):294-303.
173. Shannon TM: **Development of an apparatus to evaluate Adolescent Idiopathic Scoliosis by dynamic surface topography.** *Stud Health Technol Inform* 2008, **140**:121-127.
174. Michoński J, Glinkowski W, Witkowski M, Sitnik R: **Automatic recognition of surface landmarks of anatomical structures of back and posture.** *Journal of Biomedical Optics* 2012, **17**(5):056015.
175. Komeili A, Westover LM, Parent EC, Moreau M, El-Rich M, Adeeb S: **Surface topography asymmetry maps categorizing external deformity in scoliosis.** *The spine journal : official journal of the North American Spine Society* 2014, **14**(6):973.
176. Rigo M: **Patient evaluation in idiopathic scoliosis: Radiographic assessment, trunk deformity and back asymmetry.** *Physiotherapy Theory & Practice* 2011, **27**(1):7-25.

177. Pazos V, Cheriet F, Song L, Labelle H, Dansereau J: **Accuracy assessment of human trunk surface 3D reconstructions from an optical digitising system.** *Med Biol Eng Comput* 2005, **43**(1):11-15.
178. de Seze M, Randriaminahisoa T, Gaunelle A, de Korvin G, Mazaux JM: **Inter-observer reproducibility of back surface topography parameters allowing assessment of scoliotic thoracic gibbosity and comparison with two standard postures.** *Annals of physical and rehabilitation medicine* 2013, **56**(9-10):599-612.
179. Debanne P, Pazos V, Labelle H, Cheriet F: **Evaluation of reducibility of trunk asymmetry in lateral bending.** *Stud Health Technol Inform* 2010, **158**:72-77.
180. Hackenberg L, Hierholzer E, Bullmann V, Liljenqvist U, Gotze C: **Rasterstereographic analysis of axial back surface rotation in standing versus forward bending posture in idiopathic scoliosis.** *Eur Spine J* 2006, **15**(7):1144-1149.
181. Patias P, Grivas TB, Kaspiris A, Aggouris C, Drakoutos E: **A review of the trunk surface metrics used as Scoliosis and other deformities evaluation indices.** *Scoliosis and spinal disorders* 2010, **5**(1):12.
182. Suzuki N, Inami K, Ono T, Kohno K, Asher M: **Analysis of posterior trunk symmetry index (POTSI) in Scoliosis. Part 1.** *Studies in Health Technology and Informatics* 1999:81-84.
183. Inami K, Suzuki N, Ono T, Yamashita Y, Kohno K, Morisue H: **Analysis of posterior trunk symmetry index (POTSI) in scoliosis. Part 2.** *Studies in Health Technology and Informatics* 1999:85-88.
184. Asher M, Lai SM, Burton D, Manna B: **Maintenance of trunk deformity correction following posterior instrumentation and arthrodesis for idiopathic scoliosis.** *Spine* 2004, **29**(16):1782-1788.

185. Minguez MF, Buendia M, Cibrian RM, Salvador R, Laguia M, Martin A, Gomar F: **Quantifier variables of the back surface deformity obtained with a noninvasive structured light method: evaluation of their usefulness in idiopathic scoliosis diagnosis.** *Eur Spine J* 2007, **16**(1):73-82.
186. Hackenberg L, Hierholzer E, Pötzl W, Götze C, Liljenqvist U: **Rasterstereographic back shape analysis in idiopathic scoliosis after anterior correction and fusion.** *Clinical Biomechanics* 2003, **18**(1):1-8.
187. Kinel E, Kotwicki T, Stryla W, Szulc A: **Corrective bracing for severe idiopathic scoliosis in adolescence: influence of brace on trunk morphology.** *Scientific World Journal* 2012, **2012**(1):435158.
188. Berryman F, Pynsent P, Fairbank J: **Thoracic kyphosis angle measurements with ISIS2.** *Stud Health Technol Inform* 2008, **140**:68-71.
189. Berryman F, Pynsent P, Fairbank J: **Measuring the rib hump in scoliosis with ISIS2.** *Stud Health Technol Inform* 2008, **140**:65-67.
190. Berryman F, Pynsent P, Fairbank J, Disney S: **A new system for measuring three-dimensional back shape in scoliosis.** *Eur Spine J* 2008, **17**(5):663-672.
191. McArdle F, Griffiths C, Macdonald A, Gibson M: **Monitoring the thoracic sagittal curvature in kyphoscoliosis with surface topography: a trend analysis of 57 patients.** *Studies in Health Technology and Informatics* 2001, **91**:199-203.
192. Schulte TL, Hierholzer E, Boerke A, Lerner T, Liljenqvist U, Bullmann V, Hackenberg L: **Raster stereography versus radiography in the long-term follow-up of idiopathic scoliosis.** *Journal of spinal disorders & techniques* 2008, **21**(1):23-28.



193. Knott P, Mardjetko S, Tager D, Hund R, Thompson S: **The influence of body mass index (BMI) on the reproducibility of surface topography measurements.** *Scoliosis* 2012, **7**(Suppl 1):O18.
194. Melvin M, Sylvia M, Udo W, Helmut S, Paletta JR, Adrian S: **Reproducibility of rasterstereography for kyphotic and lordotic angles, trunk length, and trunk inclination: a reliability study.** *Spine* 2010, **35**(14):1353-1358.
195. Darrieutortlaffite C, Hamel O, Glémarec J, Maugars Y, Le GB: **Ultrasonography of the lumbar spine: sonoanatomy and practical applications.** *Joint Bone Spine* 2014, **81**(2):130-136.
196. Finnoff JT, Hall MM, Adams E, Berkoff D, Concoff AL, Dexter W, Smith J: **American Medical Society for Sports Medicine (AMSSM) Position Statement: Interventional Musculoskeletal Ultrasound in Sports Medicine.** *Clinical Journal of Sport Medicine Official Journal of the Canadian Academy of Sport Medicine* 2015, **7**(2):151-168.
197. Letts M, Quanbury A, Gouw G, Kolsun W, Letts E: **Computerized ultrasonic digitization in the measurement of spinal curvature.** *Spine* 1988, **13**(10):1106-1110.
198. Li M, Cheng J, Ying M, Ng B, Zheng YP, Lam TP, Wong WY, Wong MS: **Application of 3-D ultrasound in assisting the fitting procedure of spinal orthosis to patients with adolescent idiopathic scoliosis.** *Studies In Health Technology And Informatics* 2010, **158**:34-37.
199. Li M, Cheng J, Ying M, Ng B, Zheng Y, Lam T, Wong W, Wong M: **Could clinical ultrasound improve the fitting of spinal orthosis for the patients with AIS?** *European Spine Journal* 2012, **21**(10):1926-1935.

200. Meng L, Wong M, Keith D, Kenneth W, Cheung KM: **Time-dependent response of scoliotic curvature to orthotic intervention: When should a radiograph be taken after putting on or taking off a spinal orthosis?** *Spine (Phila Pa 1976)* 2014, **39**(17):1408-1416.
201. Lam TP, Hung VWY, Yeung HY, Chu WCW, Ng BKW, Lee KM, Qin L, Cheng JCY: **Quantitative Ultrasound for Predicting Curve Progression in Adolescent Idiopathic Scoliosis: A Prospective Cohort Study of 294 Cases Followed-Up Beyond Skeletal Maturity.** *Ultrasound in medicine & biology* 2013, **39**(3):381-387.
202. Suzuki S, Yamamuro T, Shikata J, Shimizu K, Iida H: **Ultrasound measurement of vertebral rotation in idiopathic scoliosis.** *J Bone Joint Surg Br* 1989, **71**(2):252-255.
203. Koo TK, Guo J-Y, Ippolito C, Bedle JC: **Assessment of Scoliotic Deformity Using Spinous Processes: Comparison of Different Analysis Methods of an Ultrasonographic System.** *Journal of manipulative and physiological therapeutics* 2014, **37**(9):667-677.
204. Thaler M, Kaufmann G, Steingruber I, Mayr E, Liebensteiner M, Bach C: **Radiographic versus ultrasound evaluation of the Risser Grade in adolescent idiopathic scoliosis: a prospective study of 46 patients.** *Eur Spine J* 2008, **17**(9):1251-1255.
205. Kennelly KP, Stokes MJ: **Pattern of asymmetry of paraspinal muscle size in adolescent idiopathic scoliosis examined by real-time ultrasound imaging. A preliminary study.** *Spine (Phila Pa 1976)* 1993, **18**(7):913-917.
206. Paweł L, Edward S, Michał K, Tomasz W: **Ultrasound Assessment of the Abdominal Muscles at Rest and During the ASLR Test Among Adolescents with Scoliosis.** *Journal of spinal disorders & techniques* 2014, **110**(s 3–4):207-215.

207. Yang HS, Yoo JW, Lee BA, Choi CK, You JH: **Inter-tester and Intra-tester Reliability of Ultrasound Imaging Measurements of Abdominal Muscles in Adolescents with and without Idiopathic Scoliosis: A Case-controlled Study.** *Bio-medical materials and engineering* 2014, **24**(1):453-458.
208. Linek P, Saulicz E, Wolny T, Myśliwiec A, Gogola A: **Ultrasound evaluation of the symmetry of abdominal muscles in mild adolescent idiopathic scoliosis.** *Journal of Physical Therapy Science* 2015, **2**(27):465-468.
209. Zapata KA, Wang-Price SS, Sucato DJ, Dempsey-Robertson M: **Ultrasonographic Measurements of Paraspinal Muscle Thickness in Adolescent Idiopathic Scoliosis: A Comparison and Reliability Study.** *Pediatric Physical Therapy* 2015, **27**(2):119-125.
210. Richter A, Parent EC, Kawchuk G, Moreau M, Hedden D, Lou E: **Ultrasound image measurements of erector spinae muscle thickness at four spinal levels in adolescents with idiopathic scoliosis: reliability and concave-convex comparison.** *Scoliosis* 2013, **8**(Suppl 2):O36.
211. Wagner U, Diedrich V, Schmitt O: **Determination of skeletal maturity by ultrasound: a preliminary report.** *Skeletal radiology* 1995, **24**(6):417-420.
212. Torlak G, Kiter E, Oto M, Akman A: **Ultrasonographic evaluation of the Risser sign. Is it a reliable and reproducible method?** *Spine (Phila Pa 1976)* 2012, **37**(4):316-320.
213. Pitlovic H, Jovanovic S, Pitlovic V, Saric G, Crnkovic T: **A Validity of Ultrasound Subdivision of Risser Grade 4 in Assessment of Skeletal Maturity.** *Collegium Antropologicum* 2013, **37**(4):1105–1109.

214. Baroncelli GI: **Quantitative ultrasound methods to assess bone mineral status in children: technical characteristics, performance, and clinical application.** *Pediatric Research* 2008, **63**(3):220-228.
215. Lam TP, Hung VWY, Yeung HY, Tse YK, Chu WCW, Ng BKW, Lee KM, Qin L, Cheng JCY: **Abnormal bone quality in adolescent idiopathic scoliosis: a case-control study on 635 subjects and 269 normal controls with bone densitometry and quantitative ultrasound.** *Spine* 2011, **36**(15):1211-1217.
216. Tsz Ping L, Hung VWY, Hiu Yan Y, Yee Kit T, Chu WCW, Ng BKW, Kwong Man L, Ling Q, Cheng JCY: **Abnormal Bone Quality in Adolescent Idiopathic Scoliosis.** *Spine* 2011, **36**(15):1211-1217.
217. Du Q, Zhou X, Li JA, He XH, Liang JP, Zhao L, Yang XY, Chen N, Zhang SX, Chen PJ: **Quantitative Ultrasound Measurements of Bone Quality in Female Adolescents With Idiopathic Scoliosis Compared To Normal Controls.** *Journal of manipulative and physiological therapeutics* 2015, **38**(6):434-441.
218. Wang H, Du Q, Chen P, Li J, He X: **Quantitative ultrasound measurements of bone strength in female adolescent idiopathic scoliosis patients.** *Scoliosis* 2013, **8**(Suppl 1):O7.
219. Zhou X, Du Q, Li J, He X, Zhao L, Chen P: **Is it worthwhile to measure bone quality in patients with adolescent idiopathic scoliosis?** *Scoliosis* 2014, **9**(Suppl 1):O14.
220. Berton F, Azzabi W, Cheriet F, Laporte C: **Automatic Segmentation of Vertebrae in Ultrasound Images.** In: *Image Analysis and Recognition.* edn.: Springer; 2015: 344-351.
221. Carbajal G, Gómez Á, Fichtinger G, Ungi T: **Portable Optically Tracked Ultrasound System for Scoliosis Measurement.** In: *Recent Advances in*

- Computational Methods and Clinical Applications for Spine Imaging*. edn.: Springer; 2015: 37-46.
222. Solomon E, Shortland A, Lucas J: **The Development and Validation of a 3D Ultrasound System for Monitoring Curve Progression of Patients with Scoliosis.** *Bone & Joint Journal* 2015, **97**(SUPP 9):P1.
223. Lou E, Zheng R, Chan AC, Hill DL, Moreau MJ, Hedden DM, Mahood JK, Southon S: **Reliability of coronal curvature measurements on 3D ultrasound images for AIS.** *Scoliosis* 2015, **10**(Suppl 1):O37.
224. Ungi T, King F, Kempston M, Keri Z, Lasso A, Mousavi P, Rudan J, Borschneck DP, Fichtinger G: **Spinal curvature measurement by tracked ultrasound snapshots.** *Ultrasound in medicine & biology* 2014, **40**(2):447-454.
225. Kottner J, Audigé L, Brorson S, Donner A, Gajewski BJ, Hróbjartsson A, Roberts C, Shoukri M, Streiner DL: **Guidelines for reporting reliability and agreement studies (GRRAS) were proposed.** *International journal of nursing studies* 2011, **48**(6):661-671.
226. Burwell RG, Aujla KK, Cole AA, Kirby AS, Pratt KK, Webb JK, Moulton A: **Anterior universal spine system for adolescent idiopathic scoliosis: a follow-up study using scoliometer, real-time ultrasound and radiographs.** *Stud Health Technol Inform* 2002, **91**:473-476.
227. Burwell RG, Aujla RK, Cole AA, Kirby AS, Pratt RK, Webb JK, Moulton A: **Preliminary study of a new real-time ultrasound method for measuring spinal and rib rotation in preoperative patients with adolescent idiopathic scoliosis.** *Stud Health Technol Inform* 2002, **91**:262-266.
228. Burwell RG, Aujla RK, Cole AA, Kirby AS, Pratt RK, Webb JK, Moulton A: **Spine-rib rotation differences at the apex in preoperative patients with adolescent**

- idiopathic scoliosis: evaluation of a three-level ultrasound method.** *Stud Health Technol Inform* 2002, **91**:246-250.
229. Burwell RG, Aujla RK, Kirby AS, Moulton A, Webb JK: **The early detection of adolescent idiopathic scoliosis in three positions using the scoliometer and real-time ultrasound: should the prone position also be used?** *Stud Health Technol Inform* 2002, **88**:74-80.
230. Chen W, Lou E, Le LH: **A Reliable Semi-automatic Program to Measure the Vertebral Rotation Using the Center of Lamina for Adolescent Idiopathic Scoliosis.** In: *5th International Conference on Biomedical Engineering in Vietnam: 2015*: Springer; 2015: 159-162.
231. Vo QN, Lou EH, Le LH: **Measurement of axial vertebral rotation using three-dimensional ultrasound images.** *Scoliosis* 2015, **10**(Suppl 2):S7.
232. Takács M, Rudner E, Kovács A, Orlovits Z, Kiss RM: **The Assessment of the Spinal Curvatures in the Sagittal Plane of Children Using an Ultrasound-Based Motion Analysing System.** *Annals of biomedical engineering* 2015, **43**(2):348-362.
233. Mauritzson L, Ilver J, Benoni G, Lindström K, Willner S: **Two-dimensional airborne ultrasound real-time linear array scanner—Applied to screening for scoliosis.** *Ultrasound in Medicine & Biology* 1991, **17**(5):519.
234. Lou E, Zheng R, Le L, Hill D, Raso J, Hedden D, Mahood J, Moreau M: **Curve flexibility assessment on AIS surgical candidates using ultrasonic imaging method—a preliminary study.** *Scoliosis* 2015, **10**(Suppl 1):O39.
235. Zheng R, Lou E, Le LH, Hedden D, Mahood J, Moreau M: **Assessment of Curve Flexibility by Ultrasonic Imaging—A Pilot Study.** In: *5th International Conference on Biomedical Engineering in Vietnam: 2015*: Springer; 2015: 167-170.

236. Kotani T, Minami S, Takahashi K, Isobe K, Nakata Y, Takaso M, Inoue M, Nishikawa S, Maruta T, Tamaki T: **Three dimensional analysis of chest wall motion during breathing in healthy individuals and patients with seoliosis using an ultrasonography-based system.** *Studies in Health Technology & Informatics* 2002, **91**:135-139.
237. Berteau JP, Pithioux M, Follet H, Guivier-Curien C, Lasaygues P, Chabrand P: **Computed tomography, histological and ultrasonic measurements of adolescent scoliotic rib hump geometrical and material properties.** *Journal of Biomechanics* 2012, **45**(14):2467-2471.
238. Chalmers E, Hill D, Donauer A, Tilburn M, Zhao V, Lou E: **How does pressure configuration affect Cobb angle during AIS brace casting?** *Scoliosis* 2015, **10**(Suppl 1):O60.
239. Lou E, Chan A, Donauer A, Tilburn M, Hill D: **Ultrasound-assisted brace casting for adolescent idiopathic scoliosis.** *Scoliosis* 2015, **10**(Suppl 1):O38.
240. Stokes OM, O'Donovan EJ, Samartzis D, Bow CH, Luk KD, Cheung K: **Reducing radiation exposure in early-onset scoliosis surgery patients: novel use of ultrasonography to measure lengthening in magnetically-controlled growing rods.** *The Spine Journal* 2014, **14**(10):2379-2404.
241. Yoon WW, Chang AC, Tyler P, Butt S, Raniga S, Noordeen H: **The use of ultrasound in comparison to radiography in magnetically controlled growth rod lengthening measurement: a prospective study.** *European Spine Journal* 2014, **24**(7):1422-1426.
242. Hong JY, Suh SW, Modi HN, Hur CY, Song HR, Ryu JH: **Centroid method: reliable method to determine the coronal curvature of scoliosis: a case control**

- study comparing with the Cobb method.** *Spine (Phila Pa 1976)* 2011, **36**(13):855-861.
243. Currier DP: **Elements of research in physical therapy**, 3rd edn: Williams & Wilkins; 1984.
244. Bland JM, Altman DG: **Statistical methods for assessing agreement between two methods of clinical measurement.** *The lancet* 1986, **327**(8476):307-310.
245. Bland JM, Altman DG: **Comparing methods of measurement: why plotting difference against standard method is misleading.** *The Lancet* 1995, **346**(8982):1085-1087.
246. Bland JM, Altman DG: **Measuring agreement in method comparison studies.** *Statistical methods in medical research* 1999, **8**(2):135-160.
247. Bland JM, Altman DG: **Applying the right statistics: analyses of measurement studies.** *Ultrasound in obstetrics & gynecology* 2003, **22**(1):85-93.
248. Zaki R, Bulgiba A, Ismail R, Ismail NA: **Statistical methods used to test for agreement of medical instruments measuring continuous variables in method comparison studies: a systematic review.** *PloS one* 2012, **7**(5):e37908.
249. Lonstein JE, Carlson JM: **The prediction of curve progression in untreated idiopathic scoliosis during growth.** *Journal of Bone & Joint Surgery American Volume* 1984, **66**(7):1061-1071.
250. Wu H, Ronsky JL, Cheriet F, Harder J, Küpper JC, Zernicke RF: **Time series spinal radiographs as prognostic factors for scoliosis and progression of spinal deformities.** *European Spine Journal* 2011, **20**(1):112.
251. Adam CJ, Askin GN, Percy MJ: **Gravity-induced torque and intravertebral rotation in idiopathic scoliosis.** *Spine* 2008, **33**(2):E30-E37.



252. Hong JY, Suh SW, Easwar TR, Modi HN, Yang JH, Park JH: **Evaluation of the three-dimensional deformities in scoliosis surgery with computed tomography: efficacy and relationship with clinical outcomes.** *Spine (Phila Pa 1976)* 2011, **36**(19):E1259-1265.
253. Vrtovec T, Likar B, Pernuš F: **Analysis of four manual and a computerized method for measuring axial vertebral rotation in computed tomography images.** *Spine* 2010, **35**(12):E535-E541.
254. Vrtovec T, Pernuš F, Likar B: **Determination of axial vertebral rotation in MR images: comparison of four manual and a computerized method.** *European Spine Journal* 2010, **19**(5):774-781.
255. Wang W, Wang Z, Liu Z, Zhu Z, Zhu F, Sun X, Lam TP, Cheng JC, Qiu Y: **Are there gender differences in sagittal spinal pelvic inclination before and after the adolescent pubertal growth spurt?** *Eur Spine J* 2015, **24**(6):1168-1174.
256. Newton PO, Fujimori T, Doan J, Reighard FG, Bastrom TP, Misaghi A: **Defining the "Three-Dimensional Sagittal Plane" in Thoracic Adolescent Idiopathic Scoliosis.** *The Journal of bone and joint surgery American volume* 2015, **97**(20):1694-1701.
257. Upasani VV, Tis J, Bastrom T, Pawelek J, Marks M, Lonner B, Crawford A, Newton PO: **Analysis of sagittal alignment in thoracic and thoracolumbar curves in adolescent idiopathic scoliosis: how do these two curve types differ?** *Spine* 2007, **32**(12):1355-1359.
258. Hu P, Yu M, Liu X, Zhu B, Liu X, Liu Z: **Analysis of the relationship between coronal and sagittal deformities in adolescent idiopathic scoliosis.** *Eur Spine J* 2016, **25**(2):409-416.

259. Liu T, Hai Y: **Sagittal plane analysis of selective posterior thoracic spinal fusion in adolescent idiopathic scoliosis: a comparison study of all pedicle screw and hybrid instrumentation.** *J Spinal Disord Tech* 2014, **27**(5):277-282.
260. Anwer S, Alghadir A, Abu Shaphe M, Anwar D: **Effects of Exercise on Spinal Deformities and Quality of Life in Patients with Adolescent Idiopathic Scoliosis.** *BioMed research international* 2015, **2015**:123848.
261. Fang MQ, Wang C, Xiang GH, Lou C, Tian NF, Xu HZ: **Long-term effects of the Cheneau brace on coronal and sagittal alignment in adolescent idiopathic scoliosis.** *Journal of neurosurgery Spine* 2015, **23**(4):505-509.
262. Torell G, Nachemson A, Haderspeck-Grib K, Schultz A: **Standing and supine Cobb measures in girls with idiopathic scoliosis.** *Spine* 1985, **10**(5):425-427.
263. Yazici M, Acaroglu ER, Alanay A, Deviren V, Cila A, Surat A: **Measurement of vertebral rotation in standing versus supine position in adolescent idiopathic scoliosis.** *Journal of Pediatric Orthopaedics* 2001, **21**(2):252-256.
264. Keenan BE, Izatt MT, Askin GN, Labrom RD, Percy MJ, Adam CJ: **Supine to standing Cobb angle change in idiopathic scoliosis: the effect of endplate pre-selection.** *Scoliosis* 2014, **9**(1):16.
265. Shi B, Mao S, Wang Z, Lam TP, Ping Yu FW, Wah Ng BK, Chu WC, Zhu Z, Qiu Y, Yiu Cheng JC: **How does the supine MRI correlate with standing x-ray of different curve severity in adolescent idiopathic scoliosis?** *Spine (Phila Pa 1976)* 2015, **40**(15):1206-1212.
266. Lee MC, Solomito M, Patel A: **Supine magnetic resonance imaging Cobb measurements for idiopathic scoliosis are linearly related to measurements from standing plain radiographs.** *Spine* 2013, **38**(11):E656-E661.

267. Zetterberg C, Hansson T, Lidström J, Irstam L, Andersson GB: **Postural and time-dependent effects on body height and scoliosis angle in adolescent idiopathic scoliosis.** *Acta Orthopaedica* 1983, **54**(6):836-840.
268. Cheh G, Lenke LG, Lehman RA, Jr., Kim YJ, Nunley R, Bridwell KH: **The reliability of preoperative supine radiographs to predict the amount of curve flexibility in adolescent idiopathic scoliosis.** *Spine (Phila Pa 1976)* 2007, **32**(24):2668-2672.
269. Sabharwal S, Apazidis A, Zhao C, Hullinger H, Vives M: **Comparison of intraoperative supine and postoperative standing radiographs after posterior instrumentation for adolescent idiopathic scoliosis.** *Journal of pediatric orthopedics Part B* 2011, **20**(6):389-396.
270. Ohrt-Nissen S, Hallager DW, Gehrchen M, Dahl B: **Supine lateral bending radiographs predict the initial in-brace correction of the Providence brace in patients with Adolescent Idiopathic Scoliosis.** *Spine (Phila Pa 1976)* 2016.
271. Little JP, Pearcy MJ, Izatt MT, Boom K, Labrom RD, Askin GN, Adam CJ: **Understanding how axial loads on the spine influence segmental biomechanics for idiopathic scoliosis patients: A magnetic resonance imaging study.** *Clinical biomechanics (Bristol, Avon)* 2016, **32**:220-228.
272. Duval-Beaupere G: **Rib hump and supine angle as prognostic factors for mild scoliosis.** *Spine* 1992, **17**(1):103-107.

**- END -**